

Investigation of the impact of prebiotics and polyphenols on intestinal physiology and immunity

Harry Shaw

A thesis submitted to Lancaster University for the degree of

Master of Science Biomedical Science

Supervised by Dr Rachael Rigby

August 2025

Declaration

I declare that this thesis is entirely my own work submitted for the degree of Masters (by Research) in Biomedical Science at Lancaster University and has not been previously submitted to any other University or Institute of Learning for the award of a higher degree.

Acknowledgments

I would first like to give thanks to Dr Rachael Rigby for her guidance and support throughout my research project and subsequent write up period. Thank you also to the participants and staff at Lancashire Teaching Hospitals NHS involved in our stoma study, particularly Arnab Bhowmick and Amanda Alty. I also want to express my immense gratitude to my mum, Jill who has given me unconditional love and support throughout the completion of this project. Finally, I dedicate this thesis to my late grandma, who sadly passed away shortly before the submission of this work.

Table of contents

Declaration	2
Acknowledgements	3
Table of contents	4
List of abbreviations	.11
Abstract	.17
1. Literature Review	.18
1.1. Overview	.18
1.2. The gastrointestinal tract	.19
1.3. The gut microbiome	.21
1.3.1. Gastrointestinal microbial composition	.22
1.3.1.1. Bacterial composition	.22
1.3.1.2. Fungal composition	.23
1.3.1.3. Viral composition	.24
1.4. Substrates that influence microbial composition	.24
1.4.1.Probiotics	.25
1.4.2.Short chain fatty acids	.25
1.4.3. Prebiotics	.27
1.4.3.1. Polyphenols	.28
1.5. Enteric bacteria and intestinal barrier function and	
repair	.29
1.5.1. Dysbiosis hinders damage repair	.30
1.6. Gastrointestinal immunity	.31
1.6.1.Innate intestinal immunity	.31
1.6.1.1. Dendritic cells	.32
1.6.1.1.1. CD103 ⁺ / ₋ DC subsets	.32
1.6.2. Adaptive intestinal immunity	.33
1.6.2.1. T cell activation by CD103 ⁺ /- DC subsets	
1.7. Nutrient deprivation disrupts microbial composition and	
intestinal physiology	
1.7.1.Total parenteral nutrition	
1.7.2.Loop ileostomy and loop ileostomy reversal	
1.7.2.1. Altered physiology in the defunctioned ileum	

	1.7.2.2. Dysbiosis in the defunctioned ileum	38
	1.7.2.3. Intestinal atrophy is associated with dysbiosis	39
	1.7.2.4. Possible immune dysregulation in the	
	defunctioned ileum	40
	1.8. Distal limb stimulation	40
	1.9. Polyphenols: a proposed addition to DLS	42
	1.9.1. Effect of polyphenols on pathologies	42
	1.9.2. Polyphenol influence on intestinal barrier integrity ar	
	repair	44
	1.9.3. Extra virgin olive oil	44
	1.9.4. Polyphenol metabolism and bioavailability	46
	1.10. Solid lipid nanoparticles	49
	1.10.1. Potential incorporation of SLN-tagged polyphenol	S
	in DLS	50
	1.11. Hypotheses	52
	1.12. Research aims	53
2.	Methods	54
	2.1. Model maintenance	54
	2.1.1.Cell line maintenance	54
	2.1.2. Murine model maintenance	54
	2.1.2.1. Ethics statement	54
	2.1.2.2. Husbandry	55
	2.2. Obtaining human intestinal tissue	55
	2.2.1. Declaration and informed patient consent	55
	2.2.2. Distal limb stimulation protocol	56
	2.2.3. Tissue fixation and embedding	56
	2.3. Histochemistry	58
	2.3.1.H&E staining	58
	2.4. Microscopy	58
	2.5. Flow cytometry	
	2.5.1. Sample preparation	
	2.5.2. Flow cytometry acquisition	
	2.6. in vivo polyphenol feeding	
	2.6.1. Preparation of treatments	
	2.6.1.1. Polyphenol extraction from EVOO	
	2.6.1.2. SLN synthesis for polyphenol tagging	
	2.6.2. Experimental procedure	63

	2.7.	Fluorescence imaging	.64
	2.8.	High performance liquid chromatography	.65
	2.	8.1. HPLC tissue preparation	.65
	2.	8.2. HPLC analysis	.66
	2.9.	in vitro polyphenol translocation	.67
	2.	9.1. Experimental set up	.67
		2.9.1.1. Transwell set up and monolayer establishment	.67
		2.9.1.2. Polyphenol preparation	.68
	2.	9.2. Experimental procedure	.68
3.	Resu	ılts	.69
	3.1.	Stoma participant demographics	.69
	3.2.	Effects of loop ileostomy on immune cell populations	
		in the defunctioned ileum	.70
	3.	2.1. Immune cell selection and gating strategy	.70
	3.	2.2. Stoma formation does not affect dendritic cell	
		populations in the defunctioned ileum	.72
	3.	2.3. Stoma formation does not affect T cell populations in	
		the defunctioned ileum	.74
	3.3.	Characterising the physiological impacts of loop	
		ileostomy and distal limb stimulation in the	
		defunctioned ileum	.75
	3.	3.1. Crypt depth as an indicator of stem cell	
		proliferation	.75
	3.	3.2. Villus atrophy in the defunctioned ileum	
		persisted with DLS	.76
	3.	3.3.The physiological effect of stoma formation and	
		DLS on crypt depth in the defunctioned ileum	
		Bioavailability of polyphenols	
	3.	4.1. in vitro polyphenol translocation	
		3.4.1.1. Optimising polyphenol detection	.80
		3.4.1.2. Polyphenol transport through an intestinal	
	_	epithelial monolayer	.81
	3.	4.2. in vivo assessment of solid lipid nanoparticles on	
		polyphenol absorption	
		3.4.2.1. Experimental monitoring	.83
		3.4.2.1.1. Physical observations suggest	_ =
		treatments were well tolerated	.83

		3.4.2	.1.2.	Body mass was not affected by	
				treatments	83
		3.4.2	.1.3.	Treatments did not impact food intake	84
		3.4.2	.1.4.	Organ mass after experiment	85
		3.4.2.2.	Colo	nic crypt depth is not altered by	
			poly	phenol administration	87
		3.4.2.3.	Fluo	rescence imaging	88
		3.4.2.4.	Poly	phenol detection using HPLC	92
4.	Disc	ussion	•••••		93
	4.1.	Immund	ologic	al state of the defunctioned ileum prior	
		to reana	astom	nosis	93
	4.2.	Physiol	ogica	l state of the defunctioned ileum prior	
		to reana	astom	nosis	95
	4.3.	Physiol	ogica	l impacts of DLS in the defunctioned ileun	n 97
	4.4.	Investig	ating	polyphenol bioavailability	100
	4.	4.1.Poly	ohend	ol translocation through an intestinal	
		epith	elial	monolayer	100
	4.	4.2. Atter	npts t	to improve polyphenol bioavailability	101
		4.4.2.1.	Impa	act of SLNs and EVOO extracts on colonic	
			phys	siology	101
		4.4.2.2.	Impa	act of SLNs on polyphenol bioavailability	101
		4.4.2.3.	Suita	ability for SLN-tagged EVOO extracts in	
			DLS		103
	4.5.	Conclus	sion		104
5.	Appe	endix	• • • • • • • • • •		106
	5.1.	APES-co	oated	microscope slides	106
	5.2.	Flow cy	tome	try	106
	5.	2.1.Cell :	surfac	ce antibodies	106
	5.	2.2. Patie	nt filt	ter panels	107
6	Dofo	rancas			112

List of figures

Figure 1.1. Organisation of the gastrointestinal tract	19
Figure 1.2. Mucosal physiology in the ileum	21
Figure 1.3. Changes in environment and common taxa along the GI tract	23
Figure 1.4. Classes and subclasses of prebiotics	27
Figure 1.5. The four main groups (and sub-groups) of dietary polyphenols	28
Figure 1.6. Process of loop ileostomy reversal surgery (reanastomosis)	37
Figure 1.7. Common polyphenolic extracts from extra virgin olive oil (EVOO)	45
Figure 1.8. Process of polyphenol absorption, metabolism, transport, and removal	47
Figure 1.9. Proposed mechanism for ECG influx and efflux through the apical membrane	49
Figure 2.1. Example of villus and crypt measurements acquired in ImageJ	59
Equation 2.1. One-tailed independent sample t-test	60
Equation 2.2. Correlated total cell fluorescence	65
Figure 2.2. Transwell set up for <i>in vitro</i> polyphenol translocation experiment	67
Figure 3.1. Flow cytometry gating strategy for DC and T cell populations	71
Figure 3.2. Neither DC, nor CD103 ⁺ DC, proportions were affected by nutrient deprivation in the defunctioned ileum	73
Figure 3.3. Nutrient deprivation did not affect CD3 ⁺ T cell populations in the defunctioned ileum	74
Figure 3.4. Epithelial physiology in the functional and defunctioned ileum of stoma patients	76
Figure 3.5. DLS did not increase villus height in the defunctioned ileum	77
Figure 3.6. DLS significantly increased crypt depth in the defunctioned ileum	79
Figure 3.7. Apigenin and ferulic acid were detected in the apical and basolatera sides of the transwell epithelial monolayer	
Figure 3.8. Average daily mouse mass was not affected by any treatments	84
Figure 3.9. Food intake was not disrupted in any treatment groups	85
Figure 3.10. Comparison of average organ mass between treatment groups	86

Figure 3.11. Colonic crypt depth following seven days of polyphenol administration
Figure 3.12. Fluorescence imaging of the gastrointestinal tract following
seven days of treatment89
Figure 3.13. Fluorescence imaging of liver following seven days of treatment90
Figure 3.14. Correlated total cell fluorescence for the liver and gastrointestinal organs following treatment
Figure 3.15. Chromatograms from HPLC analysis of liver tissue between Untagged Control and Tagged Control treatments92
List of Tables
Table 1.1. Abundant short chain fatty acids and common species by which they are produced
Table 1.2. FoxP3 ⁺ Tregs and T helper cells are activated by specific CD103 ⁺ /. DC subsets
Table 1.3. Changes in proportions of beneficial and harmful bacteria in the defunctioned ileum following stoma formation
Table 2.1. Tissue processing protocol for human and mouse tissue57
Table 2.2. Contents of each treatment delivered via oral gavage63
Table 2.3. Reverse-phase elution for HPLC analysis of polyphenols in mouse tissue
Table 3.1. Stoma study participant demographics69
Table 3.2. Wavelength optimisation for detection of ferulic acid and apigenin via HPLC
Table 5.1. Cell surface antibody panels used in flow cytometry acquisition107
Table 5.2. Flow cytometry filter panel for Patient BCRG003108
Table 5.3. Flow cytometry filter panel for Patient BCRG004108
Table 5.4. Flow cytometry filter panel for Patient BCRG006109
Table 5.5. Flow cytometry filter panel for Patient BCRG007109
Table 5.6. Flow cytometry filter panel for Patient BCRG018110
Table 5.7. Flow cytometry filter panel for Patient BCRG020110

Table 5.8. Flow cytometry filter panel for Patient BCRG021	111
Table 5.9. Flow cytometry filter panel for Patient BCRG022	111
Table 5.10. Flow cytometry filter panel for Patient BCRG023	112

List of abbreviations

16S rDNA- 16S ribosomal deoxyribonucleic acid
16S rRNA- 16S ribosomal ribonucleic acid
ABC- ATP-binding cassette
AhR- aryl hydrocarbon receptor
APC- antigen-presenting cell
APES- aminopropyltriethoxysilane
AWERB- Animal Welfare and Ethics Review Boards (Lancaster University)
BODIPY- 4,4-difluoro-4-bora-3a,4a-diaza-s-indacene
CAT- catalase
CD103- cluster of differentiation 103
CD11b- cluster of differentiation 11b
CD11c- cluster of differentiation 11c
CD14- cluster of differentiation 14
CD19- cluster of differentiation 19
CD20- cluster of differentiation 20
CD25- cluster of differentiation 25
CD3- cluster of differentiation 3
CD4- cluster of differentiation 4
CD45- cluster of differentiation 45
CD56- cluster of differentiation 56
cDC1- conventional dendritic cell type 1
cDC2- conventional dendritic cell type 2
CFU- colony forming units

COX-2- cyclooxygenase-2
DC- dendritic cell
DLS- distal limb stimulation
DPX- dibutyl phthalate polystyrene xylene
dsDNA- double stranded deoxyribonucleic acid
DSS- dextran sulphate sodium
DTT- dithiothreitol
ECG- epicatchin-3-gallate
EDTA- ethylenediaminetetraacetic acid
EGCG- epigallocatechin gallate
EGF- epidermal growth factor
ELISA- enzyme-linked immunosorbent assay
ENS- enteric nervous system
EVOO- extra virgin olive oil
F:B- Firmicutes : Bacteroidetes
FACS- fluorescence-activated cell sorting
FBS- foetal bovine serum
FITC- fluorescein isothiocyanate
FOS- fructooligosaccharides
FOXP3- Forkhead Box P3
FSC-A- forward scatter- area
FSC-H- forward scatter- height
GALT- gut-associated lymphoid tissue
GF- germ-free
GI- gastrointestinal

GLP-1- glucagon-like peptide-1
GLP-2- glucagon-like peptide-2
GOS- galactooligosaccharides
GPE- grape pomace extract
GSH- glutathione
GTE- green tea extract
GVHD- graft-versus-host disease
HBSS- Hanks' Balanced Salt Solution
HD5- human alpha-defensin 5
HD6- human alpha-defensin 6
HFD- high fat diet
HIV- human immunodeficiency virus
HLA-DR- human leukocyte antigen- DR isotype
HPLC- high performance liquid chromatography
IBD- inflammatory bowel disease
IBS- irritable bowel syndrome
IEC- intestinal epithelial cell
IFN-γ- interferon γ
IgA- immunoglobulin A
IL-10- interleukin 10
IL-12- interleukin 12
IL-1β- interleukin 1β
IL-2- interleukin 2
IL-21- interleukin 21
IL-6- interleukin 6

IL-8- interleukin 8
IL-0- Interteuxin o
IRF4- interferon regulatory factor 4
ISC- intestinal stem cell
IVC- individual ventilated cage
KC-1- CXCL1 (C-X-C motif chemokine ligand 1)
LP- lamina propria
LTH-NHS- Lancashire Teaching Hospital, National Health Service
MCT- monocarboxylate transporter
MEM- minimal essential media
MHC Class II- major histocompatibility complex Class II
MLN- mesenteric lymph node
mRNA- messenger ribonucleic acid
MRP- multidrug resistant protein
MS- metabolic syndrome
MUC2- mucin 2
NE-AA- non-essential amino acids
NK- natural killer cells
NRF2-KEAP1- nuclear factor erythroid 2-related factor 2-Kelch-like ECH-associated protein 1
OATP- organic anion transporting polypeptides
OLE- olive leaf extract
PCNA- proliferating cell nuclear antigen
PNS- painong-san extract
pO₂- partial oxygen pressure
POI- postoperative ileus
PP- Peyer's patch

PUFA- polyunsaturated fatty acids
PYY- peptide YY
Reg3γ- regenerating family member γ
RFU- relative fluorescence units
ROS- reactive oxygen species
SCFA- short chain fatty acid
SIRPα- signal-regulatory protein alpha
SLN- solid lipid nanoparticle
SOD- superoxide dismutase
SPF- specific pathogen-free
sPLA2- secreted phospholipase 2
SSC-A- side scatter- area
SSC-H- side scatter- height
ssDNA- single stranded deoxyribonucleic acid
STAT3- signal transducer and activator of transcription 3
TC- Tagged Control
TGFβR1- transforming growth factor β receptor 1
TGF-β- transforming growth factor $β$
Th1- T helper 1
Th17- T helper 17
Th2- T helper 2
TLR- toll-like receptor
TNF-α- tumour necrosis factor α
TNF-β- tumour necrosis factor β
TP- Tagged Polyphenol

PN- total parenteral nutrition
regs- regulatory T cells
JC- Untagged Control
JP- Untagged Polyphenol
/LP- virus-like particles
Vnt- Wingless-related integration site
(CR1- X-C motif chemokine receptor 1

Abstract

Patients who undergo loop ileostomy surgery experience nutrient deprivation in the distal, defunctioned ileum. As a result, dysbiosis, intestinal atrophy (particularly reduced villus height), and potential immune dysregulation occurs. Following stoma closure (reanastomosis), patients experience high incidence of post-operative morbidity including post-operative ileus (POI) and anastomotic leak. This pilot study consisted of two cohorts; one employed to elucidate the immune environment in the defunctioned ileum and the second to investigate the physiological impacts of distal limb stimulation (DLS). In stoma patients which had not received DLS, immune cell populations (dendritic cells, CD103⁺ dendritic cells, and T cells) were not impacted by long-term nutrient deprivation, so the immunological impacts of DLS were not investigated. Histochemical analysis showed DLS did not reverse villus atrophy in the defunctioned ileum, but crypt depth was significantly increased, suggesting a potential increase in proliferative activity in the crypt base.

Polyphenols, plant secondary metabolites, were considered for future inclusion in DLS due to their anti-inflammatory and prebiotic properties. However, their impact is limited by their poorly elucidated and generally low bioavailability in the small intestine. Solid lipid nanoparticles (SLNs) were tagged to polyphenolic compounds extracted extra virgin olive oil (EVOO) and a murine model was utilised to determine whether SLNs improved polyphenol bioavailability. Initial data from high performance liquid chromatography indicate SLN-tagged polyphenols were not detected in the liver, suggesting polyphenols were not systemic and bioavailability was not improved.

This study has demonstrated an initial mucosal response to DLS, supporting its use prior to reanastomosis, and with a greater duration of DLS and larger cohort, intestinal atrophy may be reversed. At present, it is still unknown whether polyphenols are absorbed in the small intestine, whether they exert their prebiotic abilities on the resident microflora, and whether SLNs impact these events. Therefore, this study is unable to provide sufficient evidence to support the inclusion of polyphenols in DLS.

1. Literature Review

1.1. Overview

Loop ileostomy surgery is required when pathologies of the lower gastrointestinal (GI) tract, such as colon cancer and inflammatory bowel disease (IBD), arise. Surgery results in stoma formation which separates the ileum into two environments either side of the stoma: the proximal, functional ileum and the distal, defunctioned ileum. As waste is released via the stoma, the defunctioned ileum experiences nutrient deprivation, causing microbial dysbiosis, characterised by a reduction in bacterial load and number of beneficial species (Beamish et al., 2023; Lee et al., 2023). This contributes to intestinal atrophy, such as reduced villus height, a decrease in Paneth and goblet cells, and diminished stem cell activity (Beamish et al., 2017; Wieck et al., 2017). Immunological homeostasis, although not thoroughly elucidated in stoma patients, is also suggested to be disrupted by nutrient deprivation.

Loop ileostomy reversal (reanastomosis), which can be performed in approximately 75% of patients, is associated with high morbidity such as post-operative ileus (POI) and anastomotic leak (El-Hussuna et al., 2012). Previous attempts to increase the success of reanastomosis have implemented distal limb stimulation (DLS) (Abrisqueta et al., 2014; Garfinkle et al., 2014), which is proposed to boost the depleted microbiome and restore intestinal homeostasis. However, studies are scarce and have only aimed to reduce post-operative morbidity, not investigate the impact of DLS on the gut microbiome or intestinal physiology.

Dietary polyphenols, plant metabolites praised for their anti-inflammatory and prebiotic properties (Márquez-Flores et al., 2016; Li et al., 2021), have not previously been incorporated into DLS due to their poor bioavailability, particularly in the small intestine (Clifford, 2004). However, intestinal polyphenol absorption may be improved by solid lipid nanoparticles (SLNs), a drug delivery system, previously shown to enhance the bioavailability of other nutraceuticals (Neves et al., 2013). Enhancing the bioavailability of potentially beneficial compounds may improve their suitability for inclusion in DLS, increasing its efficacy.

1.2. The gastrointestinal tract

The gastrointestinal (GI) tract is a collection of organs spanning from the oral cavity to the anal canal, responsible for food digestion and absorption of nutrients. The majority of digestion takes place in the stomach while absorption of nutrients occurs in the small intestine (Cheng et al., 2010). The large intestine (colon) is the site of waste desiccation and compaction as well as water, vitamin, and metabolic ion absorption (Kiela and Gishan, 2016). The small intestine is divided into three sections: the duodenum (most proximal to the stomach), the jejunum, and the ileum (Figure 1.1.).

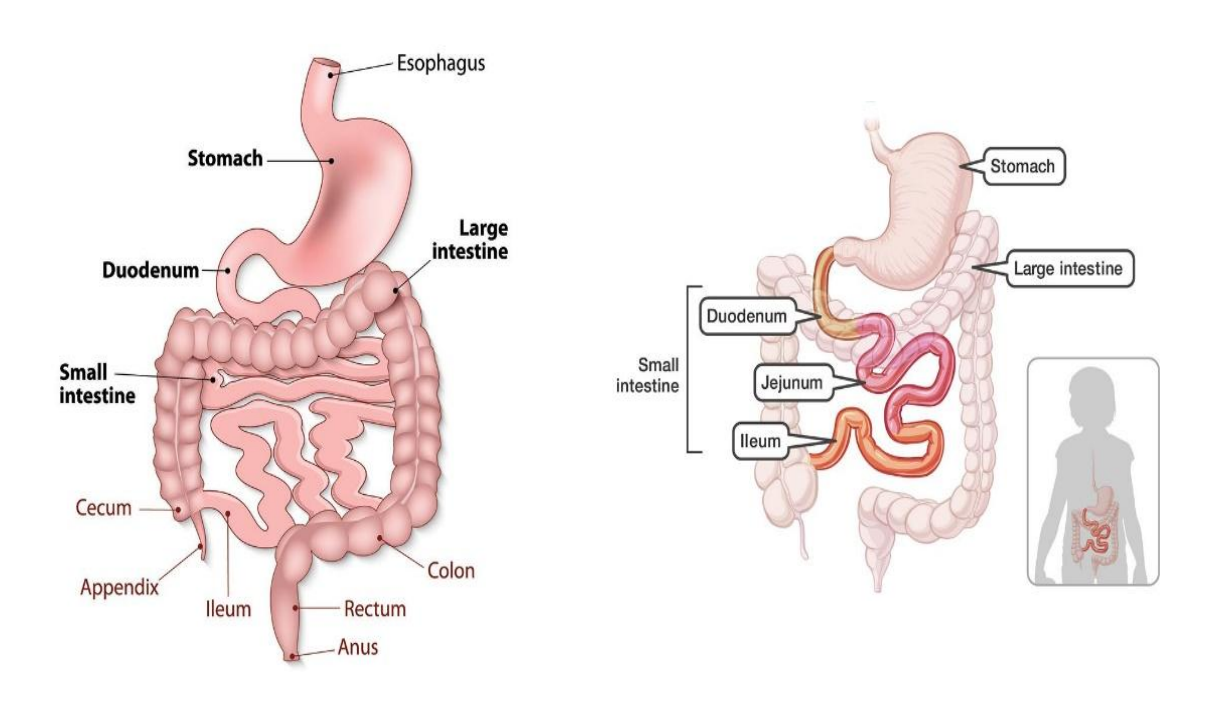


Figure 1.1. Organisation of the gastrointestinal tract from oesophagus to anus (left) and particular focus on the three distinct regions of the small intestine: duodenum, jejunum, and ileum (right) (Palade et al., 2022; AboutKidsHealth.ca).

Small intestinal tissue is composed of several layers, the innermost being the mucosa, made up of a monolayer of intestinal epithelial cells (IECs) also known as enterocytes. The mucosal layer, responsible for nutrient absorption and mucus secretion, importantly forms the barrier between the luminal contents and the underlying tissue.

Distinct features of the mucosa are the villi and crypts (Figure 1.2.). Villi are luminal protrusions mostly composed of enterocytes and are maintained by intestinal stem cells (ISCs) located in the crypt base. When activated, ISCs migrate out of the crypts and differentiate into enterocytes, contributing to villus structure.

ISC activity is regulated by the stem cell niche, a micro-environment which supports the self-renewal and differentiation of ISCs in the crypt base. Paneth cells, also located in the crypt base, maintain the stem cell niche by secreting signals such as Wnt, epidermal growth factor (EGF), and Notch (Bai et al., 2025). Paneth cells also contribute to innate immunity by secreting antimicrobial peptides including α-defensins like HD5 and HD6 which prevent pathogenic invasion (Porter et al., 2002). Goblet cells are also located in the mucosal layer and are essential for preventing infection through production of mucus. This mucus forms a barrier to protect the intestine from toxins and aid the passage of faecal waste along the GI tract. The lamina propria (LP) is the layer situated below the mucosa and, exclusively in the ileum, is the location of Peyer's patches (PPs). These are a collection of lymphoid nodules also involved in intestinal immunity and contain specialised microfold (M) cells which capture and deliver antigens to immune cells (Mabbott et al., 2013). PPs are also connected to mesenteric lymph nodes (MLNs) responsible for activating adaptive immunity.

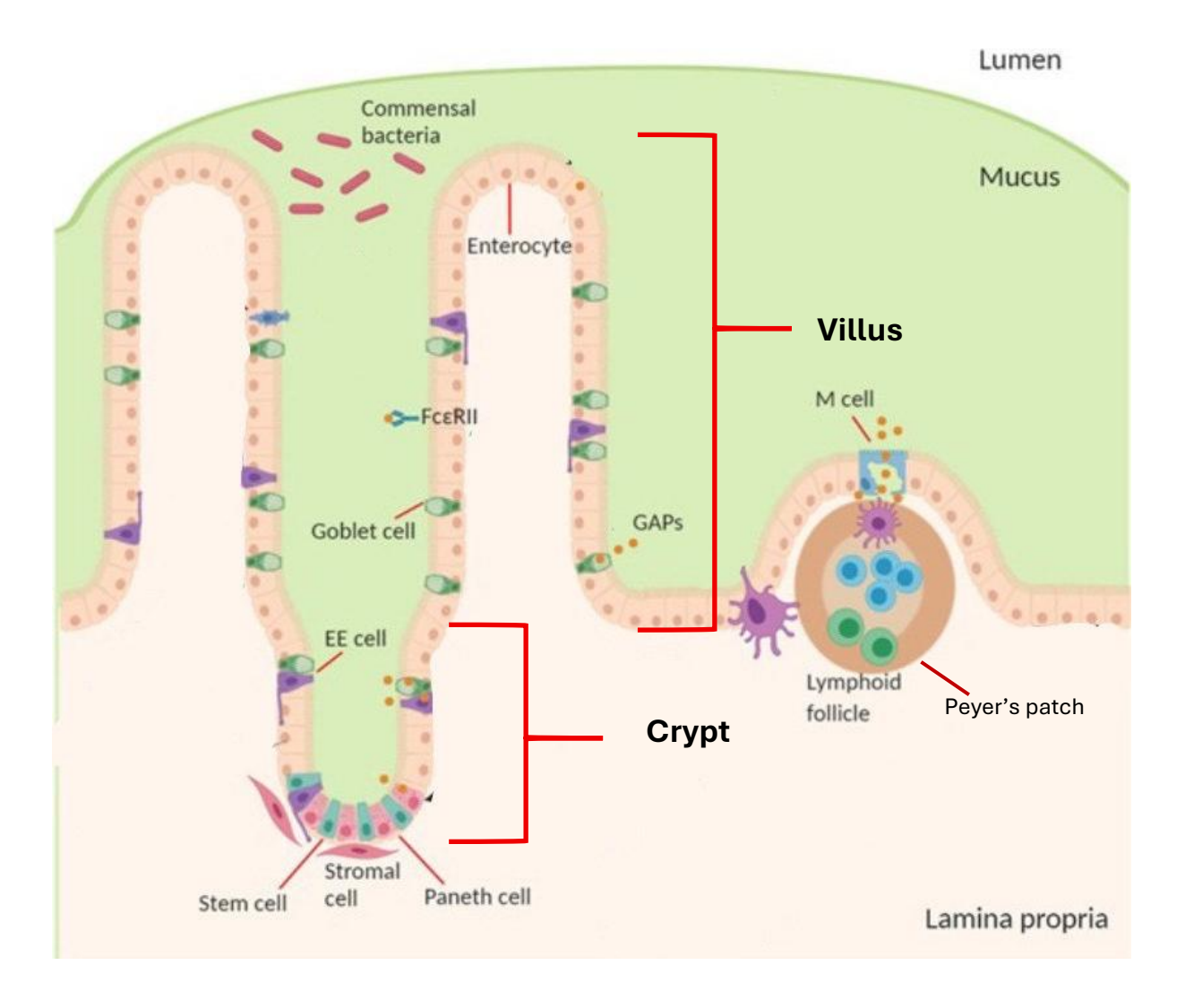


Figure 1.2. Mucosal physiology in the ileum with particular focus on the Paneth and stem cells in the crypt base and differentiated enterocytes which contribute to villus structure (Ali et al., 2020).

1.3. The gut microbiome

The breakdown and absorption of available nutrients in the GI tract is dependent on the resident microflora, comprised of bacteria, fungi, viruses, and archaea. Most of the estimated one hundred trillion microorganisms in and on the body are confined to the lower GI tract (Turnbaugh et al., 2007). A mutualistic relationship exists between the host and the gut (enteric) microbiome; resident microorganisms secrete digestive enzymes required for food metabolism and nutrient absorption by the host and, in

exchange, the microbiota exist in a hospitable environment with all necessary nutrients available. Another benefit from the enteric microbiota is their production of metabolic end-products utilised by host cells (Savage, 1986). These include short chain fatty acids (SCFAs), produced through fermentation of dietary fibres (Topping and Clifton, 2001) involved in modulating intestinal motility, immunity, and gut barrier function (Martin-Gallausiaux et al., 2021) (1.4.2.).

Native microflora also prevents the colonisation and infection of pathogenic microorganisms (Libertucci and Young, 2018); germ-free (GF) mice (which have no established microbiome) were unable to prevent *Campylobacter jejuni* infection whereas conventionally raised mice cleared the pathogen within two days, proving the importance of the microbiome in preventing pathogenic translocation (Bereswill et al., 2011).

1.3.1. Gastrointestinal microbial composition

1.3.1.1. Bacterial composition

Despite similarities in genera and species, an individual's microbial composition is completely unique (Gilbert et al., 2018) as it is determined by multiple factors including diet, age, and genetics (Wen and Duffy, 2017). Indicated in Figure 1.3., the bacterial composition (bacteriome) and bacterial load varies between regions of the GI tract, with the colon having the greatest bacterial density of approximately 10^{12} CFU/ml (Rastall, 2004). In comparison bacterial load in the small intestine increases from approximately 10^{4-5} CFU/ml to 10^{7-8} CFU/ml from the duodenum to the ileum (Kastl Jr et al., 2020). A unique feature of the ileum is its two most abundant phyla are Firmicutes and Actinobacteria rather than Firmicutes and Bacteroidetes which are most abundant in other regions of the GI tract (Villmones et al., 2018). Alterations in bacterial species, even between sections of the small intestine, result from changes in environment including a decrease in oxygen content along the GI tract (Albenberg et al., 2014). Decreasing partial oxygen pressure (pO_2) leads to the highest proportion of obligate anaerobes in the ileum compared to the duodenum and jejunum and an even greater proportion in the colon (Hayashi et al., 2005).

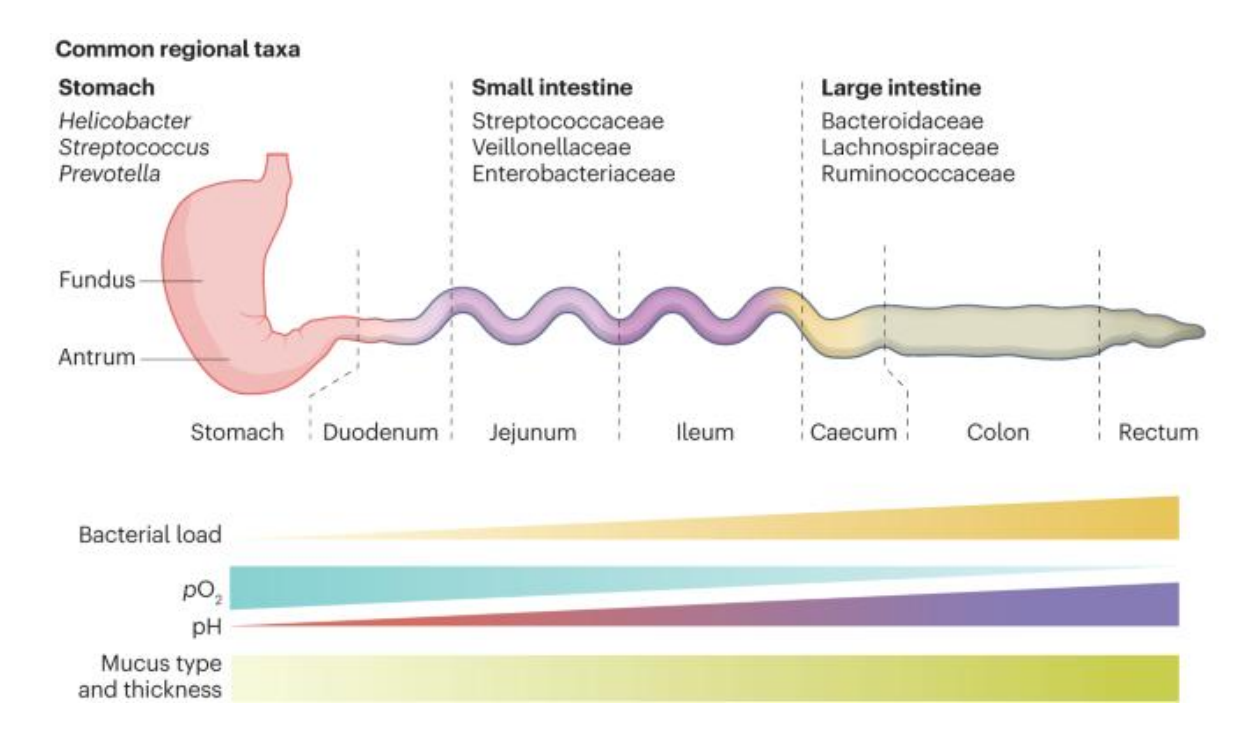


Figure 1.3. Changes in environment and common taxa along the GI tract. While partial oxygen pressure (pO_2) decreases, bacterial load, pH, and mucus thickness increase from stomach to rectum (McCallum and Tropini, 2024).

As previously mentioned, the most abundant phyla in the GI tract are Firmicutes and Bacteroidetes which account for approximately 90% of all bacteria (Eckburg et al., 2005). Many studies examine the ratio between these two phyla (Firmicutes: Bacteroidetes, F:B) to identify changes in microbial composition. Also frequently used to track changes to the microbiome are *Bifidobacteria* (Firmicutes) and *Lactobacillus* (Actinobacteria), beneficial due to their association with immunomodulation and infection prevention (Vlasova et al., 2016).

1.3.1.2. Fungal composition

The fungal populations that exist along the GI tract (mycobiota) only account for approximately 0.1% of the total microbial DNA (Qin et al., 2013) and the composition of

the mycobiome is determined by similar factors as the bacteriome (Mims et al., 2021). Mycobial composition is not thoroughly elucidated but *Ascomycota* and *Basidiomycota* are reported as dominant phyla while abundant genera include yeasts, namely *Saccharomyces*, *Malassezia*, and *Candida* (Nash et al., 2017). Despite their lower abundance, the resident fungi are still important for maintaining gut homeostasis and preventing infection (Pareek et al., 2019; Markey et al., 2018).

1.3.1.3. Viral composition

The gut virome consists of all viruses found within the GI tract, the composition and physiological effect of which is largely unknown. It is estimated there are over 10¹² virus-like particles (VLPs) per adult human, approximately 90% capable of infecting prokaryotes (Shkoporov and Hill, 2019). The composition of the virome is considerably less elucidated than the bacteriome or mycobiome, but the most abundant order and family are reported to be dsDNA *Caudovirales* and ssDNA *Microviridae* respectively (Manrique et al., 2016; Minot et al., 2013). As with bacteria and fungi, the viral composition of the gut is influenced by lifestyle and genetics (Cao et al., 2022) although the function of the virome is generally unknown. However, viruses in the GI tract are proposed to regulate the host's innate and adaptive immune system (Popescu et al., 2021).

1.4. Substrates that influence micobial composition

As previously mentioned, several factors influence gut microbial composition, an important aspect being diet. Different foods have either positive or negative effects on the microbiome, either contributing to microbial homeostasis or leading to an increase in harmful bacteria. Compounds reported to positively influence microbial composition include diet-based probiotics and prebiotics and bacteria-produced SCFAs.

1.4.1. Probiotics

Probiotics are described as "live microorganisms that, when administered in adequate amounts, confer a health benefit on the host" (Hill et al., 2014). Probiotics are reported to improve gut microbial composition by producing antimicrobial agents which suppress and outcompete harmful microbes for attachment (Spinler et al., 2008; O'Shea et al., 2011; Collado et al., 2007). However, probiotics have had disputed success, as studies have shown the enteric microbial composition is unchanged following probiotic intake. For example, several studies have demonstrated that administration of probiotics such as Lactobacillus acidophilus NCFM, Bifidobacterium animalis subsp. lactis Bi-07 (Larsen et al., 2011), and Lactobacillus rhamnosus (Laursen et al., 2017) did not significantly alter the gut microbial compositon. This suggests probiotics are not capable of restoring eubiosis, possibly due to poor attachment and colonisation of the GI tract. Comparitively, administration of Lactobacillus plantarum 299V successfully reduced inflammatory bowel disease (IBD)related symptoms, such as abdominal pain and stool inconsistency (Niedzielin et al., 2001) and administration of probiotics to colorectal cancer patients increased transepithelial resistance and enhanced mucosal tight junction protein expression (Liu et al., 2011). Therefore, despite limited evidence to support their influence on the microbiome, probiotics may improve intestinal barrier integrity in pathology models which experience dysbiosis (Hemarajata and Versalovic, 2013).

1.4.2. Short chain fatty acids

Short chain fatty acids (SCFAs), most abundantly butyrate, propionate, and acetate are produced by beneficial gut bacteria through anaerobic fermentation of non-digestible dietary residues. This is most commonly performed by colonic bacteria (Table 1.1.), with lesser amounts produced in the small intestine. SCFAs are capable of lowering colonic pH (Cummings et al., 1987), creating a more favourable environment for SCFA-producing bacteria like *Roseburia spp.* and *Faecalibacterium prausnitzii* (Walker et al., 2005) and preventing the overgrowth of harmful bacteria such as *Escherichia coli*

(Wolin, 1969). This creates a virtuous cycle of greater SCFA production and greater abundance of beneficial bacteria, improving the intestinal environment.

As well as influencing microbial composition, SCFAs also maintain gut barrier integrity (Kelly et al., 2015; Peng et al., 2009) and influence host metabolism and immunity (Vinolo et al., 2011). In particular, butyrate reduces the number of pro-inflammatory dendritic cells (DCs) (Andrusaite et al., 2024) and other SCFAs have been shown to regulate pro- and anti-inflammatory T cell responses (Park et al., 2015; Zhou et al., 2018). Additionally, SCFAs decrease pro-inflammatory cytokine expression such as TNF-α and boost metabolism by increasing levels of Peptide YY (PYY) and glucagon-like peptide-1 (GLP-1) (Freeland and Wolever, 2010).

Table 1.1. Abundant short chain fatty acids and common species by which they are produced.

Short-chain fatty acid	Known bacterial producers	Reference
Butyrate	 Ruminococcus bromii Eubacterium rectale Eubacterium hallii Coprococcus catus Faecalibacterium prausnitzii Clostridium butyricum 	(Rb) Sasaki et al., 2022 (Er) Rivière et al., 2016 (Eh) Duncan et al., 2004 (Cc) Holderman and Moor, 1974 (Fp) Zhou et al., 2018 (Cb) Stoeva et al., 2021
Propionate	 Akkermansai muciniphula Bacteroides thetaiotaomicron Veillonella parvula Coprococcus catus Lactobacillus plantarum 	(Ak) Derrien et al., 2004 (Cc) Reichardt et al., 2014 (Bt) Wrzosek et al., 2013 (Vp) Ng and Hamilton, 1971 (Lp) Hong et al., 2021
Acetate	 Prevotella spp. Streptococcus spp. Bacteroides spp. Bifidobacterium spp. Clostridium spp. Blautia hydrogenotrophica 	(Bh) Wang et al., 2023 (C spp.) Guo et al., 2020 (Bi spp.) Fukuda et al., 2012 (Ba spp.) Horvath et al., 2022 (S spp.) Tagaino et al., 2019 (P spp.) Hosmer et al., 2024

1.4.3. Prebiotics

A separate category of substrates proven to alter intestinal microbial composition are prebiotics, compounds metabolised by the gut microbiome, improving its composition and activity. There is a broad spectrum of prebiotics (Figure 1.4.) and their ability to improve the gut microbiome in turn confers beneficial physiological effects to the host (Bindels et al., 2015).

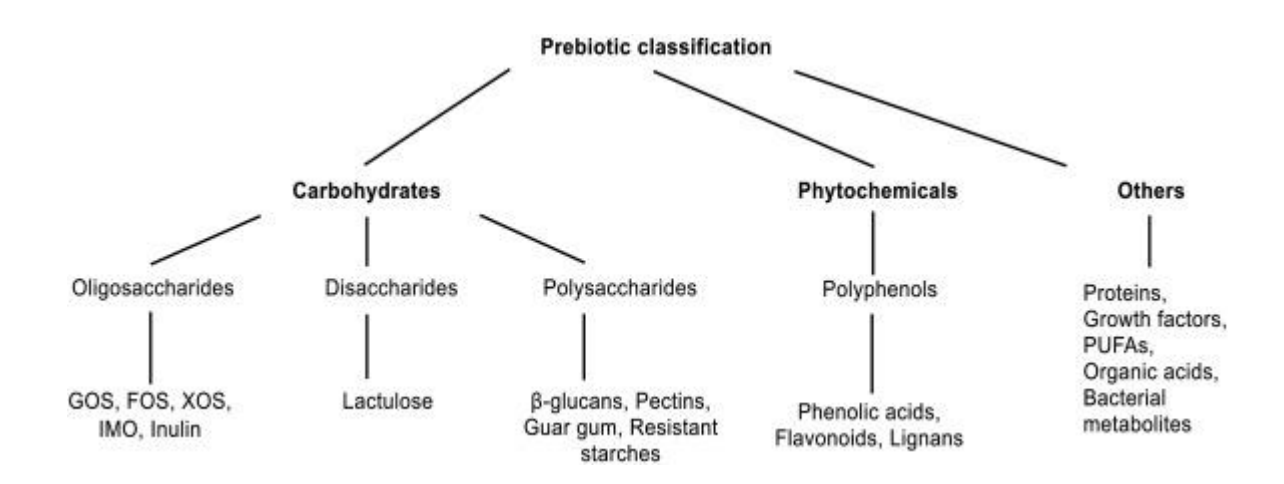


Figure 1.4. Classes and subclasses of prebiotics (Hurtado-Romero et al., 2020).

There is substantial evidence supporting the ability of prebiotics to change microbial populations; Jerusalem artichoke-derived inulin (Ramnani et al., 2010), the dietary fibre, gum Arabic (Calame et al., 2008), and fructooligosaccharides (FOS) (Tandon et al., 2019) increased the abundance of beneficial genera, *Bifidobacteria* and *Lactobacillus*. Additionally, wheat dextrin consumption decreased the abundance of harmful *Clostridium* and increased the abundance of beneficial *Bacteroides* (Lefranc-Millot et al., 2012). As well as directly influencing bacterial populations, prebiotic components of chicory root extract including inulin, sesquiterpene lactones, and FOS correlated to an increase in SCFA levels (Baxter et al., 2019) and a decrease in pro-inflammatory TNF-α, IL-1β, and IL-8 expression (Pouille et al., 2022).

Similarly to probiotics, prebiotics can reduce the severity of certain diseases; administration of galactooligosaccharides (GOS) to IBS patients increased *Bifidobacteria* abundance as well as reducing IBS-associated side effects like bloating, stool inconsistency, and flatulence (Silk et al., 2009). Prebiotics, namely dietary fibres, can also prevent infection by increasing GI mucin production, reducing the risk of pathogenic translocation through the mucosa (Satchithanandam et al., 1990).

1.4.3.1. Polyphenols

A sub-class of prebiotics are polyphenols; a group of over 8000 compounds defined as plant secondary metabolites which can be divided into four broad categories (Figure 1.5.) (Wang et al., 2022).

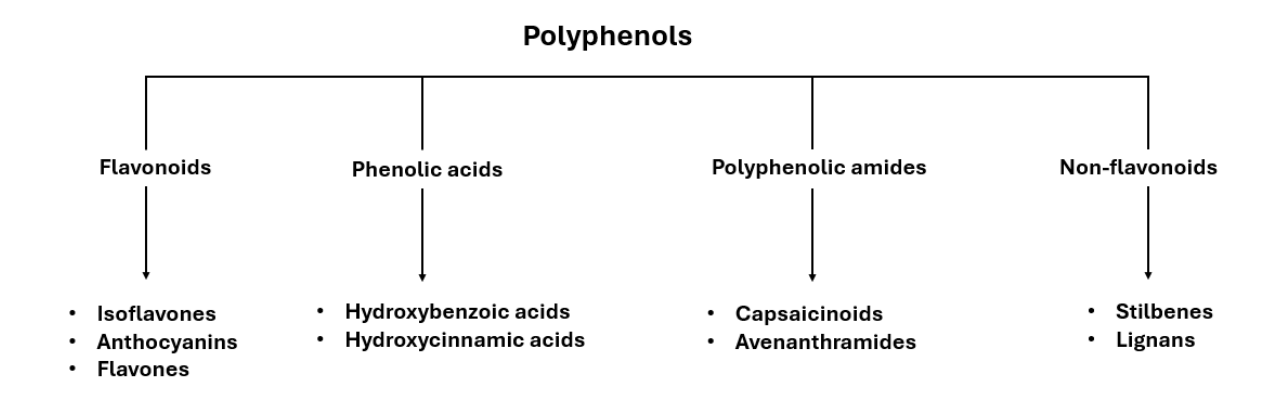


Figure 1.5. The four main groups (and sub-groups) of dietary polyphenols.

Numerous studies have demonstrated the ability of polyphenols to influence the gut microbial composition, suggesting they possess prebiotics properties. Multiple polyphenols have increased the abundance of gut barrier protectors, *Lactobacillus*, *Bifidobacteria*, and *Bacteroides* and decreased the abundance of harmful bacteria such as *Clostridium spp*. (Molan et al., 2014; Liu et al., 2014; Wang et al., 2020).

SCFA-producing bacteria were also increased following polyphenol consumption such as $Faecalibacterium\ prausnitzii$ and Roseburia (Moreno-Indias et al., 2016). This increased SCFA production corresponded to reduced inflammation, indicating polyphenols influence the intestinal environment (Xu et al., 2022). Polyphenol consumption also decreased β -glucuronidase activity, a bacterial enzyme associated with increased risk of colorectal cancer, suggesting microbial activity is also affected by polyphenols (Jurgoński et al., 2014).

1.5. Enteric bacteria and intestinal barrier function and repair

The importance of the gut microbiome in maintenance of intestinal epithelial barrier function has been demonstrated and, additionally, how a disrupted gut microbiome leads to impaired barrier function and diminishes damage repair. A large proportion of intestinal cell types are mediated by the gut microbiota, particularly enteric bacteria; for example, the gut microbiome mediates goblet cell differentiation in intestinal crypts through TLR (toll-like receptor) signalling (Engevick et al., 2019). Goblet cells and IECs are also indirectly controlled by the gut microbiota; IL-10, which influences goblet cell differentiation and IEC proliferation is upregulated by gut bacteria-produced indole, acting upon the xenobiotic aryl hydrocarbon receptor (AhR) (Powell et al., 2020).

GF mouse models have demonstrated the involvement of enteric bacteria in gut barrier function. Colonisation of GF mice with *Bacteroides thetaiotaomicron* proved its involvement in nutrient absorption, mucosal barrier fortification, and angiogenesis (Hooper et al., 2001). Although Paneth cell differentiation can occur independently of microbial stimuli (Putsep et al., 2000), enteric microbiota can induce their activity, such as increase expression of antimicrobial peptide, Reg3y (Schoenborn et al., 2019). Paneth cell activity can also be triggered by the MyD88-dependent TLR pathway, activated by the gut microbiome (Cheng et al., 2019). Additionally, GF mice experience a reduction in Paneth cell numbers (Schoenborn et al., 2018) suggested to result from reduced intestinal turnover (Hassan et al., 2023). Furthermore, intestinal motility is regulated by bacteria-produced SCFAs via serotonin production (Buey et al., 2023) and

enteric nervous system (ENS) development, which controls gut motor and sensory function, is also mediated by the gut microbiome (Collins et al., 2014).

1.5.1. Dysbiosis hinders damage repair

Disruption to the enteric microbial composition (gut dysbiosis) can be characterised by an increase in harmful bacteria, a reduction in beneficial bacteria, or a reduction in total bacterial load. Stress and lack of sleep or changes in lifestyle or diet can cause dysbiosis (Madison and Kiecolt-Glaser, 2019; Sun et al., 2023). For example, increased fat consumption increases the abundance of *Erysipelotrichales*, *Bacilli*, and *Clostridiales* which can detrimentally raise the F:B ratio (Velasquez., 2018). Antibiotic treatments can also cause dysbiosis by reducing microbial diversity and abundance of beneficial bacteria which contributes to intestinal permeability (Palleja et al., 2018).

During dysbiosis, intestinal barrier physiology cannot be maintained, and damage repair mechanisms are diminished. GF mice took significantly longer to recover from dextran sodium sulphate (DSS)-induced damage compared to partially colonised specific pathogen-free (SPF) mice (Zhan et al., 2013). Additionally, antibiotic-treated mice were more susceptible to DSS damage compared to fully colonised mice (Hernández-Chirlaque et al., 2016) and halting antibiotic treatment and restoring a healthy gut microbiome improved mucosal repair mechanisms (Rakoff-Nahoum et al., 2004).

Via TLR signalling, the gut microbiome influences mucosal repair through activation of IL-6, TNF, and KC-1 release. This activation was diminished in GF mice which experienced greater haemorrhage, epithelial injury, and mortality due to a weakened intestinal barrier (Hernández-Chirlaque et al., 2016). The hindered colonic damage repair observed in GF mice was also associated with a reduction in epithelial proliferation, indicating the gut microbiome influences intestinal proliferative activity (Pull et al., 2005). Intestinal weight and length were also reduced in GF mice, further supporting the association of enteric bacteria with proliferative activity. Additionally, angiogenesis, the process of vasculature formation, was also arrested in GF mice and

forty-nine angiogenesis-associated genes were downregulated, leading to a decline in villus microvasculature (Stappenbeck et al., 2002; Romero et al., 2022). This gives further evidence that effective intestinal barrier integrity is reliant on eubiosis.

Several diseases have been associated with bacterial dysbiosis, including the inflammatory bowel diseases, Crohn's disease and ulcerative colitis (Tamboli et al., 2003) and other inflammatory diseases like rheumatoid arthritis (Zhang et al., 2015) and atherosclerosis (Karlsson et al., 2012). Other pathologies include polycystic ovary syndrome and type II diabetes mellitus (Duan et al., 2021) and there is also a correlation between gut dysbiosis and depression and anxiety (Naseribafrouei et al., 2014; Carabotti et al., 2015).

1.6. Gastrointestinal Immunity

Intestinal immunity is extremely important and expansive, with approximately 70% of total immune cells located in the gut-associated lymphoid tissue (GALT) (Vighi et al., 2008). The primary role of the GALT is to prevent pathogenic infection whilst maintaining tolerance towards resident microorganisms, preventing unnecessary immune responses (autoimmunity) as well as supporting immune cell development. Intestinal immunity also maintains gut barrier function by influencing IEC proliferation and differentiation (Soderholm and Pedicord, 2019). Immune populations and the gut microbiota interact with each other to maintain homeostasis and preserve intestinal barrier integrity.

1.6.1. Innate intestinal immunity

There are two branches of the immune system: innate and adaptive immunity. Innate, or 'non-specific' immunity, is the first line of defence against infection and encompasses immune cells such as macrophages, neutrophils, and DCs. Many innate immune cells are phagocytic antigen presenting cells (APCs), recognising, engulfing, and digesting foreign material then displaying the pathogen's antigens to activate adaptive immune cells (Martins et al., 2023). Enterocyte-produced antimicrobial

peptides including defensins, Reg3γ, and cathelicidins are also an essential element of innate immunity in the GI tract by either killing pathogens or promoting their clearance (Zong et al., 2020; Vaishnava et al., 2011). Immunoglobulin A (IgA), an antibody produced by adaptive immune cells is also involved in innate immunity by binding to pathogens and preventing adherence to the mucosa.

1.6.1.1. Dendritic cells

DCs are bone-marrow-derived APCs that exist in several layers of the small intestine, including the mucosa, LP (Mayrhofer et al., 1983) (particularly in PPs (Kelsall and Strober, 1996)), and the MLNs. Depending on the organ, intestinal DCs represent between 1-5% of tissue cells (Merad et al., 2013) and have important roles in connecting innate and adaptive immunity and maintaining intestinal homeostasis. DCs are of particular interest as different subsets are involved in either protection against pathogens or tolerance towards commensal bacteria (Fucikova et al., 2019). All DCs constitutively express surface markers including MHC Class II (also known as HLA-DR), CD11c, and CD45 (Inaba et al., 1992) but can be separated into distinct subsets, categorised by their expression of surface proteins CD103 and CD11b.

1.6.1.1.1. CD103⁺/₋ DC subsets

Conventional DC1 (cDC1) are a CD103⁺ CD11b⁻ subset whereas cDC2 are primarily CD103⁺ CD11b⁺ with an additional population of CD103⁻ CD11b⁺ DCs. cDC1 can also be identified by XCR1 (X-C motif chemokine receptor 1) expression whereas cDC2 express SIRPα (signal-regulatory protein alpha) (Gurka et al., 2015). Of the cDCs that reside in the LP prior to migration to MLNs, approximately 64% are CD103⁺ (Johansson-Lindbom et al., 2005) but cDC populations vary along the GI tract. In the small intestine and associated MLNs, cDC1 are most abundant whereas in the colon and associated MLNs, cDC2 are most abundant (Houston et al., 2016). cDCs are responsible for eliciting both tolerogenic and inflammatory responses by activating the adaptive immune response (Table 1.2.).

1.6.2. Adaptive intestinal immunity

Also known as acquired or specific immunity, and contrastingly to the nonspecific activity of innate immune cells, specific antigens on pathogens are identified by adaptive immune cells (Ahuja, 2008). T and B lymphocytes are immune cells involved in adaptive immunity; B cells elicit a humoral immune response by interacting with a pathogenic antigen, causing the synthesis and secretion of immunoglobulins including IgA which neutralize the pathogen (Alberts et al., 2002). T cells are involved in cell-mediated immune responses; specifically, helper T (Th) cells are stimulated by APCs, allowing activation and expansion of cytotoxic T cells, launching a sufficient immune response. Adaptive immunity also ensures lifelong protection from pathogens via memory T cells.

T cells are either pro- or anti-inflammatory, depending on their function and the type of T cell that is activated is dependent on which immune response is required. For example, regulatory T cells (Tregs) are activated for intestinal tolerance towards commensal microorganisms to prevent autoimmunity and chronic inflammation (Sakaguchi et al., 2001). All Tregs are suppressive to autoimmunity as well as helping the immune system control its response to foreign antigens. The FoxP3⁺ subset of Tregs additionally has the capacity to suppress the activity of other immune cells, contributing to immune homeostasis (Gavin et al., 2007). Oppositely to the anti-inflammatory activity of Tregs, under pathogenic invasion, helper T cells like Th1 and Th17 release proinflammatory cytokines like IFN-γ, IL-2, and TNF-β to activate cytotoxic T cells capable of killing pathogens (Sallusto et al., 1998).

1.6.2.1. T cell activation by CD103⁺/₋DC subsets

Different CD103⁺/- DC subsets are responsible for the activation of the appropriate T cell type, depending on the required immune response. DCs migrate from the LP to the MLNs where immature T cells are activated (Shiokawa et al., 2017). To launch an anti-inflammatory response, CD103⁺ CD11b⁻ (cDC1) and CD103⁺ and CD11b⁺ (cDC2) DCs activate Tregs (Welty et al., 2013; Bain et al., 2017); DCs express aldhla1 (Coombes et al., 2007), a retinal dehydrogenase involved in conversion of retinal (from Vitamin A) to

retinoic acid (RA) needed for FoxP3⁺ Treg migration to the LP. FoxP3⁺ Treg migration is also reliant on TGF- β (Chen et al., 2003), activated by the expression of $\alpha V\beta 8$, ltbp3 and plat by CD103⁺ DC subsets (Worthington et al., 2011; Siddiqui and Powrie, 2008; Annes et al., 2003).

To launch a pro-inflammatory response, Th1 and Th17 cells are activated. Th1 is activated by both cDC subsets (Liang et al., 2016; Luda et al., 2016) whereas Th17 is solely activated by the cDC2 subset and is reliant on IL-6 and interferon regulatory factor 4 (IRF4) production (Persson et al., 2013). Another helper T cell is Th2, which is primarily activated by cDC2 and protects against parasitic infection (Redpath et al., 2018). Th2 cells are anti-inflammatory and produce cytokines such as IL-4 and IL-21, which inhibit Th1 activation, and IL-10, which inhibits the release of pro-inflammatory cytokines from Th1 cells (Wurster et al., 2002; Fiorentino et al., 1991). While they are activated by the cDC2 subset, Th2 cells can also be suppressed by cDC1 through their constitutive expression of IL-12 (Everts et al., 2016). The subset of cDC1 that performs this differs between the small intestine (CD103+ CD11b+) and colon (CD103- CD11b+) (Mayer et al., 2017).

Table 1.2. FoxP3⁺ Tregs and T helper cells are activated by specific CD103⁺/. DC subsets.

	cDC1	cDC2	
	CD103⁺ CD11b⁻	CD103 ⁺ CD11b ⁺	CD103 ⁻ CD11b ⁺
(FoxP3 ⁺) Tregs	~	~	×
Th1	~	~	~
Th2	×	✓	✓
Th17	×	~	~

1.7. Nutrient deprivation disrupts the microbial composition and intestinal physiology

Nutrient deprivation occurs when the faecal stream is ceased, preventing luminal stimulation in the GI tract. Nutrient deprivation models, discussed below, experience physiological and immunological changes, which studies propose are caused by the disruption of the intestinal microbial composition experienced in these models.

1.7.1. Total Parenteral Nutrition

An example of nutrient deprivation is total parenteral nutrition (TPN) which eliminates the faecal stream from the intestine as the patient receives all necessary nutrients intravenously. Dysbiosis associated with TPN is characterised by a reduction in Firmicutes and an increase in Bacteroidetes and Proteobacteria (Heneghan et al., 2014). In rodent studies, the physiological changes caused by TPN have been highlighted, for example, a reduction in ileal Paneth cell activity and a concomitant decrease in antimicrobial proteins such as Reg3 γ and cryptdin-4. Other physiological changes include intestinal atrophy, characterised by a reduction in ileal thickness and villus height (Chance et al., 1998). This atrophy was associated with a decrease in gut barrier and immune function (Alverdy and Burk, 1992; Alverdy et al., 1985) causing an increase in potential bacterial translocation across the gut wall (Alverdy et al., 1988). TPN also caused a 46% reduction in enterocyte proliferation rate, a three-fold increase in enterocyte apoptosis, and a 3.5-fold increase in pro-inflammatory IFN- γ expression (Yang et al., 2003).

TPN-induced physiological changes have also been demonstrated in human studies, namely a reduction in jejunal villus height and area and a decrease in crypt depth (Feng et al., 2009). Although villus and crypt reductions were not significant in the ileum, ileal tissue mass and protein content were reduced following TPN (Kansagra et al., 2003). This atrophy and decline in epithelial barrier function has been proven to result from a decrease in growth factors, diminishing proliferative activity and increasing apoptosis (Demehri et al., 2013).

TPN also causes many immunological changes in the intestine, particularly disruption to the GALT, leading to the upregulation of pro-inflammatory cytokines such as IFN-γ and TNF-α (Yang et al., 2008). This upregulation increases intestinal inflammation, eventually resulting in mucosal atrophy, characterised by a reduction in IEC proliferation and increase in apoptosis (Wildhaber et al., 2002). TPN is also detrimental to cell recruitment, decreasing lymphocyte populations in the GALT which decreases IgA levels (King et al., 1997). A reduction in IgA decreases antimicrobial production, and levels of antimicrobial signals such as secretory phospholipase A2 (sPLA2) from Paneth cells and MUC2 from goblet cells are decreased (Heneghan et al., 2014). Lower IgA also dampens adaptive immune cell activation as IgA is involved in immune tolerance (Patel and Jialal, 2023). PPs also experience atrophy, leading to decreased mucosal lymphocyte activation (Nakasaki et al., 1996). These alterations to intestinal physiology and immunity are associated with shifts in enteric microbial composition, namely an increase in Gram-negative Proteobacteria associated with increased expression of proinflammatory cytokines and inflammation (Mukhopadhya et al., 2012).

1.7.2. Loop ileostomy and loop ileostomy reversal

Loop ileostomy is a surgery required under certain pathologies of the lower GI tract such as colon cancer and IBD (Banaszkiewicz et al., 2015; Estrada et al., 2021). Patients are left with a stoma (Figure 1.6.A.) which diverts faecal waste through the abdominal wall, preventing it passing through the terminal section of the small intestine and the colon (Beamish et al., 2017). Therefore, the distal, defunctioned ileum experiences nutrient deprivation.

When the lower GI tract has healed (typically after approximately six to twelve months), patients can undergo reversal surgery (reanastomosis). This involves reattaching the proximal (functional) and defunctioned sections of the ileum (Figure 1.5.B) and pushing it back through the abdominal wall. Reanastomosis is possible in approximately 75% of patients, however, approximately 25% (some reports as high as 40% (Beamish et al., 2023)) of cases experience post-operative morbidity such as temporary bowel paralysis

(ileus), anastomotic leak into the abdominal cavity, and infection (El-Hussuna et al., 2012).

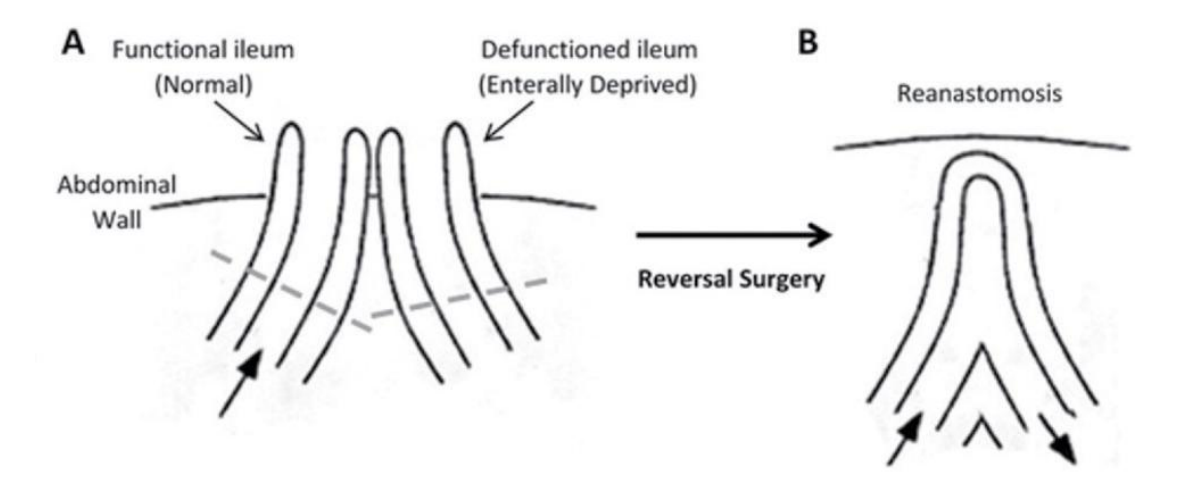


Figure 1.6. Process of loop ileostomy reversal surgery: (A)- diversion of faecal stream (stoma), (B)- reconnected ileum following reversal surgery (reanastomosis) (Beamish et al., 2017).

1.7.2.1. Altered physiology in the defunctioned ileum

Diversion of the faecal stream detrimentally alters the intestinal physiology, particularly in the mucosal layer. Healthy small intestinal mucosa is characterised by long villi and shallow crypts, but intestinal damage and inflammation is associated with shorter villi and deeper crypts (Ducatelle et al., 2018). Nutrient deprivation in the defunctioned ileum causes a reduction of villus height as well as reduced proliferation, contributing to ileal atrophy characterised by a reduction in villus height (Beamish et al., 2017). Unlike in TPN patients which experience an increase in apoptosis, the reduction in villus height in the defunctioned ileum was suggested to result solely from halted epithelial proliferation possibly due to a decline in pro-proliferative microbial-produced signals (Beamish et al., 2017). The defunctioned ileum also experiences a loss of both circular and longitudinal smooth muscle, reduced isometric contractility (Williams et al., 2007), and reduced intestinal motility (Burghgraef et al., 2020; Huang et al., 2017).

Goblet cells and Paneth cells both saw a mean reduction in the defunctioned ileum (Watanabe et al., 2022; Wieck et al., 2017) which may contribute to mechanical and immunological dysregulation.

1.7.2.2. Dysbiosis in the defunctioned ileum

In addition to changes to intestinal physiology, microbial composition in the defunctioned ileum is also disrupted. Ileostomy caused a reduction in microbial complexity and proportions of beneficial bacteria whilst increasing the abundance of harmful bacteria in the defunctioned ileum (Table 1.3.) (Lee et al., 2023). A reduction in microbial diversity and abundance has been proposed (Sakai et al., 2022) however, another study did not find a reduction in species diversity, only a reduction in bacterial load by approximately 64% (Beamish et al., 2023; Beamish et al., 2017). Additionally, Beamish et al., 2023 reported that patients with a greater decrease in bacterial load in the defunctioned ileum experienced a higher incidence of post-operative morbidity, highlighting the importance of the gut microbiome in maintaining intestinal homeostasis.

SCFA levels were also reduced in the defunctioned ileum (Sakai et al., 2022), expected to be detrimental to intestinal barrier integrity and immunity which are influenced by SCFAs (Martin-Gallausiaux et al., 2021). Additionally, an increase in oxygen content in the defunctioned ileum resulted in a switch from obligate anaerobes (predominantly *Bacteroides* and *Clostridia*) to facultative anaerobes (most abundantly *Lactobacilli* and *Enterobacteria*) (Hartman et al., 2009).

Table 1.3. Changes in proportions of beneficial and harmful bacteria in the defunctioned ileum following stoma formation. Loop ileostomy causes an increase in harmful bacteria and a decrease in beneficial bacteria (Lee et al., 2023).

Bacterial genus	Beneficial or Harmful	Control proportion (%)	lleostomy proportion (%)
Lachnospiraceae	Beneficial	29.9	3.8
Ruminococcaceae	Beneficial	18.4	0.6
Blautia	Beneficial	9.1	0.1
Faecalibacterium	Beneficial	7.5	0.2
Proteobacteria	Harmful	5.1	17.9
Clostridium	Harmful	1.1	16.2
Streptococcus	Harmful	1.6	17.7

1.7.2.3. Intestinal atrophy is associated with dysbiosis

Intestinal atrophy in ileostomy patients has previously been attributed to reductions in bacterial load and diversity (Williams et al., 2007; Lapthorne et al., 2013). As previously discussed (1.5.), the gut microbiome is essential for intestial barrier function and repair, demonstrated by GF and TPN models. The absence of an established microbiome results in a reduction in goblet cell abundance (Yousefi et al., 2025) and Paneth cell numbers (Schoenborn et al., 2018), changes which are also observed in the defunctioned ileum (Watanabe et al., 2022; Wieck et al., 2017). Mucosal atrophy such as reduced villus height is observed in both TPN and ileostomy patients (Feng et al., 2009; Beamish et al., 2017) supporting the association of intestinal atrophy with dysbiosis. Therefore, the alterered intestinal physiology and post-operative

complications associated with reanastomosis can be attributed to dysbiosis in the defunctioned ileum and restoring eubiosis may reverse intestinal atrophy.

1.7.2.4. Possible immune dysregulation in the defunctioned ileum

The impacts of ileostomy on physiology and microbial composition are vastly more investigated than the immunological state of the defunctioned ileum. The studies that have compared immune cell populations between the functional and defunctioned ileum are limited and have solely focused on adaptive immune cells. Some studies witnessed a decline in T cell populations (Watanabe et al., 2022; Li et al., 2022) whereas others did not (Turki et al., 2019). None of these studies have investigated innate immune cell populations and give limited insight into the potential immune dysregulation in the defunctioned ileum. Other nutrient deprivation models have experienced changes in immune cell activity (Yang et al., 2008; King et al., 1997) so this is also likely experienced by stoma patients.

1.8. Distal limb stimulation

Previous studies have demonstrated that restimulation following nutrient deprivation has contributed to the reversal of intestinal atrophy and immune dysregulation; stimulation with enteral feeding in TPN rodent models increased villus height and gut weight (Mukau et al., 1994) and swiftly restored lymphocyte numbers in the GALT (Janu et al., 1997). Distal limb stimulation (DLS) describes the process of pre-operatively stimulating the defunctioned ileum of ileostomy patients prior to reanastomosis to improve intestinal barrier integrity (Blanco et al., 2023). DLS can range from saline solutions, prebiotic suspensions, or faecal recycling and aims to reduce post-operative morbidity.

There have been few attempts to reverse this atrophy and reduce related complications and the mechanistic effects of DLS are poorly elucidated. Early studies, such as Wong et al., 2004, demonstrated DLS was a safe practice and, injection of proximal effluents in to the defunctioned ileum (faecal recycling) decreased post-operative complications

like anastomotic leakage (Lau et al., 2016). However, not all studies yielded success, as DLS with succus entericus (intestinal juice) did not reduce post-operative ileus (POI) incidence (Liu et al., 2021).

The gut microbiome contributes to intestinal barrier function, and the decrease in epithelial proliferation in the defunctioned ileum is suggested to be caused by a decline in pro-proliferative microbial signals (Beamish et al., 2017). Therefore, restoration of the ileal microbiome has been of particular interest in recent DLS studies which have utilised either probiotics or prebiotics to reverse dysbiosis. These studies hypothesise that restoring eubiosis prior to reanastomosis will reverse intestinal atrophy and improve gut barrier function, reducing post-operative morbidity.

One study introduced a probiotic cocktail containing *Lactobacillus*, *Bifidobacterium*, and *Streptococcus* strains into the defunctioned ileum (Rodríguez-Padilla et al., 2021) but did not find a significant reduction in POI incidence compared to control groups and oral tolerance and hospital stay also did not differ. This could suggest probiotics are unable to restore eubiosis; as previously mentioned (1.4.1.), the ability for probiotics to influence microbial composition is disputed so administration is unlikely to reverse intestinal atrophy or reduce post-operative morbidity.

Alternatively, two studies assessed the impact of prebiotic DLS prior to reanastomosis, utilising a prebiotic suspension of saline and thickening agent (Nestle® Thicken-up®) (Abrisqueta et al., 2014; Garfinkle et al., 2023). Although microbial populations were not investigated, POI incidence was significantly lower in both studies as well as shorter hospital stay and return to oral tolerance. These studies may support the use of prebiotics over probiotics to reduce post-operative complications as their ability to reverse dysbiosis has been proven (Ramnani et al., 2010). A separate study implemented faecal recycling as DLS for fifteen days prior to reanastomosis also significantly reduced POI incidence as well as shorter time to restoration of bowel function and shorter time to tolerance of liquids (Ocaña et al., 2022). Additionally, the inclusion of SCFAs in DLS has also reduced post-operative morbidity, namely a reduction in hospital stay duration (Fernández López et al., 2019).

Unfortunately, previous prebiotic studies have only examined morbidity incidence and not investigated the impact of DLS on the microbial composition or mucosal physiology (Dilke et al., 2020). However, a murine study reversed mucosal atrophy by injecting discharged stool from the functional ileum into the defunctioned ileum. This faecal recycling increased the ratio of defunctioned vs functional villous height (0.81 control, 0.97 after DLS) supporting the hypothesis that DLS restores intestinal physiology (Uga et al., 2021). Additionally, DLS increased proliferating cell nuclear antigen (PCNA) expression, suggesting a restoration in proliferative activity and potential reversal of atrophy (Zhu et al., 2011). Therefore, the reduced incidence of post-operative morbidity observed in human DLS studies are likely attributed to a reversal in mucosal atrophy and restoration of intestinal barrier integrity. The success of prebiotic studies indicates that targeting the microbiome is essential for reversing intestinal atrophy, although this can only be hypothesised.

1.9. Polyphenols: a proposed addition to DLS

As previously mentioned (1.4.3.1), polyphenols are plant secondary metabolites known to have anti-inflammatory, anti-cancer and, importantly, prebiotic abilities.

Polyphenols can be found in either free form (aglycones), bound as sugars with other compounds (glycosides), or bound to the plant's cell wall. Around two thirds of polyphenols consumed in a typical human diet are flavonoids (mostly flavanols and anthocyanins) with other polyphenols ingested in smaller quantities (Scalbert and Williamson, 2000). The intestinal atrophy observed in the defunctioned ileum of stoma patients is proposed to be caused by a reduction in bacterial load (Beamish et al., 2017) and, therefore, targeting the microbiome with prebiotics like polyphenols could resolve mucosal atrophy.

1.9.1. Effect of polyphenols on pathologies

Inclusion of polyphenols in the diet is associated with numerous health benefits and increased intake has successfully reduced the severity of several diseases including

cancer and heart disease. Studies have shown a positive association with flavonoid intake and reduced risk of lung (Christensen et al., 2012), breast (Hui et al., 2013), and gastric cancer (Woo et al., 2014), although the latter is disputed by a separate study (Petrick et al., 2015). Flavonoids have also successfully reduced the risk of cardiovascular diseases like coronary heart disease (Knekt et al., 1996) and other polyphenols have demonstrated benefits all around the body including the brain and liver. For example, administration of quercetin upregulated the NRF2-KEAP1 antioxidant response pathway (Arredondo et al., 2010) and increased expression of antioxidant enzymes superoxide dismutase (SOD), catalase and glutathione peroxidase (Molina et al., 2003).

The effects of polyphenols on gut-related pathologies have also been investigated through numerous clinical trials. Daily consumption of epigallocatechin gallate (EGCG) and apigenin decreased the incidence of neoplasia recurrence in patients with resected colorectal cancer (Hoensch et al., 2008) and green tea extract (GTE) consumption decreased metachronous adenoma occurrence by 50% in high-risk patients (Shimizu et al., 2008). The beneficial effects of polyphenols on ulcerative colitis have been demonstrated in DSS-induced colitis models; apigenin decreased macroscopic and microscopic signs of colitis and reduced pro-inflammatory IL-1β and TNF-α production (Márquez-Flores et al., 2016).

Their ability to improve intestinal pathologies has been attributed to their prebiotic properties; Painong-San (PNS) extract suppressed the overgrowth of pathogenic bacteria including *Oscillospiraceae* and *Helicobacter* while increasing *Lactobacillus*, *Bifidobacterium*, and *Akkermansia* in an ulcerative colitis mouse model (Wang et al., 2022). These changes subsequently improved intestinal function by enhancing damage repair and reducing colonic inflammation. Another study showed polyphenols decreased the abundance of Bacteroidaceae, Deferribacteraceae, and Enterobacteriaceae and downregulated the expression of pro-inflammatory cytokines like IL-6 and TNF-α, reducing colon shortening and histological injury (Ren et al., 2021).

1.9.2. Polyphenol influence on intestinal barrier integrity and repair

Experimentally, polyphenols have boosted intestinal repair mechanisms and contributed to normal barrier function. Colitis models have been employed to assess the capabilities of polyphenols to reverse intestinal epithelial damage, improving barrier integrity. In colitis models, resveratrol, curcumin, and simvastatin reduced proinflammatory cytokine expression (IFN-γ, TNF-α, and IL-6), preventing inflammation and inhibiting bacterial translocation (Bereswill et al., 2010). Another study found that polyphenol-rich grape pomace extract (GPE) prevented DSS-induced colon shortening and colitis in rats and reduced the extent of ulceration, destruction of epithelial cells, and oedema (Boussena et al., 2016a). Epithelial architecture, particularly crypt structure, was also improved, demonstrating the ability of polyphenols to improve colonic barrier integrity. Additionally, colon shortening and colitis symptoms including weight loss and decreased appetite were prevented by GPE supplementation (Boussena et al., 2016b). Polyphenols administered to IL-10 deficient ileitis models reduced inflammation by restoring the normal ratio of villi/crypt length (Yang et al., 2014). However, success varied between different polyphenols (Boussena et al., 2016a), suggesting their capabilities are not uniform.

1.9.3. Extra Virgin Olive Oil

Extra virgin olive oil (EVOO) is rich in a variety of polyphenolic compounds (Figure 1.7.) and exhibits the same anti-inflammatory and prebiotic capabilities as polyphenols. This has been demonstrated in DSS-colitis mouse models where EVOO administration reversed the loss of mucosal crypts and reduced ulceration (Sánchez-Fidalgo et al., 2011). EVOO also promoted reepithelialisation corresponding to improved disease index, reduced mortality by 50%, and reduced TNF-α and IL-10 expression. However, a later study did not find a significant reduction in these pro-inflammatory cytokines but showed EVOO prevented inflammation by downregulating COX-2 and STAT3 expression (Takashima et al., 2014). EVOO also decreased neutrophil infiltration, dystrophic goblet cell numbers, and presence of crypt abscesses associated in mucosal damage (Cariello et al., 2020).

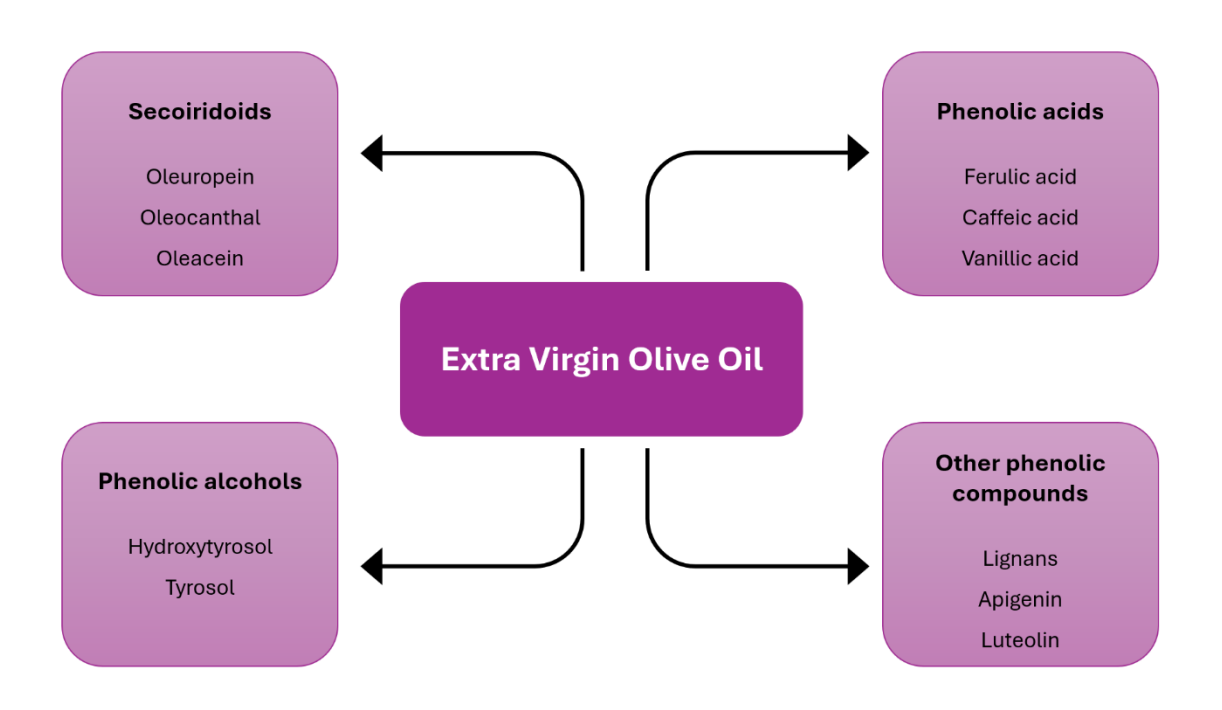


Figure 1.7. Common polyphenolic extracts from extra virgin olive oil (EVOO).

EVOO has exhibited its prebiotic abilities and its potential to resolve pathology-related dysbiosis. For example, in combination with thyme phenolic compounds, EVOO increased numbers of *Bifidobacteria* groups in hypercholesterolemic patients (Martín-Peláez et al., 2017). EVOO also increased α- and β-diversity in high fat diet (HFD)-mice, preventing metabolic syndrome (MS) and upregulated antimicrobial Reg3γ in the ileum which prevented bacterial translocation (Millman et al., 2020; Zhao et al., 2019). Similarly, olive leaf extract (OLE) reversed dysbiosis in HFD-mice by decreasing the F:B ratio and increasing the abundance of beneficial *Cytophaga* (Bacteroidetes) and *Akkermansia* (Verrumicrobia) (Vezza et al., 2019). HIV-associated dysbiosis has also been improved by EVOO intake; beneficial genera were increased in both males (*Prevotella*, *Bacteroidetes*, and *Bifidobacterium*) and females (*Ruminococcus*, *Lachnospiraceae*, and *Akkermansia*) (Olalla et al., 2019).

The success of polyphenol-rich compounds like EVOO to improve microbial composition and resolve intestinal atrophy may make them useful additions to DLS. Currently, no previous studies have included polyphenols in DLS, potentially due to their limitations, discussed below.

1.9.4. Polyphenol metabolism and bioavailability

Polyphenol metabolism and bioavailability is unique to each compound and is highly variable. Generally, their bioavailability is low, partly due to low water solubility and instability in low pH environments, leaving a large proportion of ingested polyphenols unabsorbed. Bioavailability differs between monomeric and multimeric polyphenols (Monagas et al., 2010); monomeric polyphenols such as phenolic acids and flavonoids are much more bioaccessible and undergo covalent modifications in the small and large intestine. This is known as Phase I metabolism and includes acylation, esterification, and glycosylation (Marín et al., 2015) which make polyphenols more bioactive and readily absorbed by enterocytes. Once absorbed, Phase II metabolism including methylation, sulphation, and glucuronidation takes place before polyphenols are released into the bloodstream through the basolateral membrane. Once systemic, polyphenols are transported to the liver (Nielsen et al., 1998) where further Phase II metabolism occurs (Donovan et al., 2011) (Figure 1.8.).

Human intestinal enzymes are unable to metabolise polyphenols themselves, so their metabolism is performed by enzymes produced by the enteric microbiota. However, many bacterial species responsible for polyphenol metabolism are solely located in the colon so only approximately 10% of polyphenols are reported to be absorbed in the small intestine (Clifford, 2004). For example, no small intestinal bacteria produce α -rhamnosidase, capable of hydrolysing the α rhamnose moiety linked to flavonoids but colonic bacteria such as *Bifidobacterium dentinum* produce this enzyme, permitting flavonoid metabolism and absorption in the large intestine (Bang et al., 2015). The hydrolysis of rutin to quercetin is also only achieved by resident colonic bacteria, including several *Bacteroides spp.*, capable of producing β -glucosidase (Bokkenheuser et al., 1987). Known beneficial bacteria *Bifidobacterium* and *Lactobacillus* are also

responsible for polyphenol metabolism (Zhu et al., 2018; Gaur et al., 2020; Szwajgier and Jakubczyk, 2010) and absorption is suggested to differ between individuals due to differences in microbial compositions (Feliciano et al., 2017).

Even after metabolism and absorption, not all polyphenols become systemic, as some are secreted out of enterocytes and back out into the lumen (Villa-Rodriguez et al., 2019). Other polyphenols are unable to be absorbed entirely including proanthocyanidins and certain flavanols which have too large of a molecular weight to be absorbed by enterocytes. Additionally, intestinal bacteria do not produce enzymes capable of breaking down certain polyphenols, so they completely transit the GI tract without being absorbed (Pasinetti et al., 2018).

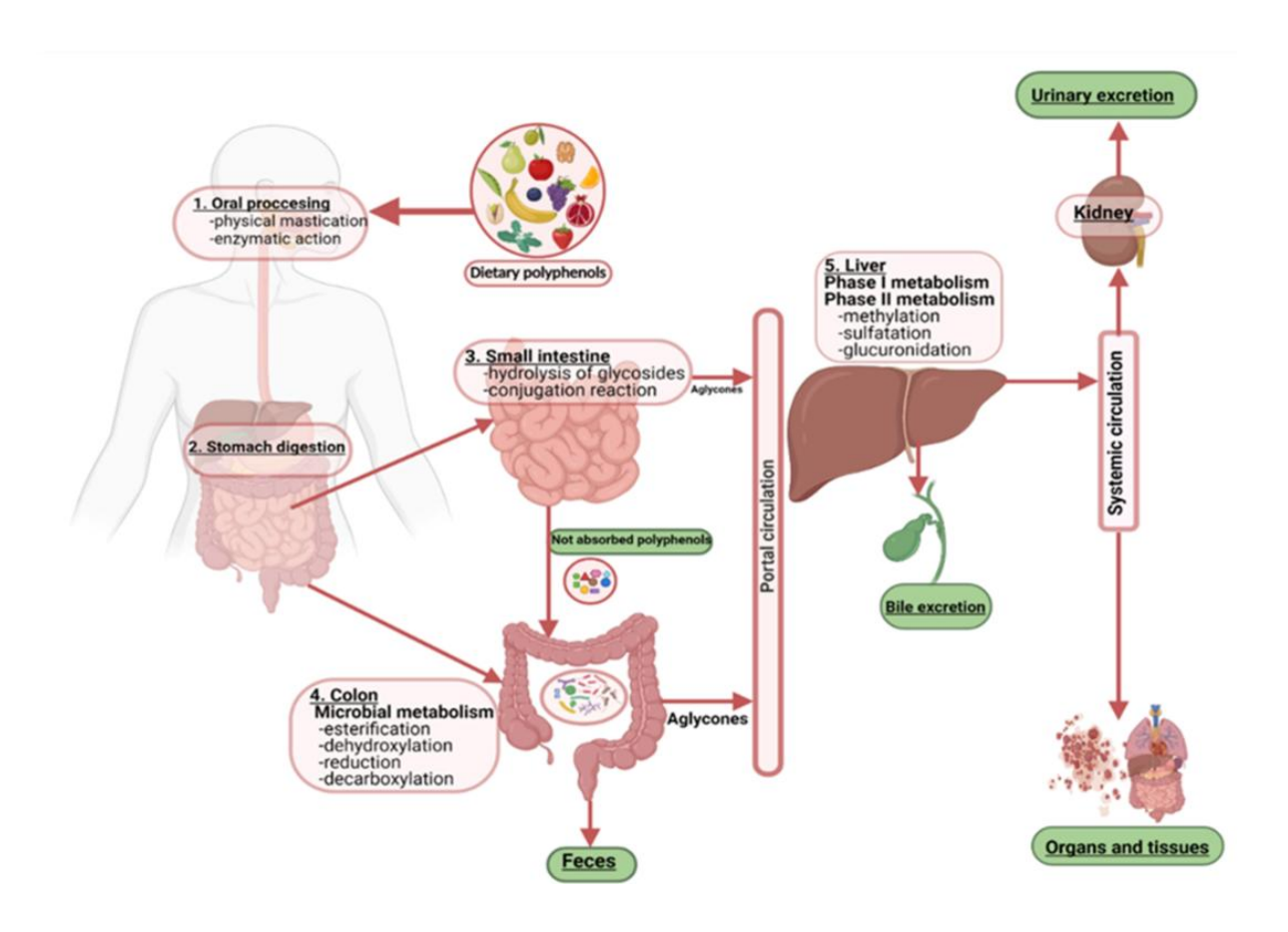


Figure 1.8. Process of polyphenol absorption, metabolism, transport, and finally removal following oral intake. Notably, Phase I and II metabolism occur in the small intestine, colon, and liver (Plamada and Vodnar, 2021).

Polyphenol bioavailability is still not well elucidated and extremely variable. Using detection in urine as an indicator of polyphenol uptake, this variability has been demonstrated. Red wine anthocyanins were detected in the urine between the range of 1.5-5.1% of the total anthocyanins ingested (Lapidot et al., 1998) whereas soybean isoflavones, daidzein and genistein were detected at 21% and 9% respectively (Xu et al., 1994). Bioavailability is also dependent on the source of polyphenols; quercetin from onion was detected at 1.39% of the original dose whereas quercetin from apples was only detected at 0.44% (Hollman et al., 1997).

in vitro studies have also aimed to characterise this variation in polyphenol bioavailability and have elucidated potential membrane transporters responsible for absorption and efflux. Caco-2 monolayers, immortalised human colorectal adenocarcinoma cell lines were set up in transwells with an apical (above) and basolateral (below) chamber either side of the monolayer. Polyphenols were added to the apical chamber to measure intracellular, apical and basolateral polyphenol concentrations following incubation. Although studies are limited, some polyphenols, like genistein and daidzein showed similar intracellular and basolateral concentrations (Murota et al., 2001) while other studies reported differences in absorption between polyphenols (Teng et al., 2012).

Influx and efflux across the epithelial apical membrane has also been elucidated (Figure 1.9.). Monocarboxylate transporter (MCT) inhibition with phloretin and benzoic acid and organic anion transporting polypeptide (OATP) inhibition using estrone-3-sulphate reduced epicatechin-3-gallate (ECG) uptake, suggesting these transporters are involved in polyphenol absorption (Vaidyanathan and Walle, 2003; Nguyen et al., 2019). Polyphenol efflux back through the apical membrane has been attributed to p-glycoprotein and multi-drug resistant protein (MRP) transporter using verapamil and cyclosporine, respectively (Teng et al., 2007), the latter also used to show ATP-binding cassette (ABC) transporters may also allow polyphenol efflux (Nguyen et al., 2019).

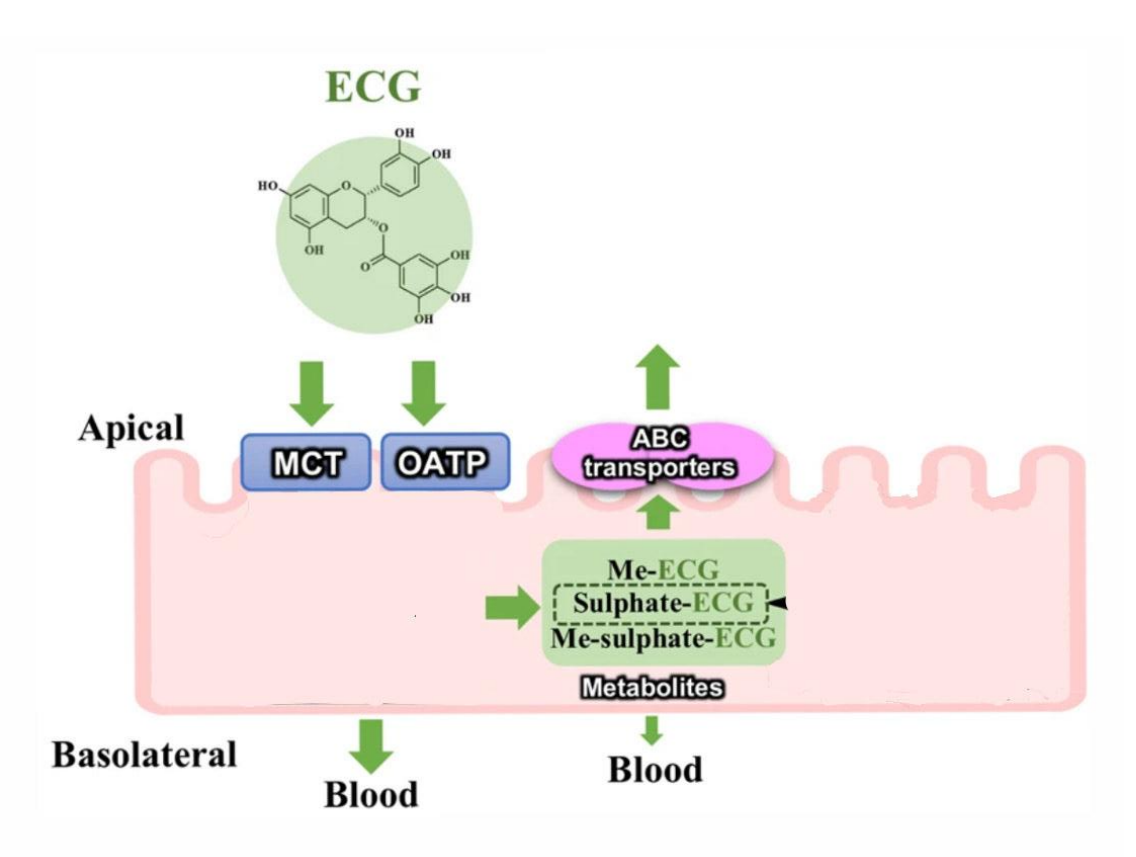


Figure 1.9. Proposed mechanism of ECG influx and efflux through the apical membrane. Apical membrane channels allow intake from the lumen and ABC transporters (and p-glycoprotein and multi-drug resistant protein transporters- not shown) allow efflux back into the lumen. ECG, epicatechin-3-gallate, MCT, monocarboxylate transporter, OATP, organic anion transporting polypeptide, ABC, ATP-binding cassette (Nguyen et al., 2019).

1.10. Solid lipid nanoparticles

Drug delivery systems have risen in popularity over recent years for their ability to ensure sufficient drug delivery and prolonged release. One type of delivery system are solid lipid nanoparticles (SLNs). With a diameter of approximately 10-1000nm, SLNs are made up of a solid lipid core, commonly composed of triglycerides, monoglycerides, and fatty acids surrounded by an external surfactant layer. This surfactant layer provides stability, allowing controlled, prolonged drug release (Weiss et al., 2008). Their ability to improve drug bioavailability has been demonstrated; for

example, SLN-tagged lumefantrine had a greater *in situ* intestinal permeability and bioavailability (Garg et al., 2017).

Several studies have also utilised SLNs to improve the poor bioavailability of polyphenols, increasing their absorption. Flavonoid bioaccessibility was increased from below 15% to over 71% when tagged with lipid nanoparticles and further investigation demonstrated a greater than twelve-fold increase in curcumin bioavailability using SLNs (Ban et al., 2020; Ji et al., 2016), proving nanoparticle delivery systems as effective vectors for enhancing polyphenol bioavailability. *in vitro* studies have proven that SLNs are protected from degradation in the mouth and stomach and allow for prolonged release in the lower GI tract. Resveratrol-loaded SLNs incubated in simulated gastric fluid for three hours only released resveratrol once transferred to simulated intestinal fluid (Neves et al., 2013). This was confirmed using flavonoid-loaded oil-based lipid nanoparticles which only released flavonoids in the *in vitro* intestine environment (Ban et al., 2015).

1.10.1. Potential incorporation of SLN-tagged polyphenols in DLS

Polyphenols have demonstrated their anti-inflammatory and prebiotic properties and their ability to improve and restore gut barrier integrity (Bereswill et al., 2010; Yang et al., 2014). Therefore, polyphenols may be a useful inclusion in DLS in the defunctioned ileum of stoma patients as they may reverse dysbiosis and atrophy as well as ameliorate any possible immune dysregulation. However, the poor bioavailability and variable activity of polyphenols (particularly in the small intestine) hinders their potential benefits and could limit their success if incorporated into DLS. Additionally, the majority of polyphenols transit the small intestine without being metabolised or absorbed, so improvements to intestinal barrier integrity may not be witnessed in the defunctioned ileum. However, polyphenol-rich EVOO was shown to upregulate Reg3y expression in the ileum, indicating polyphenols may be able to influence the environment within the defunctioned ileum (Millman et al., 2020). EVOO also contributes to wound healing (Aboui Mehrizi et al., 2016) and is anti-inflammatory which may also help to reduce post-operative complications.

SLNs are shown to overcome poor polyphenol bioavailability and are suggested to aid their absorption in the small intestine (Neves et al., 2013; Ban et al., 2015). Therefore, tagging polyphenols or polyphenol-rich compounds like EVOO may enhance their prebiotic capabilities in the defunctioned ileum and make them a useful inclusion in DLS.

1.11. Hypotheses

Nutrient deprivation in the defunctioned ileum is proposed to reduce the bacterial load (Beamish et al., 2017) which, in turn, compromises the intestinal barrier function leading to atrophy. Using GF murine models and nutrient deprivation models (TPN), we propose a mechanism where a reduction in proliferative activity and antimicrobial production from IECs, Paneth cells, and goblet cells will increase mucosal permeability and elevate the risk of bacterial translocation. The long-term immunological impact of stoma formation in the defunctioned ileum is largely unknown, but potential pathogenic invasion may trigger pro-inflammatory immune responses leading to an upregulation of innate immune cells like dendritic cells responsible for activating pro-inflammatory adaptive immunity. Specific CD103*/. DC subsets regulate pro-inflammatory T cells like Th1 and Th17 so these DC populations may be expected to increase. Additionally, prebiotic DLS is hypothesised to reverse dysbiosis in the defunctioned ileum, restoring the homeostatic gut barrier environment. Restoration of intestinal barrier function and integrity is predicted to increase proliferative activity in the defunctioned ileum, characterised by the reversal of villus atrophy.

The poor bioavailability of dietary polyphenols in the small intestine diminishes their potentially beneficial effects and excludes them from DLS. Administration of SLN-tagged EVOO extracts in a murine model is hypothesised to increase polyphenol absorption in the small intestine. This would be characterised by a greater concentration of polyphenols in the liver, indicating a greater total absorption. SLN tagging is also hypothesised to increase polyphenol absorption in the small intestine.

1.12. Research aims

Due to the absence of literature characterising the immunological impacts of loop ileostomy (particularly on innate immune cells), this project aims to use flow cytometry to compare innate (DC, CD103⁺ DC) and adaptive (T cell) immune populations between the functional and defunctioned ileum. The physiological impacts of DLS have scarcely been reported in the small number of available studies. H&E staining will characterise possible morphological changes between the defunctioned ileum of patients who had and had not received DLS prior to reanastomosis. Changes will be characterised by differences in villus height and crypt depth between cohorts.

The efficacy of SLNs to improve EVOO-extracted polyphenol bioavailability will be assessed in a murine model. After seven days of oral gavage containing either SLN-tagged or untagged polyphenols, high performance liquid chromatography (HPLC) analysis on the small intestine, colon, and liver will aim to determine whether SLNs increase polyphenol absorption, particularly in the small intestine. Fluorescence imaging will also be performed to confirm the presence of SLNs in these organs and H&E staining on colonic mucosal tissue will assess the impact of treatments on mucosal physiology.

2. Methods

2.1. Model maintenance

2.1.1. Cell line maintenance

Caco-2 cell line (European Collection of Authenticated Cell Cultures [ECACC catalogue no. 09042001]) was maintained in T75 cell culture flasks [Thermo Fisher Scientific] containing minimal essential media (MEM [Gibco®]) supplemented with 10% foetal bovine serum (FBS [Gibco®]) and 1% non-essential amino acids (NE-AA [Gibco®]). Cells were incubated at 37°C, 5% humidity and 5% CO₂ levels and all actions were performed under sterile conditions. To avoid 100% confluence, the flask was passaged every three to four days by removing the existing media, washing with 1X PBS, and adding approximately 0.5ml of 0.25% trypsin [Gibco®]. The flask was then incubated at 37°C for three to five minutes, or until all cells had detached from the bottom of the flask. After trypsinisation, the cells were resuspended in fresh, warmed media and cell counts were taken using a haemocytometer. The suspension was split between the existing flask and another flask and diluted by a ratio of 1:10 and the passage number and date were noted. The flasks were put back in the incubator until the next passage.

2.1.2. Murine model maintenance

2.1.2.1. Ethics statement

This mouse study (project license number 415-78153) was approved by Lancaster University Animal Welfare and Ethics Review Boards (AWERB) and conducted in accordance with Lancaster University Physiological Services Unit regulation for animal husbandry, ethical guidelines, and under Home Office licensing in accordance with the Animals in Scientific Procedures Act (1986).

2.1.2.2. **Husbandry**

C57/B6 wild-type mice were housed in groups of three to five per individual ventilated cage (IVC [Techniplast]), split based on sex 4 weeks after birth. Mice were kept in specific pathogen-free conditions, under a twelve-hour light/dark cycle, with ad-libitum access to food (chow) and water. Studies were carried out on adult mice age 8-12 weeks.

2.2. Obtaining human intestinal tissue

2.2.1. Declaration and informed patient consent

To investigate physiological changes and possible immune dysregulation in the defunctioned ileum, resected tissue from the functional and defunctioned ileum were obtained during reanastomosis. A separate cohort of participants received distal limb stimulation (DLS) prior to reanastomosis and, again, tissue samples were taken during reversal surgery to assess physiology. These studies were approved by the North West Research Ethics Committee (13/NW/0695) and (22/WM/0222) respectively, conducted in accordance with the Health Research Authority guidelines. Cohorts consisted of eligible and consenting patients undergoing loop ileostomy reversal surgery at Lancashire Teaching Hospitals (LTH) NHS Trust (Lancashire, UK). Participants could be male or female, 18 years or above but patients who had ongoing bowel pathologies, such as IBD, or had received antibiotic treatment within the last three months were excluded from the study. For patient anonymity, tissue samples were assigned a unique identifier: for the unfed cohort, BCRGXXX and for the DLS cohort, SFSXXX.

For the DLS cohort, participating patients were informed during a pre-feeding visit or the first visit for DLS and participant information sheets were available for patients to take home and consider. Patients were well-informed that the DLS suspension contained fibre that may increase the number of beneficial enteric bacteria and help to reduce post-operative side effects. Patients were also aware that biopsies of proximal (functional) and distal (defunctioned) bowel tissue would be taken to the laboratories at

Lancaster University to investigate the physiological impact of DLS. At the next visit, consent was obtained from participants.

2.2.2. Distal limb stimulation protocol

Approximately four weeks prior to reanastomosis, a feeding tube was inserted into the defunctioned ileum by hospital staff. Following a few days of successful administration of saline, the DLS suspension consisting of 100ml of the nutritional suspension, Ensure®, supplemented with 10g of soluble fibre rich in chicory sourced inulin (Orafti®Synergy-1) was injected daily into the defunctioned ileum. A 'feeding diary' was provided to record participant compliance with the stoma feeding, for instance whether DLS was carried out every day as advised, or whether some days were missed or partially completed. During reanastomosis, functional and defunctioned ileal tissues were obtained and transported from LTH NHS Trust to Lancaster University in MEM, on ice, before processing.

2.2.3. Tissue fixation and embedding

In a sterile tissue culture hood, the functional and defunctioned samples were removed from MEM and fixed in 4% paraformaldehyde for twenty-four hours. Samples were then rinsed with 1X PBS and submerged and stored in 70% ethanol. Samples were removed from 70% ethanol and transferred into labelled cassettes and loaded into the Excelsior AS Tissue Processor [Thermo Fisher Scientific], following the programmed protocol below (Table 2.1.). All waste was disposed of through the clinical waste route.

Table 2.1. Tissue processing protocol for human and mouse tissue in the Excelsior AS Tissue Processor [Thermo Fisher Scientific].

Process	Reagent	Time- Human	Time- Mouse	Temperature
		(min)	(min)	(°C)
Dehydration	75% ethanol	30	10	25
	90% ethanol	60	30	25
	95% ethanol	60	30	25
	100% ethanol	30	10	25
	100% ethanol	60	30	25
	100% ethanol	60	30	25
Ethanol	100% xylene	30	10	25
	100% xylene	60	30	25
extraction	100% xylene	60	30	25
Wax infiltration	Paraffin wax	60	30	64
	Paraffin wax	60	30	64
	Paraffin wax	60	30	64

After completion of the protocol, the cassettes were removed from the tissue processor and transferred to the embedding station wax chamber (HistoCore Arcadia H [Leica]). Each sample was removed from its cassette and placed into a metal wax mould on the machine's hot plate. The tissue was orientated with forceps so that cross sections of the mucosal physiology could be obtained. Once correctly positioned, molten paraffin wax was added to the mould and the labelled cassette lid was placed on top and covered in wax. The mould was then moved onto the cold plate for a minimum of ten minutes, and this process was repeated for all samples. The wax block containing the tissue was removed from the metal mould and wax was filed away into a square of

approximately 2cm x 2cm around the embedded sample. Blocks were stored at room temperature until histochemistry was performed.

2.3. Histochemistry

2.3.1. H&E staining

Following tissue processing, embedded ileal samples were sectioned using the microtome (RM2125 RTS [Leica]). The wax blocks were mounted and secured onto the microtome and sections of 7µm thickness were cut and carefully transferred onto the surface of a 45°C water bath. The sections were then transferred to labelled APEScoated microscope slides (Appendix-5.1.) and left to dry in the fume hood prior to staining. Once completely dried, the slides were immersed in two, five-minute rounds of xylene to remove the wax within the tissue. The slides were then sequentially rehydrated in two, one-minute rounds of 100% ethanol, one minute in 90% ethanol and a further minute in 70% ethanol. The slides were then rinsed under running tap water to remove the ethanol and immersed in distilled water. The slides were then submerged in filtered haematoxylin [Sigma-Aldrich®] for five minutes before being washed under warm running water for ten to twenty minutes. Once rinsed, slides were dipped up and down in eosin [Sigma-Aldrich®] and immersed for one to two minutes. Slides were then rinsed again with tap water and dehydrated in five minutes of 70%, 90% and two rounds of 100% ethanol. Following dehydration, slides were transferred to xylene for two, fiveminute rounds. Once removed, a drop of DPX mountant [Thermo Fisher Scientific] was added to the sections and a coverslip placed on top, ready for microscopic examination.

2.4 Microscopy

Microscopy was used to measure mucosal structures and compare them between the functional and defunctioned ileum of patients of the two cohorts. Slides were viewed under 100X magnification (10X objective lens) to examine intestinal villi and crypts.

Images were taken using the Moticam X³ camera [Motic®] attached to the microscope

and transferred to ImageJ for measuring. The measuring tool was calibrated using the scale bar from each image and the length of ten villi and the depth of ten crypts were measured. Seen in Figure 2.1., villi were measured from base to tip and crypts were measured from crypt base to villus base. When structures had curvature, such as the measured crypt in Figure 2.1., this was accounted for in the measurement. The average villus height and crypt depth was then calculated between the functional and defunctioned ileum between the two cohorts.

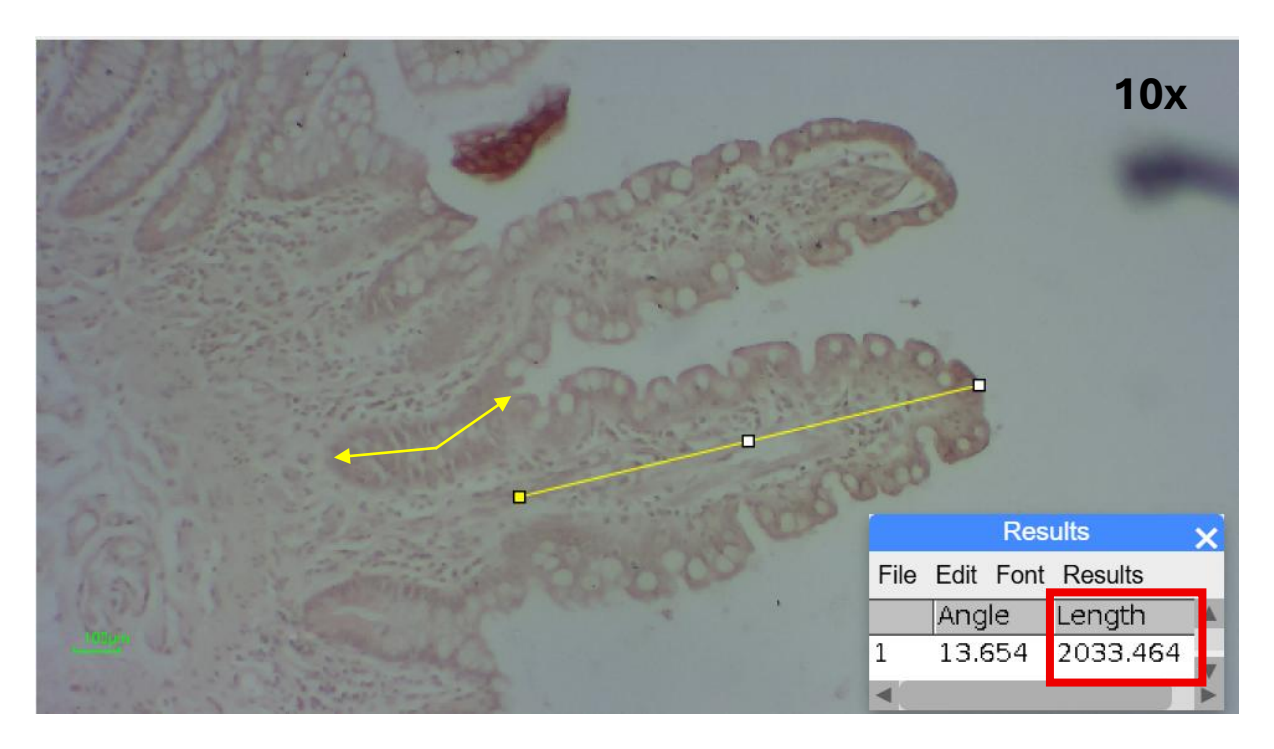


Figure 2.1. Example of villus and crypt measurements acquired in ImageJ. The depth of crypts and height of villi were calculated with the measure tool and repeated for ten crypts and villi. Objective lens 10X magnification. Example from Patient SFS002.

Mean measurements were used to perform a one-tailed independent sample t-test (Equation 2.1.) to determine whether villus height or crypt depth significantly differed between the intestinal environments and whether DLS impacted these changes.

$$t = \frac{\bar{x}_1 - \bar{x}_2}{\sqrt{\frac{s_1^2}{n_1} + \sqrt{\frac{s_2^2}{n_2}}}}$$

Equation 2.1. One-tailed independent sample t-test.

2.5. Flow cytometry

2.5.1. Sample preparation

Prior to tissue fixation (2.2.3.), sections of functional and defunctioned ileal biopsies from the unfed cohort were processed for flow cytometry to investigate the immunological effects of stoma formation. The entire procedure was performed in the tissue culture hood and waste was disposed of through the clinical waste route. Adapting the protocol from Weigmann et al., 2007, approximately 250mg of functional and defunctioned sections were first washed in Hanks' Balanced salt solution (HBSS [Thermo Fisher Scientific]) and cut into 5mm sections. The epithelium was then stripped from the intestine by incubating the gut in falcon tubes containing 1mM dithiothreitol (DTT) and 1mM EDTA in HBSS, in a shaker for twenty minutes at 37 °C. The supernatant was discarded, and the gut tissue was transferred into fresh falcon tubes containing 10ml of gut digest media (50ml HBSS, 10% FBS, 0.5mg/ml Dispase [Gibco®], and 0.5mg/ml Collagenase [Gibco®]) and incubated in the shaking incubator for sixty minutes at 37°C.

Digestion medium was then passed through 100µm cell strainers to collect cell suspensions. The filtrate was collected and centrifuged at 400g for five minutes. The supernatant was removed from each tube, and the pellet was resuspended in 8ml of

3% Percoll [Merck] before another centrifugation at 600g for twenty minutes. The supernatant containing mucus and other debris was removed and the pellet containing mononuclear cells was resuspended and washed with 4ml 1X PBS. Cell counts were performed using a haemocytometer to determine the volume of suspension required for 1-2 x10⁵ cells per fluorescent activated cell sorting (FACS) tube.

Suspensions were centrifuged for five minutes at 350g, after which, the supernatant was removed, and the pellet resuspended in FACS staining buffer (PBS with 0.1% NaN3 and 5% FBS) and maintained on ice. Cell suspensions were loaded into the 96-well plate at a concentration of 1x10⁶/ml, 200µl/tube/well. To each well, 2µl Fc block [BioLegend] was added, and the plate was left to incubate on ice for thirty minutes. At a concentration of 3µl of 0.2mg/ml 1.2µl of 0.5µg/ml, cell surface antibodies (Appendix-5.2.1.) were added and the plate was gently vortexed and incubated in the dark on ice for fifteen minutes. The plate was then centrifuged for five minutes at 350g and the supernatant was removed. Cells were then fixed with 0.5ml of 0.1% paraformaldehyde. The plate was refrigerated at 2-8°C in the dark and acquired within eighteen hours of fixation.

2.5.2. Flow cytometry acquisition

Data was obtained for each sample as well as controls for each filter and analysed in the software, Flowjo (v.10.10.0). For each patient, the samples and compensation controls were added to the software and a compensation matrix was constructed to correct fluorescence spillover. Each sample was plotted forward scatter area (FSC-A) vs side scatter area (SSC-A), presenting the cells based on their size against granularity. Viable cells were gated, avoiding dead cells or debris and events of extreme size and granularity. Side scatter height (SSC-H) was then plotted against SSC-A and doublets were excluded by gating around the true cell population. Filter panels were then plotted against each other based on individual patient filter panels (Appendix- 5.2.2.) to identify specific cell populations. Different cell populations could be identified and gated, providing the number of cells and proportion of cells compared to total cell number in the sample.

2.6. in vivo polyphenol feeding

2.6.1. Preparation of treatments

2.6.1.1. Polyphenol extraction from EVOO

Polyphenols were extracted from commercially available extra virgin olive oil (EVOO) [Yannis Fresh Greek Early Harvest Extra Virgin Olive Oil]; 10g of EVOO was dissolved in 50ml hexane to separate its non-polar components and sonicated at 20µm for five minutes to enhance dissolution. Liquid-liquid extraction was performed by loading the solution into a separatory funnel, shaking for two minutes, and polar polyphenol compounds were extracted with a mixture of methanol and water (60/40, v/v). After two further repeats, the methanolic phases containing the polyphenol extracts were collected and washed twice with hexane before refrigeration for twenty-four hours at 4°C. Methanol was removed at 40°C under reduced pressure, prior to a twenty-four hour freeze-dry cycle at -70°C and 0.0026 mbar pressure. The solid polyphenol product was weighed and resuspended in a 50/50 (v/v) methanol/water mixture to a final concentration of 10mg/ml.

2.6.1.2. SLN synthesis for polyphenol tagging

The solvent diffusion-solvent evaporation method was used to produce polyphenol-encapsulated solid lipid nanoparticles for the 'Tagged Polyphenol' treatment (Table 2.2). At 5°C above the solid lipid melting point (approximately 69°C), 500mg of stearic acid (forming the lipid core) was melted and 3.3mM of EVOO-extracted polyphenols and the fluorescent BODIPY dye dissolved in 1ml of methanol were mixed into the molten lipid. At the same temperature of the stabilising agent, the resulting organic solution was immediately injected to an aqueous poloxamer 188 non-ionic surfactant solution (1% w/v in Milli-Q water). The aqueous phase was heated and stirred at 700rpm and sonicated for five minutes producing a milky appearance, indicating formation of SLNs due to solvent diffusion and lipid precipitation. The resulting SLN dispersion was continuously stirred at 700rpm for thirty minutes on a magnetic stirrer to evaporate the solvent before storing the sample at 4°C for one hour to allow the

recrystallization and solidification of the lipid core. The dispersion was then centrifuged at 15000rpm for forty minutes at 4°C to separate the SLNs from the dissolved, unencapsulated polyphenols. The SLNs were washed three times by resuspending the nanoparticle residue in distilled water and centrifuging to ensure there were no free polyphenols present in the voids between the SLNs. SLNs used in 'Tagged Control' (suspension of SLNs lacking polyphenols) were prepared following the same protocol, but without the inclusion of polyphenols prior to dispersion into the aqueous phase.

2.6.2. Experimental procedure

Prior to the experiment, mice were housed under the conditions stated in 2.1.2.2. and conditions were kept constant throughout the experiment. The experiment consisted of four treatment groups. Mice at ten to twelve weeks of age were administered 200mg of treatment in 100µl suspension, daily for seven days via oral gavage, the time of feeding kept consistent throughout the study. The treatment groups (Table 2.2.), were 'Tagged Polyphenol' (TP) containing SLN-tagged polyphenols, 'Untagged Polyphenol' (UP) containing polyphenols without SLNs, 'Tagged Control' (TC) containing SLNs without polyphenols, and, finally, 'Untagged Control' (UC) which contained neither polyphenols or SLNs (just 1X PBS).

Table 2.2. Contents of each treatment delivered via oral gavage following the protocol in 2.6.2..

Treatment group	Abbreviation	Polyphenols	SLNs
Untagged Control	UC	×	×
Tagged Control	TC	×	~
Tagged Polyphenol	TP	~	~
Untagged Polyphenol	UP	~	×

Chow mass per cage was recorded daily to identify potential changes to food consumption while body weight and physical changes were monitored to identify negative side effects associated with treatments. Stool was also examined to ensure it resembled pellets, as looser stool indicated an inflamed or irritated intestine. On the final day of the experiment, liver, small intestine, and colon biopsies were weighed and harvested for fluorescence imaging and HPLC analysis. Colon tissue was also processed following the mouse protocol in Table 2.1. and crypt depth was measured following 2.3. and 2.4. to examine physiological changes caused by treatments.

2.7. Fluorescence imaging

Before tissue samples were fixed or frozen, the liver and lower GI tract was imaged to detect fluorescently tagged SLNs. The lumen of the small intestine, caecum, and colon were flushed with 1X PBS to remove the faecal stream and imaged using the iBright 1500 Imaging System [Invitrogen]. SLNs were tagged with the BODIPY fluorophore (excitation/emission approximately 508nm/514nm (Ikawa et al., 2008)) and organs were imaged under the FITC (fluoroscein isothiocyanate) filter (495nm/520nm) as this was the closest match to BODIPY's excitation/emission.

To quantify fluorescence, images were taken and transferred to ImageJ to calculate the correlated total cell fluorescence (CTCF, units = relative fluorescence units (RFU)) for the liver, duodenum, jejunum, ileum, caecum, and colon. Outlines were placed around the liver and each region of the GI tract, and the area, mean intensity, and integrated density were measured within the defined area. Another outline was drawn around an area with no fluorescence (the black background) and the same parameters were measured. For each region of the GI tract, CTCF was calculated using Equation 2.2. and average CTCF measurements were compared between treatment groups.

Equation 2.2. Correlated total cell fluorescence (CTCF).

2.8. High performance liquid chromatography

2.8.1. HPLC tissue preparation

To compare polyphenol absorption with and without SLN tagging, HPLC was performed on the harvested small intestine, colon, and liver. At the end of the *in vivo* experiment, small and large intestinal biopsies were flushed with 1X PBS to remove the faecal stream, and tissues were transferred to labelled eppendorfs, frozen in liquid nitrogen, and stored at -80°C. Throughout HPLC preparation, samples were kept on ice to ensure tissues did not overheat. Adapted from Lesniak et al., 2013, between 50-150mg of tissue were taken for each organ and added to tubes containing 1.4mm zirconium oxide homogenisation bead [Precellys®] and 1ml pure water (Milli-Q). Tubes were added to the RiboLyser [Hybaid] for five, twenty second rounds until tissues were homogenised. Between rounds, the tubes were placed back on ice for sixty seconds to prevent overheating. Tubes were then centrifuged at 15000rpm for ten minutes at 4°C and the supernatants were pipetted into tubes containing 3ml chloroform [Sigma-Aldrich®]. The chloroform tubes containing the homogenised tissue were briefly vortexed and centrifuged at 4000rpm for ten minutes at 4°C. A liquid disc was formed and the supernatant above the liquid disc was carefully transferred into new tubes containing

3ml acetonitrile [Sigma-Aldrich®], vortexed and centrifuged at 4000rpm for ten minutes at 4°C again. The aqueous supernatant was aliquoted into three 1ml lo-bind tubes (labelled A, B, and C) before being frozen in liquid nitrogen. The frozen samples were then freeze-dried for twenty-four hours at -80°C and 0.0026 mbar pressure, then stored at -80°C.

2.8.2. HPLC analysis

The HPLC protocol was produced and undertaken by Bakri Alaziqi in the Middleton laboratory at Lancaster University (Alaziqi et al., 2024). The NexeraX2 HPLC [Shimadzu] system was used at 40°C to separate polyphenols present in the samples. The mobile phase consisted of Solvent A (0.1% formic acid in ultrapure water) mixed with Solvent B (varying amounts of acetonitrile) while a Shim-pack XR-ODS 2.2µm (3.0 x 50mm) column represented the solid phase. At a flow rate of 1ml/min, from 1mg/ml of polyphenols, 10µl of stock solution was loaded and ran. The reverse-phase elution was as follows in Table 2.3. and the spectroscopic absorbance for each chromatographic peak was measured with a diode array detector at 240nm, 275m, and 340nm. Peaks corresponding to extracts of interest were identified by comparison to control samples and their known retention times (RT).

Table 2.3. Reverse-phase elution for HPLC analysis of polyphenols in mouse tissue. Solvent B = acetonitrile.

Solvent B concentration (%)	Duration at concentration (min)	
5	0-3	
40	3-26	
50	26-27	
5	27-32	

2.9. in vitro polyphenol translocation

2.9.1. Experimental set up

2.9.1.1. Transwell set up and monolayer establishment

Caco-2 cells were maintained as described in 2.1.1. and all preparation and running of experiments were performed under sterile conditions to prevent contamination. Cells were trypsinised, resuspended in fresh media and the concentration in the suspension was calculated using a haemocytometer. The suspension was then diluted with fresh media to $5x10^5$ cells/ml. Transwells were added to the wells of a 24-well plate [Corning Costar] and 1ml of cell suspension was pipetted into the well and 1ml of fresh media was added below the well (Figure 2.2.). The well-plate was covered and incubated at 37° C for seven days to allow the cells to become confluent and differentiate, forming a monolayer on top of the filter. For a further two weeks, the media either side of the filter were replaced with fresh media every two to three days.

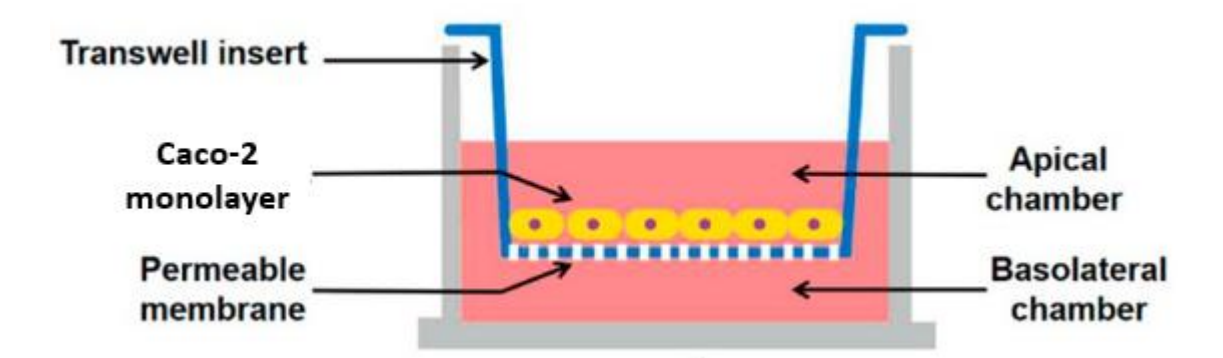


Figure 2.2. Transwell set up for *in vitro* polyphenol translocation experiment. A Caco-2 monolayer adheres to the filter within the transwell and media is added above (apical chamber) and below (basolateral chamber) the monolayer (Ding et al., 2021).

2.9.1.2. Polyphenol preparation

Polyphenols utilised in this *in vitro* experiment were ferulic acid (purity 99% [Sigma-Aldrich®]) and apigenin (purity 97% [Alfa Aesar]) stored at 4°C in 50/50 (v/v) water/methanol at concentrations 0.5mM and 1mM respectively. Polyphenols were diluted to a concentration of 10µmol/l in fresh cell culture media and incubated at 37°C prior to the experiment. Fresh cell media, with no added polyphenols represented the controls.

2.9.2. Experimental procedure

Under sterile conditions, the apical (inside the transwell) and basolateral (underneath the transwell) chambers were removed, with 1ml of fresh, warmed media pipetted underneath the filter and 1ml of either ferulic acid or apigenin-containing media pipetted into the transwell. The well-plate was covered and incubated at 37°C (5% CO₂, 5% humidity) for two hours. Following incubation, the apical and basolateral contents were removed, aliquoted into labelled eppendorfs and frozen at -80°C for HPLC analysis (2.8.). Each experiment consisted of two biological repeats and was repeated a further two times.

3. Results

3.1. Stoma participant demographics

To examine the physiological and immunological state of the defunctioned ileum following stoma formation, participants (Table 3.1.) were recruited from Lancashire Teaching Hospitals NHS. A separate cohort of participants, indicated by the code 'SFS', were administered DLS in an attempt to improve physiology in the defunctioned ileum. This investigation was deemed a pilot study as a small cohort was recruited to demonstrate that DLS is feasible in stoma patients and if physiology is improved (particularly villus atrophy), the study could be upscaled to assess other physiological aspects and whether the reduced bacterial load experienced in the defunctioned ileum can be restored in future patients.

Table 3.1. Stoma study participant demographics. Details regarding sex, age, and duration with stoma of patients in the cohort that received DLS and the cohort that did not (unfed). * = % of participants that are female (F). Average age and duration with stoma given with ± standard deviation in parentheses.

Cohort	Patient ID	Sex (M/F)	Age at reanastomosis (years)	Duration with stoma (days)
	BCRG003	М	65	259
	BCRG004	F	31	253
	BCRG006	М	69	602
	BCRG007	F	50	483
	BCRG008	M	76	815
	BCRG011	M	48	343
	BCRG017	F	17	245
	BCRG018	M	27	210
Unfed	BCRG019	F	70	301
	BCRG020	M	77	284
	BCRG021	F	71	177
	BCRG022	F	65	137
	BCRG023	F	74	977
	BCRG027	F	61	355
	BCRG040	F	45	323
	BCRG041	F	76	267
	Average	63*	58 (±19)	377 (±226)
DLS	SFS002	М	67	881
	SFS004	М	47	793
	SFS005	F	45	2030
	Average	33*	53 (±10)	1234 (±563)

3.2. Effects of loop ileostomy on immune cell populations in the defunctioned ileum

3.2.1. Immune cell selection and gating strategy

Nutrient deprivation has previously been shown to impact intestinal immunology, particularly the disruption of the GALT in TPN patients (Yang et al., 2008; King et al., 1997). Although immune cell populations have not been thoroughly investigated in stoma patients, altered microbial composition and reduced bacterial load in the defunctioned ileum are hypothesised to allow bacterial translocation and increase immune cell populations. Certain immune populations were compared between the functional and defunctioned ileum to determine whether nutrient deprivation caused immune dysregulation. DCs, and particularly the CD103⁺ subset, were investigated as they regulate adaptive immune responses as well as the T cell populations which combat infection.

Immune cell populations were compared using Flowjo, following the protocol in 2.5.. A compensation matrix was created using compensation control samples to prevent spectral overlap and was applied to the rest of the samples. A gating strategy (Figure 3.1.) was constructed and applied to all samples. Side scatter area (SSC-A) against forward scatter area (FSC-A) plots enabled a gate around cells to exclude dead cells and debris, as well as cells that were too large or too granular to be mononuclear cells (Figure 3.1.A.). Plots for FSC-height against FSC-A of the gated population removed doublets and the population of viable, single cells could then be plotted against different filters to identify DC and T cell populations. For example, in Figure 3.1.C., the HLA-DR antibody (PE-Cy7-A filter) was plotted against the antibody cocktail (CD3 (T cells), CD56 (NK cells), CD19 (B cells), CD14 (monocytes), CD20 (B cells)) (APC-A filter) to identify the DC population (HLA-DR⁺, cocktail⁻). The population of interest was gated and the proportion of cells in relation to total cells was compared between functional and defunctioned samples. The CD103⁺ DC subset was identified by plotting the HLA-DR⁺ cocktail⁻ population against the CD103 antibody. To identify T cell populations, CD3 antibody was plotted against CD19 antibody to identify the CD3⁺ CD14⁻ population (Figure 3.1.D.).

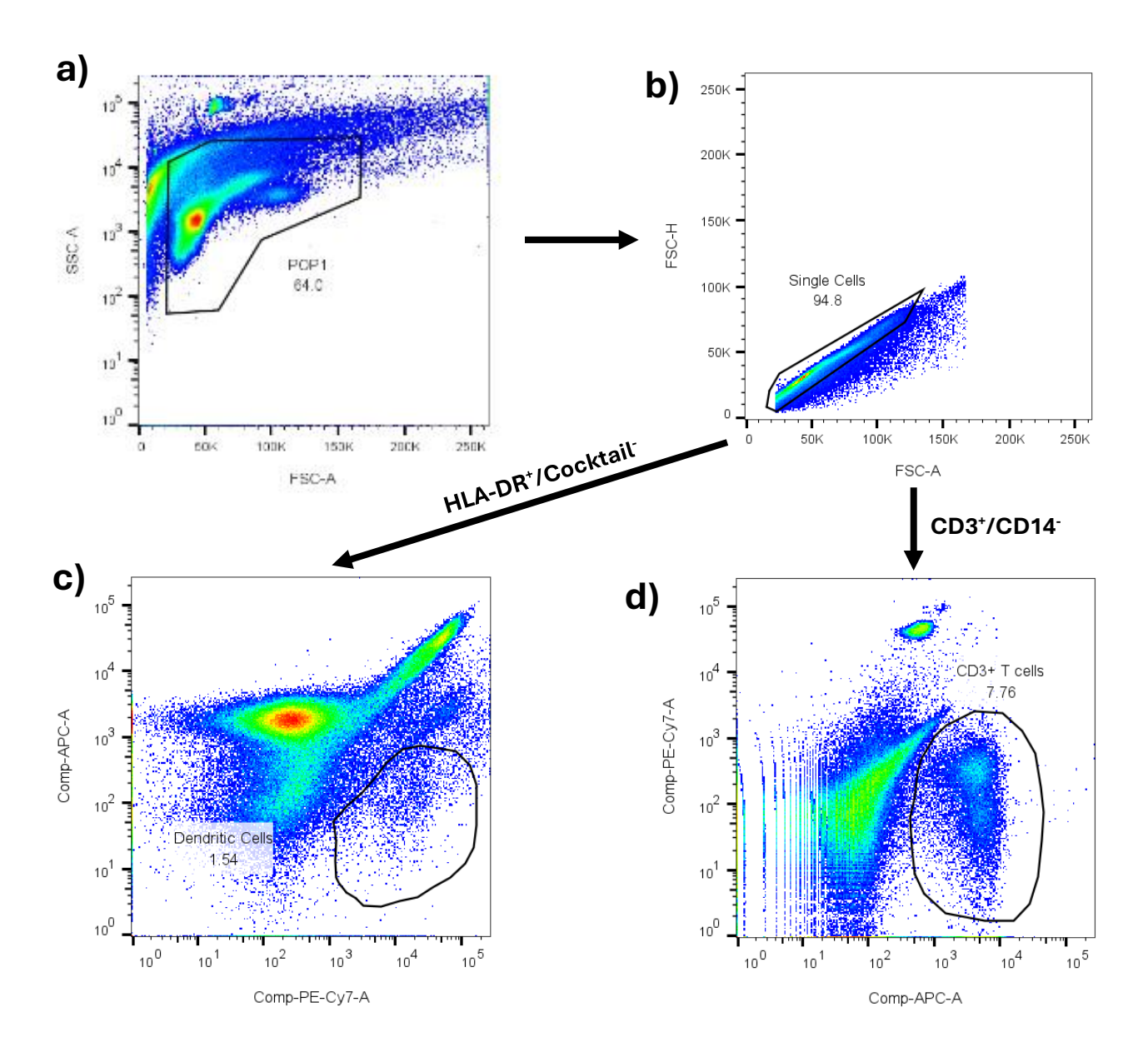


Figure 3.1. Flow cytometry gating strategy for DC and T cell populations. Using the software Flowjo, sample populations were plotted SSC-A vs FSC-A (a) then FSC-H vs FSC-A (b). Viable, single cells were gated to identify DC (c), CD103⁺ DC, and T cell (d) populations. SSC-A, side scatter areal FSC-A, forward scatter area; FSC-H, forward scatter height.

3.2.2. Stoma formation does not affect dendritic cell populations in the defunctioned ileum

DCs, particularly CD103 $^+$ /. subsets, are responsible for activating adaptive immune cells like Tregs and helper T cells and were predicted to be elevated in the defunctioned ileum. The proportion of DCs in both sections of ileum was under 10% although results varied between patients, with some individuals experiencing an over 50% increase in DCs in the defunctioned ileum whereas others had an equally as large decrease (n = 8). Despite this variation between patients, the DC population in the defunctioned ileum did not differ significantly to the functional ileal population (p > 0.05) (Figure 3.2.A.). No significant change suggests nutrient deprivation in the defunctioned ileum did not impact immune surveillance by DCs.

The proportion of CD103⁺ DCs involved in Th1 and Th17 activation were also compared to give insight into possible T cell activation; from the functional to defunctioned ileum, the average proportion of CD103⁺ DCs was 45.9% and 38.2% respectively (n=4) (Figure 3.2.B.). However, this change was not significant (p = 0.125) suggesting nutrient deprivation in the defunctioned ileum did not affect the activity of this DC subset. However, this was not consistent amongst the cohort as certain individuals experienced large declines in CD103⁺ DC populations, and a greater sample size is required. Nevertheless, it does not appear that the ability of DCs to regulate tolerance and immune responses is impacted by nutrient deprivation.

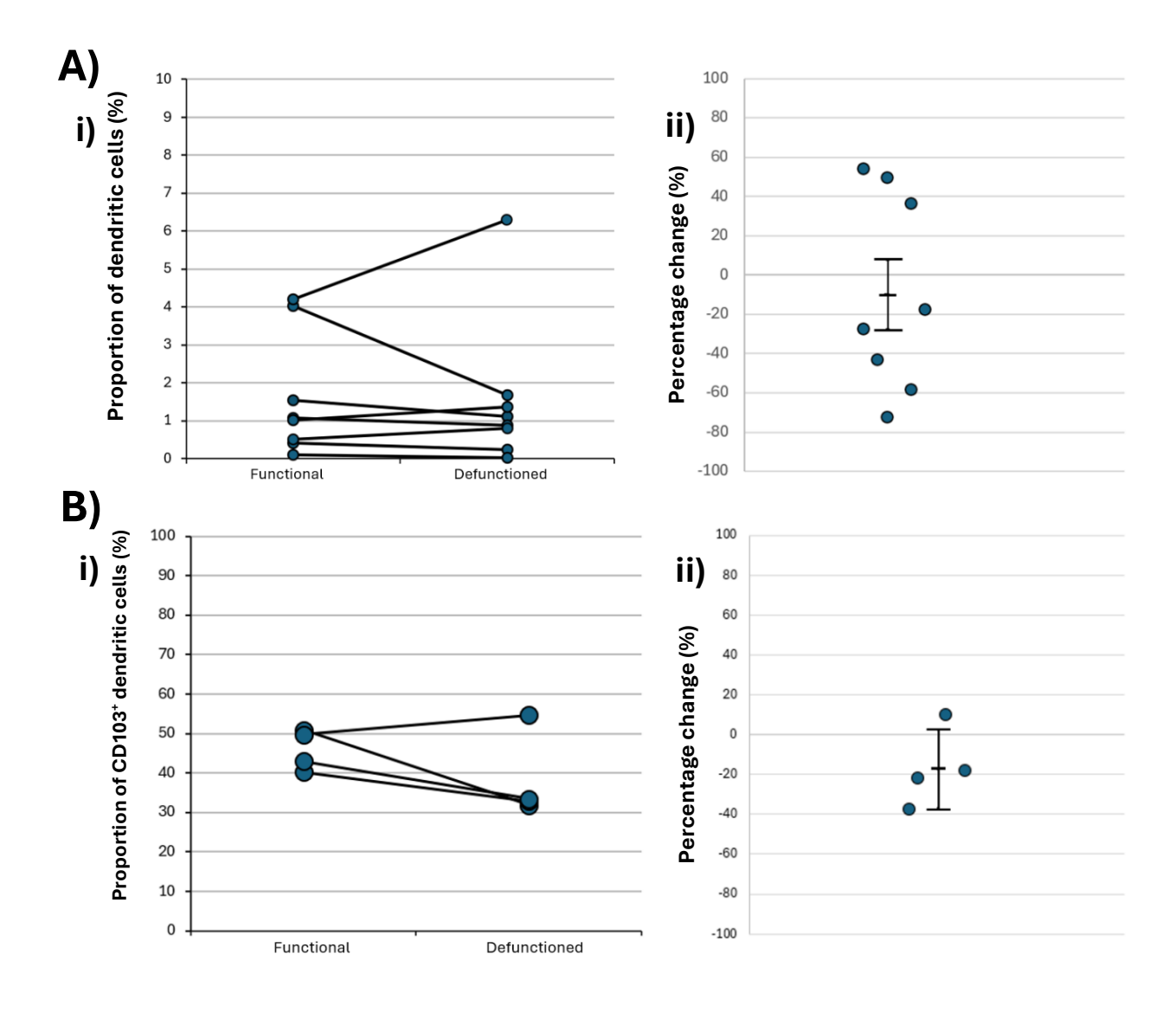


Figure 3.2. Neither DC, nor CD103 $^{+}$ DC, proportions were affected by nutrient deprivation in the defunctioned ileum. There was no significant difference in proportions of DC (ai; p > 0.05; n = 8) and CD103 $^{+}$ DC (bi; p > 0.05; n = 4) did not differ between the two sections. Percentage change in populations was also not significant (aii-DC, bii-CD103 $^{+}$, p > 0.05) (error bars = \pm SEM).

3.2.3. Stoma formation does not affect T cell populations in the defunctioned ileum

T cell populations were identified as CD3 $^+$ CD14 $^-$ and were hypothesised to be upregulated in the defunctioned ileum. The average proportion of CD3 $^+$ T cells was 14.3% and 16.9% in the functional and defunctioned ileum respectively. However, with an n of 3, these proportions did not differ significantly (p = 0.318) (Figure 3.3.), suggesting total T cell activity is not impacted by nutrient deprivation.

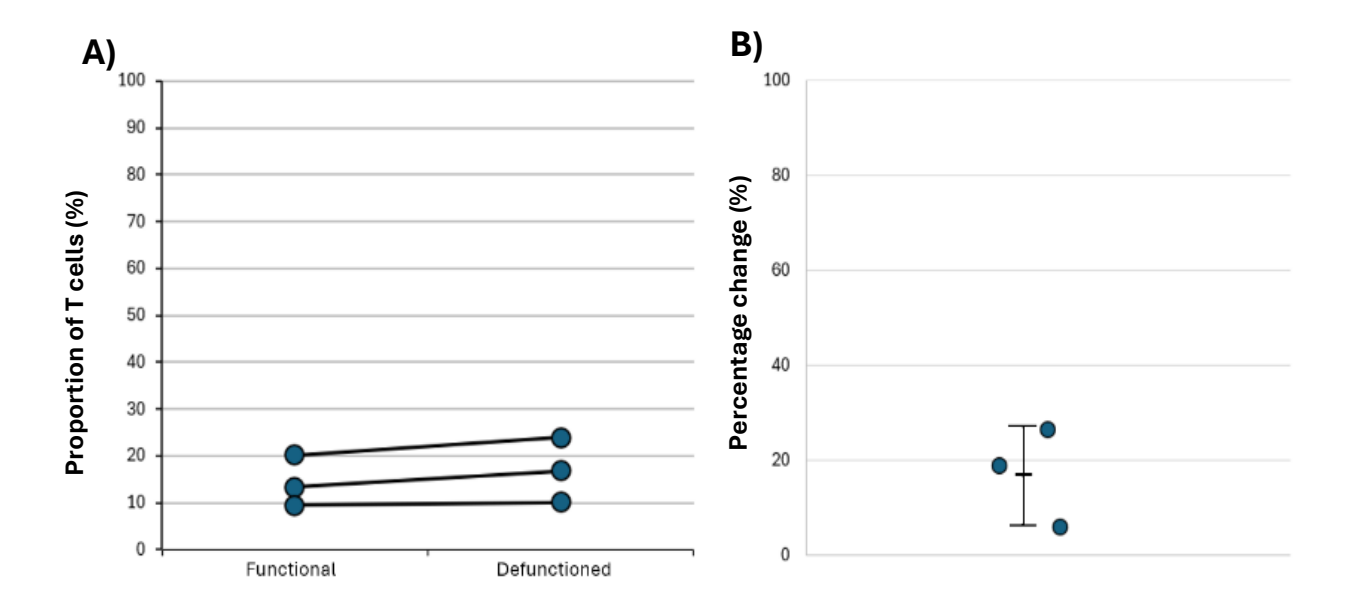


Figure 3.3. Nutrient deprivation did not affect CD3 $^{+}$ T cell populations in the defunctioned ileum. Flow cytometry was used determine whether the proportion cells that were CD3 $^{+}$ (T cells) differed between the functional and defunctioned ileum. There was no significant difference between T cell proportions between the two sections of the ileum (a, p > 0.0.5) and there was no significant percentage change (b, p > 0.05) (n = 3; error bars = \pm SEM).

No populations of immune cells investigated in this study experienced a significant change between the functional and defunctioned ileum. Despite stoma formation altering the microbiome and mucosal physiology, immune homeostasis appears to be maintained in the defunctioned ileum.

3.3. Characterising the physiological impacts of loop ileostomy and distal limb stimulation in the defunctioned ileum

3.3.1. Crypt depth as an indicator of stem cell proliferation

Beamish et al., 2017 reported a reduction in villus height and a concomitant decrease in PCNA-positive IECs, indicating a reduction in epithelial turnover in the defunctioned ileum. Crypt depth was assessed to determine whether this was an indicator of proliferative activity and, furthermore, whether this was impacted by DLS. H&E staining was performed on functional and defunctioned ileal samples from cohorts who had and had not (unfed) received DLS prior to reanastomosis. Slides were viewed under the light microscope to identify and measure villi and crypts. Figure 3.4. shows examples of the intestinal mucosa in the functional and defunctioned ileum from patients from each cohort. In the DLS cohort, macroscopically, stomas appeared more pliable and less shrunken compared to biopsies from patients in the unfed cohort. Microscopically, prebiotic feeding of the defunctioned ileum did not appear to affect the general appearance of the intestinal mucosa or crypt structure in particular.

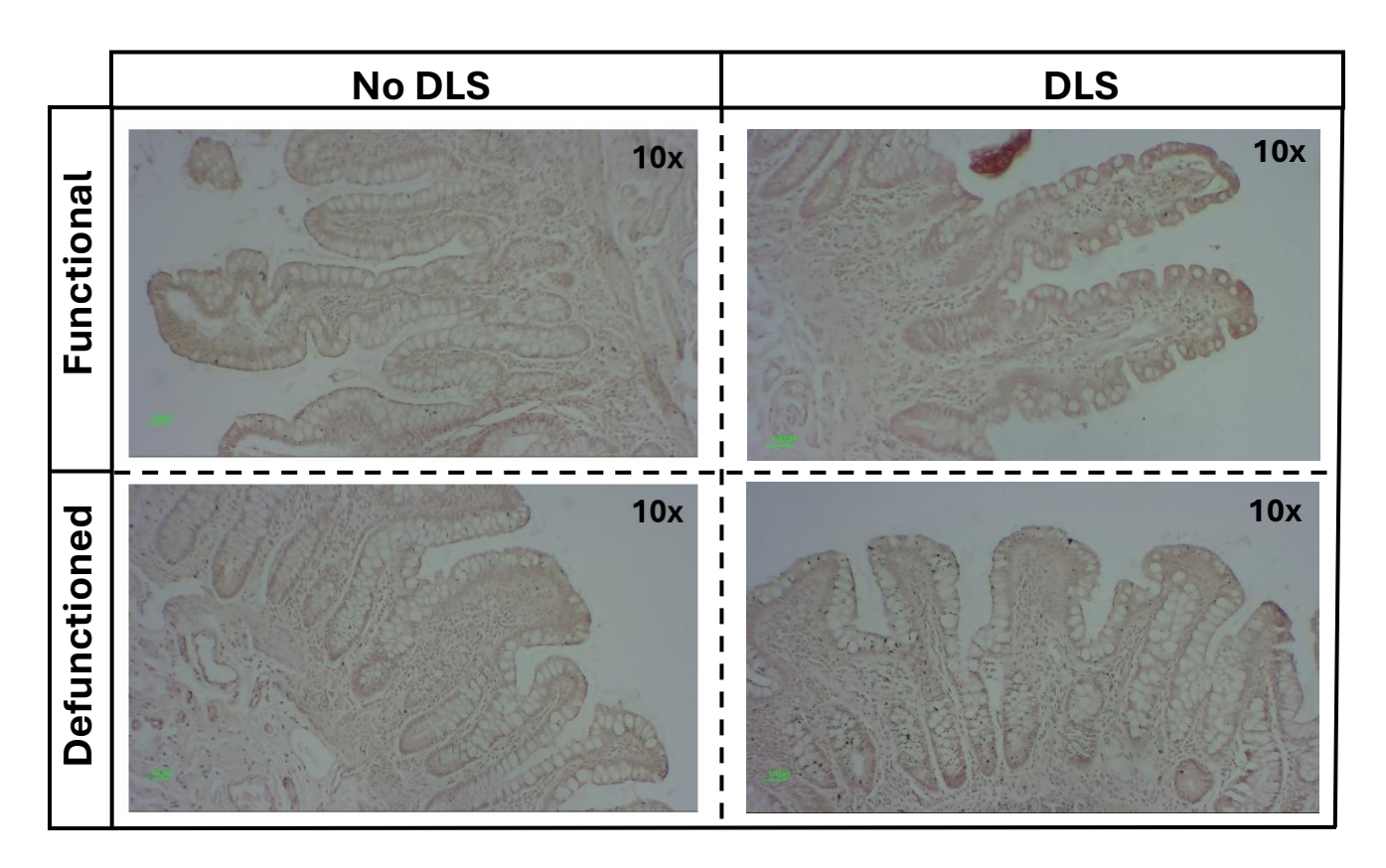


Figure 3.4. Epithelial physiology in the functional (top) and defunctioned (bottom) ileum of stoma patients prior to reanastomosis. Following H&E staining, ileal samples were viewed under the light microscope (objective lens 10X magnification) and images were captured using the Moticam X³ [Motic®]. Example images taken from Patient BCRG013 (left) and SFS002 (right).

3.3.2. Villus atrophy in the defunctioned ileum persisted with DLS

For each patient, a minimum of ten villi were measured within sections of functional and defunctioned regions of the ileum. Sufficient measurements were obtained for nine patients in the unfed group and three patients in the DLS group, and the average villus height for each patient was calculated (Figure 3.5.). As expected, a reduction in villus height from the functional to the defunctioned ileum was confirmed in all patients of the unfed cohort, with an average reduction of $-35.8\% \pm 3.8\%$ (p<00001). In the DLS group, villus height reduction was consistent ($-37.2\% \pm 1.2\%$) (p=0.00032) indicating DLS did not increase villus height, and villus atrophy was not successfully reversed.

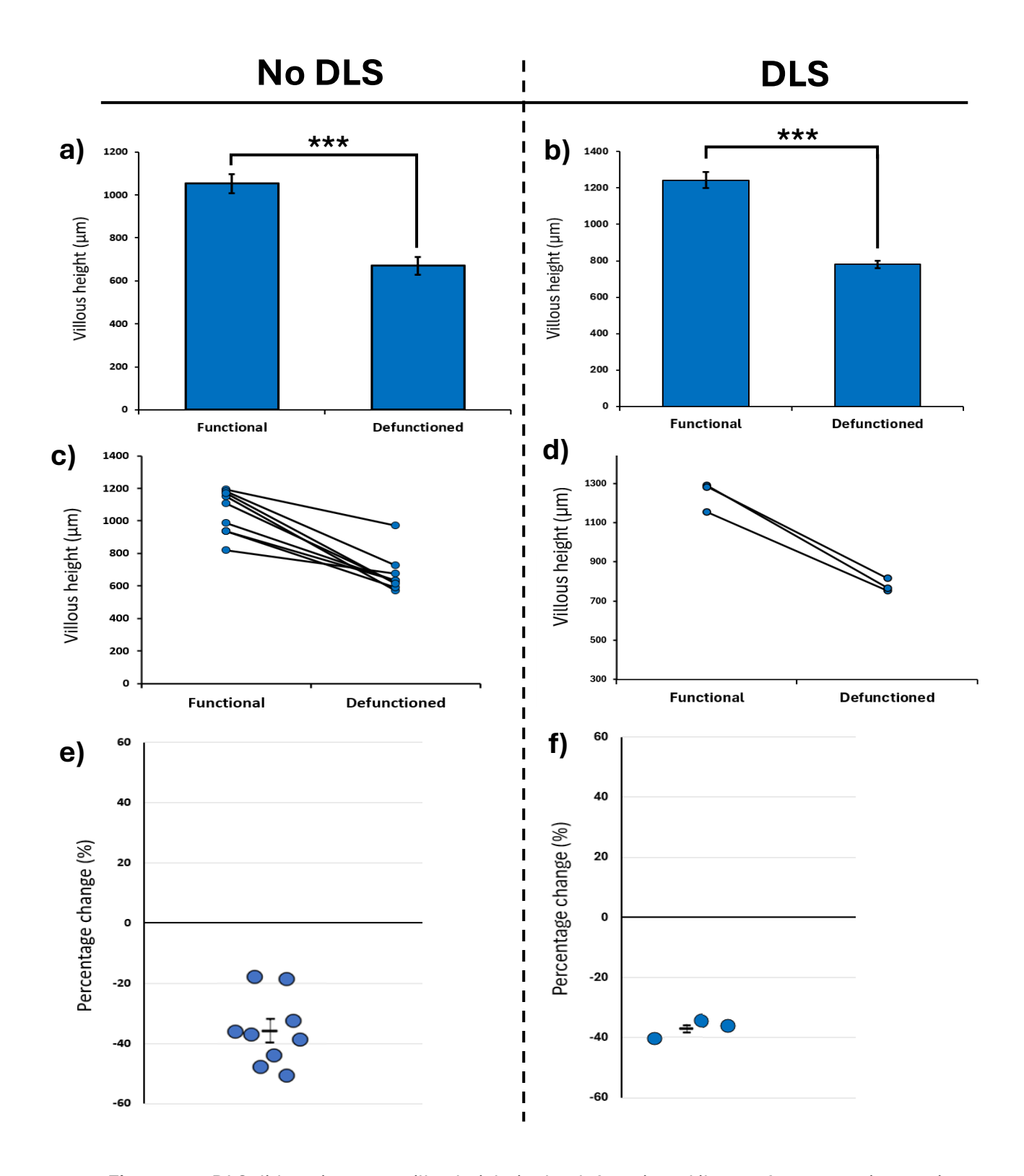


Figure 3.5. DLS did not increase villus height in the defunctioned ileum of stoma patients prior to reanastomosis. Between patients who had not received DLS (a,c,e) and those that had (b,d,f), the average villus height (a,b), paired villus height (c,d), and percentage change in villus height (d,f) were compared between the functional and defunctioned ileum. There was no significant improvement in villus atrophy following DLS and the percentage reduction from the functional to defunctioned ileum also did not differ (p > 0.05) (No DLS group, n = 9; DLS group, n = 3; error bars = \pm SEM, *** = p < 0.01).

3.3.3. The physiological effect of stoma formation and DLS on crypt depth in the defunctioned ileum

As with villus height, a minimum of ten intestinal crypts were measured in the functional and defunctioned ileum for each patient of both cohorts (unfed, n = 9; DLS, n = 3). There was no significant change in crypt depth from functional to defunctioned ileum in the unfed group prior to reanastomosis (p = 0.262) however, in the DLS group, the defunctioned ileum experienced a significant increase in crypt depth of $26.5\% \pm 14.6\%$ (p = 0.037) (Figure 3.6.). This indicates DLS has an influence on intestinal physiology and this increase may be the first sign of increased proliferative activity. A longer duration of DLS is likely required for other possible mucosal changes to be observed such as restoration of villus height.

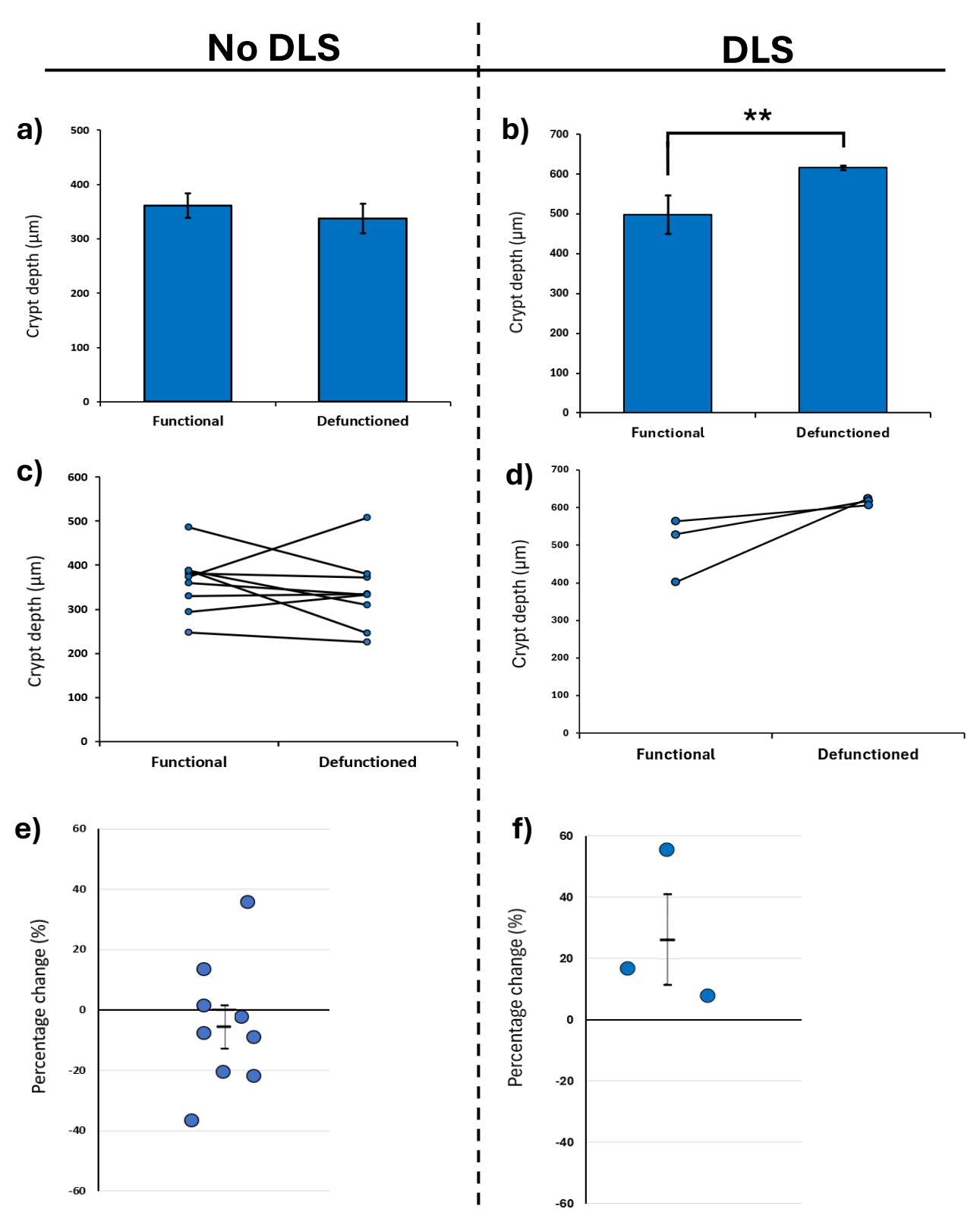


Figure 3.6. DLS significantly increased crypt depth in the defunctioned ileum of stoma patients prior to reanastomosis. Between patients who had not received DLS (a,c,e) and those that had (b,d,f), average crypt depth (a,b), paired crypt depth (c,d), and percentage change in crypt depth (e,f) were all compared between the functional and defunctioned ileum. Despite no difference in crypt depth in the unfed cohort, DLS significantly increased crypt depth in the defunctioned ileum (p = 0.037) (No DLS n = 9; DLS n = 3; error bars = \pm SEM, ** = p < 0.05).

3.4. Bioavailability of polyphenols

The study wanted to investigate the efficacy of SLNs in improving polyphenol bioavailability. Polyphenols were selected due to their prebiotic and anti-inflammatory abilities, making them a promising inclusion for DLS. However, current evidence suggests polyphenol bioavailability is low and variable which limits their beneficial effects. Firstly, an *in vitro* experiment aimed to confirm and compare the translocation of two polyphenols, ferulic acid and apigenin, through an intestinal epithelial monolayer.

3.4.1. in vitro polyphenol translocation

3.4.1.1. Optimising polyphenol detection

Following the protocol from 2.9.2., the translocation of ferulic acid and apigenin through an intestinal epithelial monolayer was assessed. A preliminary experiment was performed to optimise the detection of apigenin and ferulic acid from samples; HPLC was repeated three times at varying detection wavelengths: 240nm, 275nm, and 340nm. Seen in Table 3.2., 340nm yielded the greatest area under the peak and therefore the greatest detection of apigenin whereas for ferulic acid, 240nm was the optimal wavelength for detection. Therefore, these wavelengths were used for polyphenol detection.

Table 3.2. Wavelength optimisation for ferulic acid and apigenin detection via HPLC. HPLC was performed at three wavelengths: 240nm, 275nm, and 340nm to optimise the signal detection. The area under the chromatographic peaks were compared and the wavelength that gave the greatest area (and therefore the greatest signal) was selected for polyphenol identification. Apigenin produced the greatest signal at 340nm and ferulic acid at 240nm. (-) = no peak detected.

Polyphenol	Retention time (min)	Wavelength (nm)	Area under peak (apical)	Area under peak (basolateral)
Apigenin		240	325477	13755
	18.3	275	427489	21834
		340	649919	34772
Ferulic Acid		240	129361	11452
	9.6	275	79545	-
		340	116480	-

3.4.1.2. Polyphenol transport through an intestinal epithelial monolayer

Peaks corresponding to ferulic acid and apigenin were identified by comparison to HPLC chromatograms of media only (negative control) samples as well as using RTs from previous studies that have identified these polyphenols (Alaziqi et al., 2024). From the chomatograms in Figure 3.7., the RTs for apigenin and ferulic acid were determined to be approximately 9.6 and 18.3 minutes respectively. Although much lower than in the apical chamber, peaks for both polyphenols were identified on the basolateral side of the monolayer, indicating apigenin and ferulic acid were transported through the epithelial monolayer and released through the basolateral membrane. The area within the peaks for both polyphenols was greater in the apcial solution, suggesting a greater accumulation of polyphenols on this side of the monolayer. However, without a calibration curve, exact polyphenol concentrations cannot be calculated, so it is unknown how much of the original added dose of polyphenols are present in the basolateral chamber.

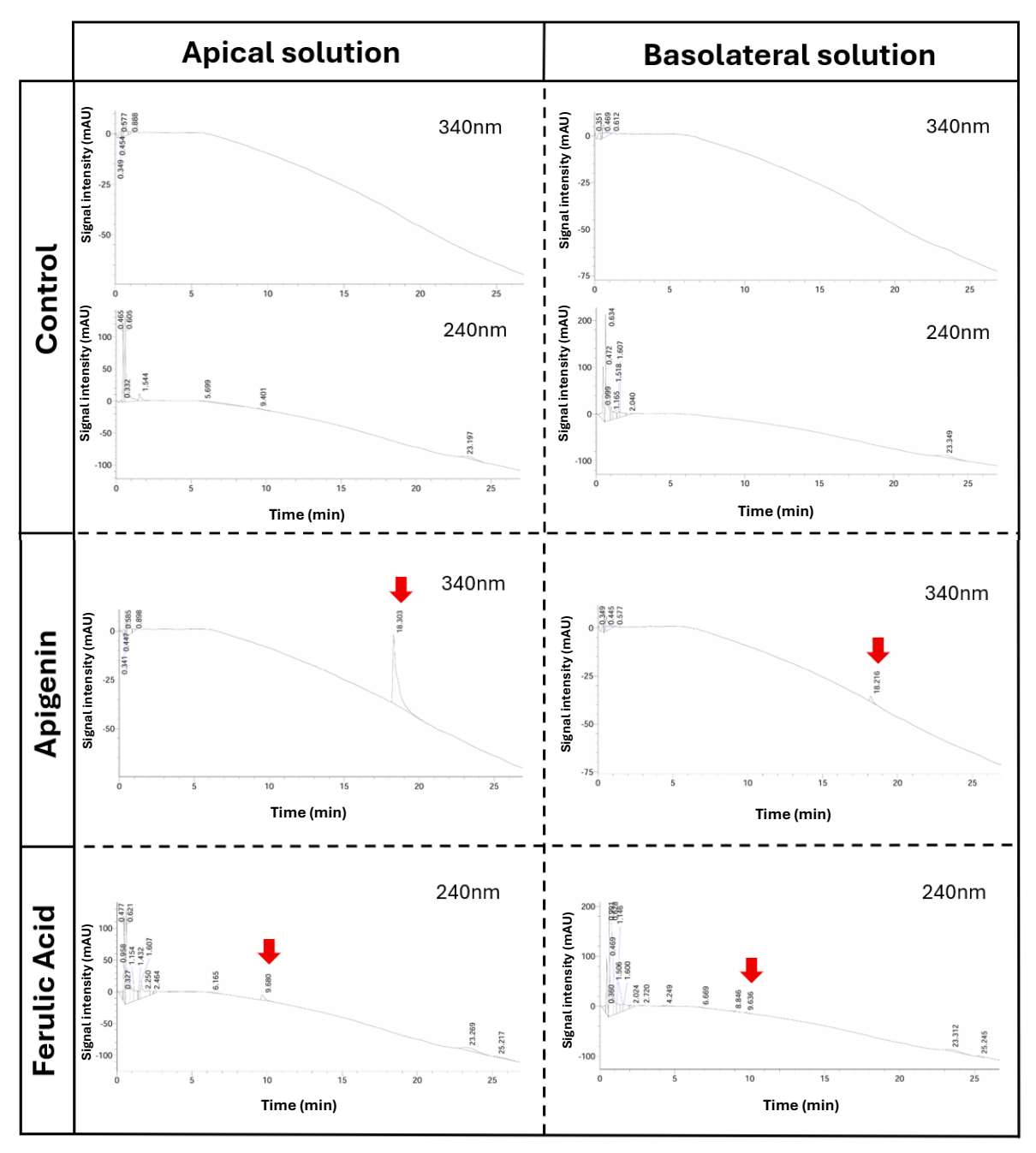


Figure 3.7. Apigenin and ferulic acid were detected in the apical and basolateral sides of the transwell epithelial monolayer. HPLC analysis was performed on the apical and basolateral suspensions following addition to the apical side of a Caco-2 monolayer. Chromatograms for the apical chamber (left) and basolateral chamber (right). Chromatographic peaks corresponding to apigenin (340nm) and ferulic acid (240nm) (indicated by red arrows) were present in both sides of the epithelial monolayer, confirmed by the absence of these peaks in the control suspensions.

3.4.2. *in vivo* assessment of solid lipid nanoparticles on polyphenol absorption

The influence of SLNs upon the absorption of EVOO extracts was investigated in a murine model. Groups received one of four treatments via oral gavage: a PBS control (Untagged Control, UC), a suspension of polyphenols (Untagged Polyphenol, UP), a suspension of SLN-tagged polyphenols (Tagged Polyphenol, TP), or a suspension containing only SLNs (Tagged Control, TC). The SLNs were tagged with the fluorophore, BODIPY and the small intestine, colon, and liver were harvested and imaged to identify SLN absorption and transport to the liver. HPLC was also performed to compare polyphenol accumulation in these organs between treatment groups.

3.4.2.1. Experimental monitoring

3.4.2.1.1. Physical observations suggest treatments were well tolerated

No changes in stool consistency were observed (no loose stool or diarrhoea), indicating treatments were well tolerated in the gut. The Mouse Grimace Scale (MGS) was used to examine any discomfort during the experiment. Developed by Langford et al., 2010, facial expressions were coded 0, 1, or 2, 'not present', 'moderate', or 'severe' respectively. Features assessed included orbital tightening, nose bulge, cheek bulge, ear position, and whisker change. No mice in any treatment group received a score above 0 for any category, suggesting SLNs and polyphenols were well tolerated.

3.4.2.1.2. Body mass was not affected by treatments

Throughout the experiment, mice were weighed before daily gavage. As seen in Figure 3.8., the mean body mass for each group remained consistent throughout the experiment with no changes greater than 1g occuring. As expected, performing an ANOVA and post-hoc test determined no treatments caused significant weight changes (p > 0.05).

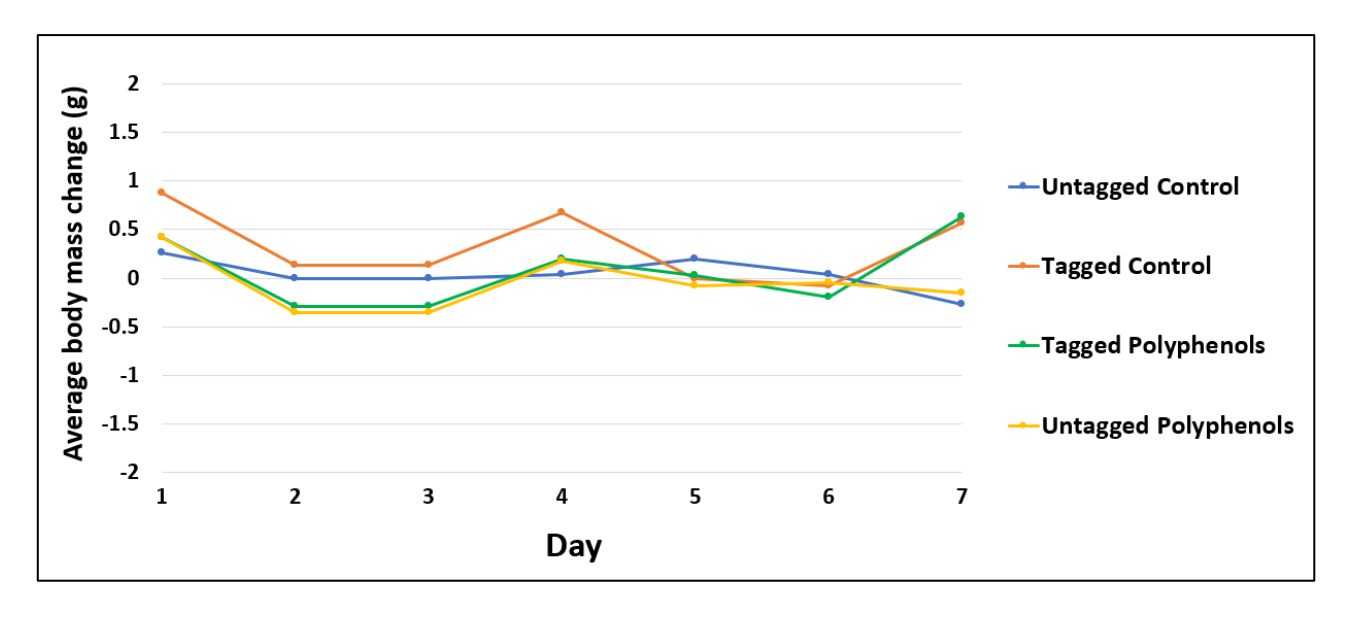


Figure 3.8. Average daily mouse mass was not affected by any treatments. Body mass of mice was monitored throughout seven days administration of either Untagged Control (blue), Tagged Control (orange), Tagged Polyphenols (green), or Untagged Polyphenols (yellow). Average body mass remained consistent for all treatment groups throughout the duration of the treatment (p > 0.05, each group, n = 4).

3.4.2.1.3. Treatments did not impact food intake

Each IVC's food was weighed each day to identify changes in apetitie. Food consumption for each IVC remained consistent throughout the study as well as between groups, indicating treatments had no impact on food intake (Figure 3.9.). As expected, there was no significant difference in food consumption between groups (p > 0.05). The anomolous results for the TC group between day four and five likely occured due to a human recording error.

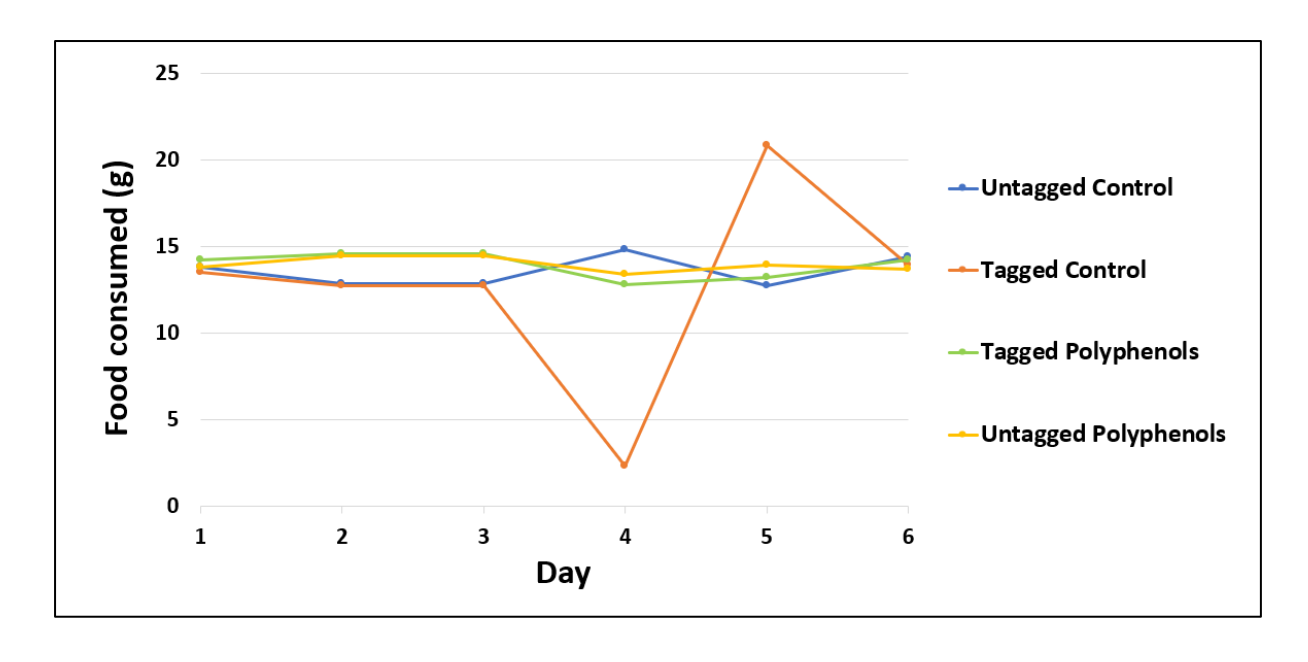


Figure 3.9. Food intake was not disrupted in any treatment groups. Daily chow consumption per group was monitored throughout seven days administration of either Untagged Control (blue), Tagged Control (orange), Tagged Polyphenols (green), or Untagged Polyphenols (yellow). There were no changes in food intake for any treatment group throughout the experiment (p > 0.05, each group, n = 4).

3.4.2.1.4. Organ mass at the end of the experiment

After completion of the study, liver, small intestine, and colon were harvested, washed with PBS (small and large intestine), and weighed. SLNs and polyphenols had no significant effect on small or large intestinal mass although liver mass was effected by polyphenol administration; an ANOVA and post-hoc test showed both TP and UP groups had a significant increase in liver mass compared to the UC group (p = 0.003 and = 0.007 respectively) and compared to the TC group (p = 0.018 and = 0.042 respectively) (Figure 3.10.A.). Despite this initial test implying polyphenol treatments alter liver mass, performing an analysis of covariance (ANCOVA) with total body as the covariate, there was no significant difference in liver mass between groups (p = 0.139).

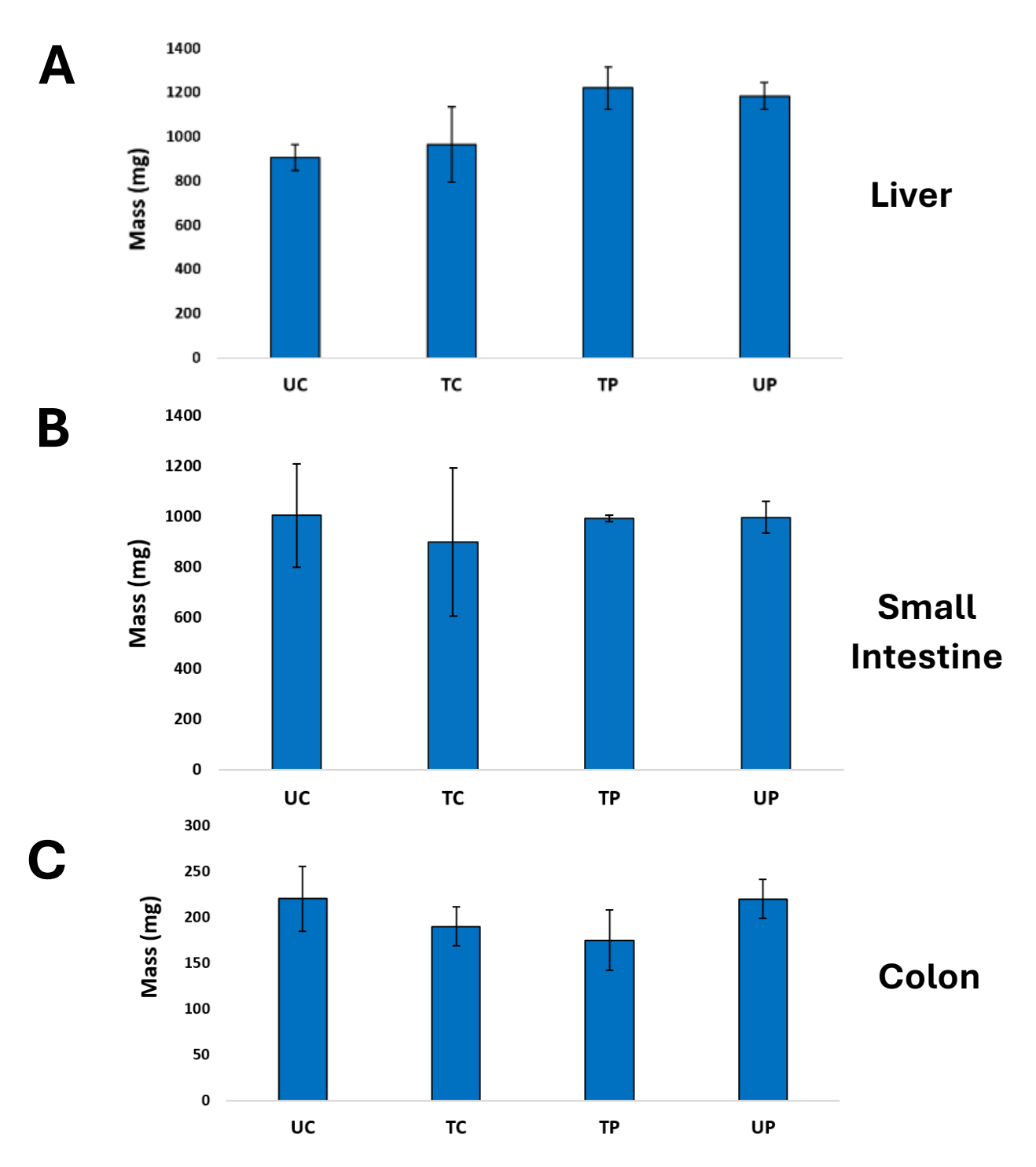


Figure 3.10. Comparison of average organ mass between treatment groups. Following seven days of administration of either Untagged Control (UC), Tagged Control (TC), Tagged Polyphenols (TP), or Untagged Polyphenols (UP), liver (a), small intestine (b), and colon (c) were all weighed. Average small and large intestine remained consistent between all treatment groups whereas polyphenol treated mice (TP and UP) had significantly increased liver mass. However, an ANCOVA revealed significant differences in liver mass was due to differences in total body mass (error bars = \pm SEM, each group, n = 4).

3.4.2.2. Colonic crypt depth is not altered by polyphenol administration

Proximal and distal colon tissue underwent histochemical analysis following the protocol in 2.2.3., 2.3., and 2.4.. Seven days of polyphenol treatments had no significant impact on crypt depth in either the proximal or distal colon compared to the untagged control group (p > 0.05, Figure 3.11.).

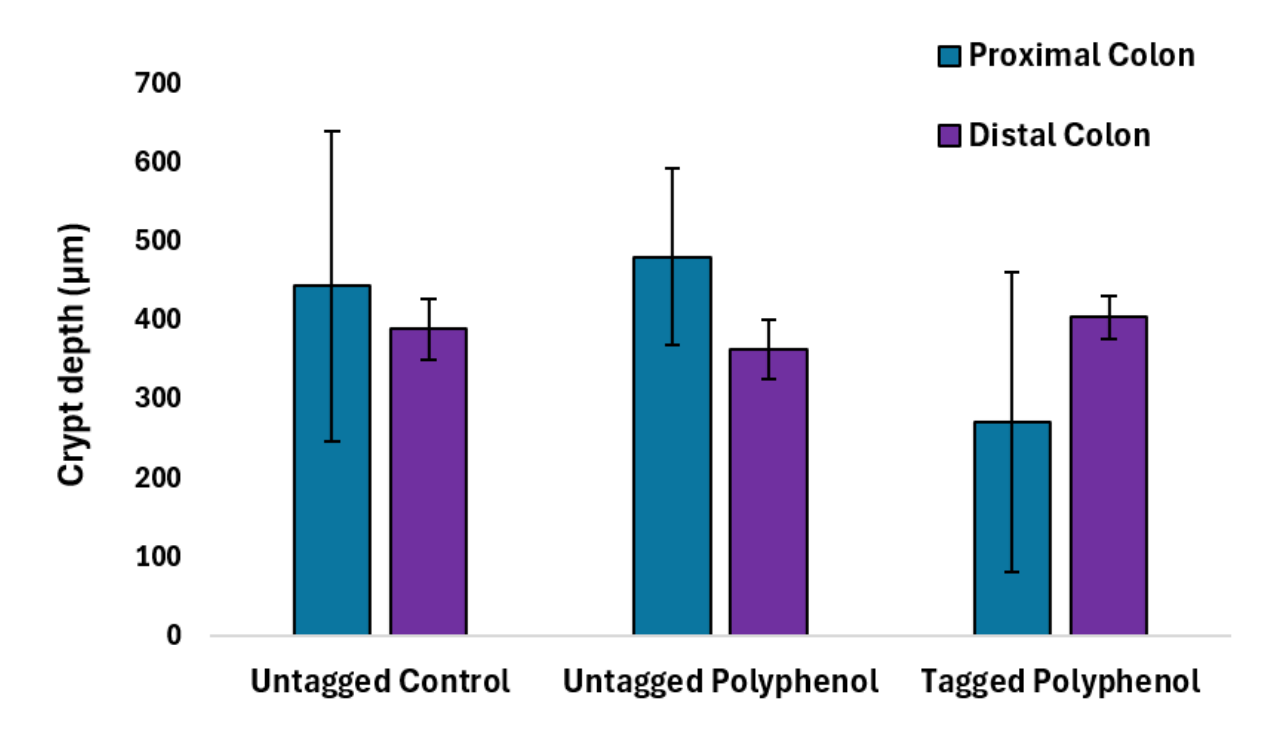


Figure 3.11. Colonic crypt depth following seven days of polyphenol administration. No polyphenol treatment resulted in a significant change in colonic crypt depth in either the proximal or distal colon compared to the untagged control (Proximal colon: blue; Distal colon: purple; error bars = ±SEM).

3.4.2.3. Fluorescence imaging

To confirm SLN absorption, the lower GI tract was harvested, flushed with PBS, and imaged using the iBright 1500 Imaging System under the FITC filter (495nm/520nm). It was expected that mice given the BODIPY-tagged SLNs (TC and TP) would exhibit greater fluorescence due to the presence of the fluorophore. However, fluorescence did not appear to differ between treatments, suggesting BODIPY (and the SLNs) were not absorbed into the tissue (Figure 3.12.).

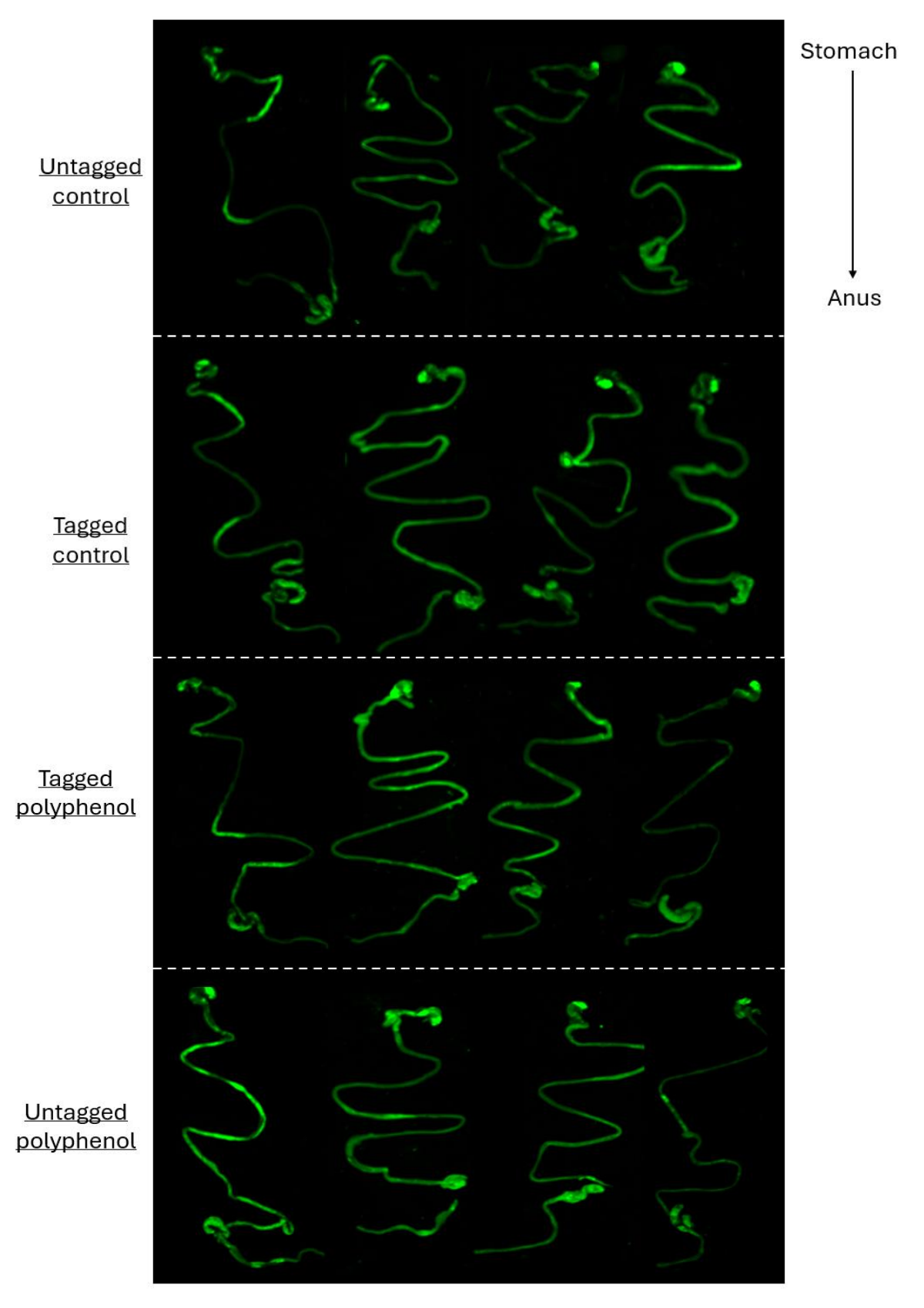


Figure 3.12. Fluorescence imaging of the gastrointestinal tract. After the seventh day of administration of either Untagged Control (1^{st} row), Tagged Control (2^{nd} row), Tagged Polyphenols (3^{rd} row), or Untagged Polyphenols (4^{th} row), the gastrointestinal tract from stomach to anus was imaged for each mouse using the iBright 1500 Imaging System under the FITC filter (495nm/520nm). No notable differences in fluorescence were observed between treatments (each group, n = 4).

Fluorescence imaging was repeated with liver samples (Figure 3.13.) and, again, no difference in fluorescence was observed between treatments. Although liver samples of certain individuals from SLN treatment groups (such as Mouse 3 of TP group) appeared to have greater fluorescence, this was minor and not consistent amongst the other liver samples within the treatment group. Therefore, it does not appear that BODIPY-tagged SLNs were present in the liver, suggesting they do not become systemic following administration.

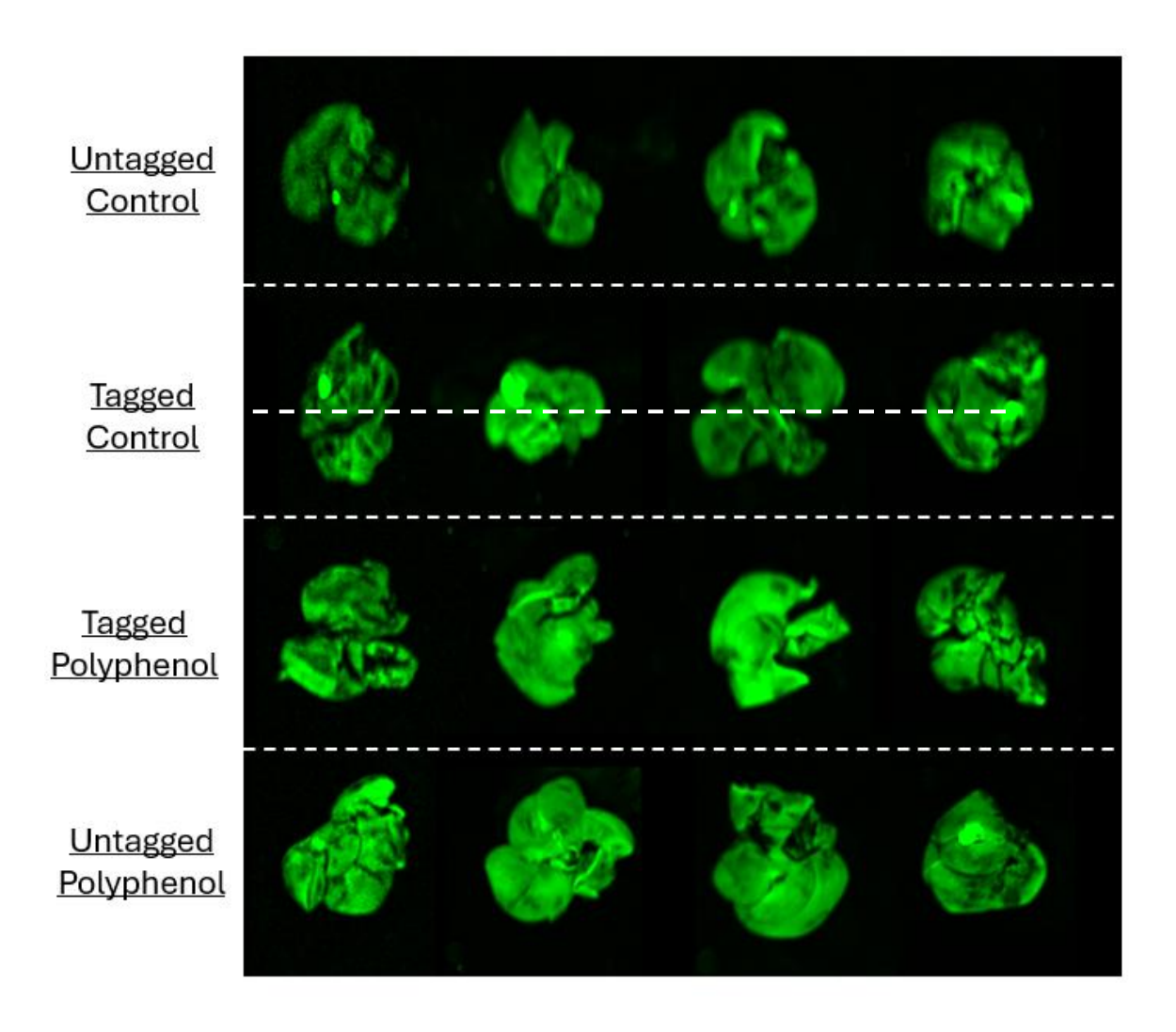


Figure 3.13. Fluorescence imaging of liver following treatment. After the seventh day of administration of either Untagged Control (1^{st} row), Tagged Control (2^{nd} row), Tagged Polyphenols (3^{rd} row), or Untagged Polyphenols (4^{th} row), liver from each mouse was imaged using the iBright 1500 Imaging System under the FITC filter (495nm/520nm). No notable differences in fluorescence were observed between treatments (each group n = 4).

To confirm if fluorescence differed between groups, the total correlated total cell fluorescence (CTCF) was calculated (Equation 2.2.) along the lower GI tract (duodenum, jejunum, ileum, caecum, and colon) and liver for each mouse. CTCF was used as it provided are more accurate reading for fluorescence as it considers the size of the tissue and any background fluorescence. For all treatments, fluorescence was low along the GI tract, with all regions measuring under 2.5RFU. Although CTCF was higher in the liver amongst all treatment groups, fluorescence did not differ significantly between treatments for any organ (p > 0.05, Figure 3.14.). The fluorescence observed may be epithelial autofluorescence or unflushed faecal matter in the lumen.

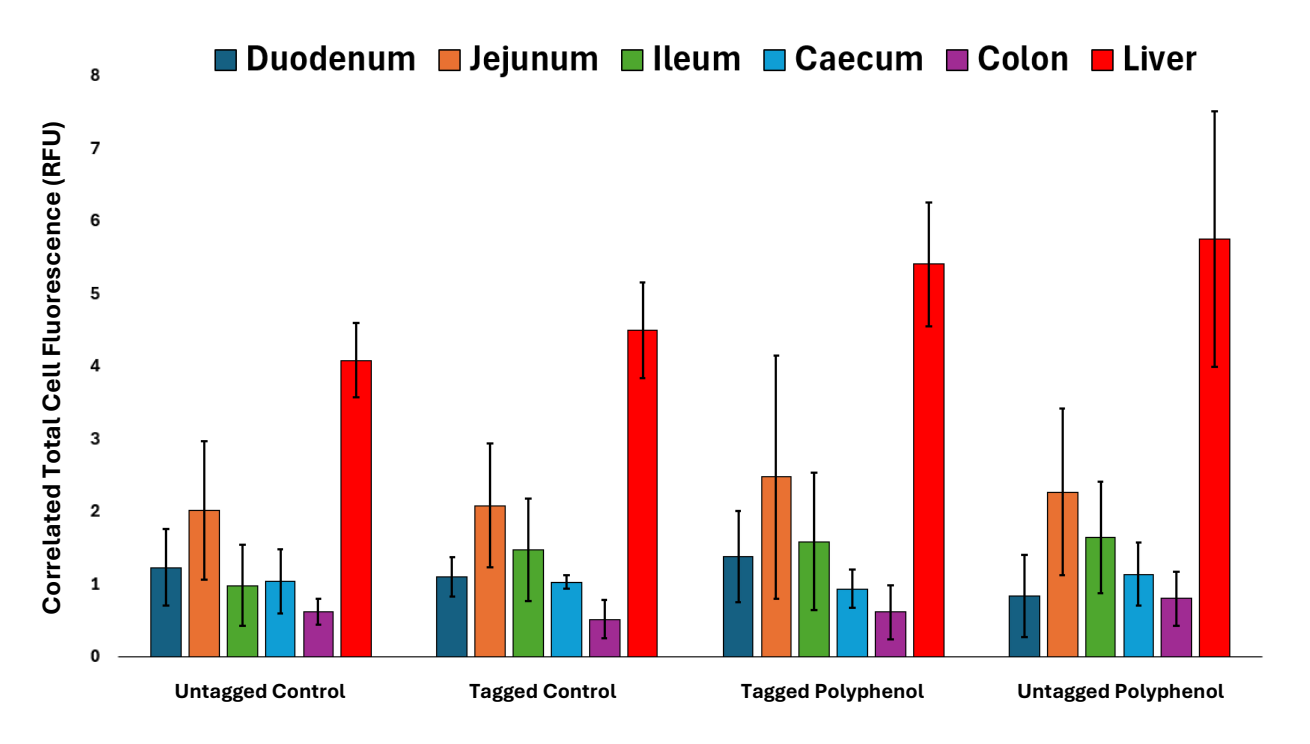


Figure 3.14. Correlated total cell fluorescence (CTCF) for the liver and gastrointestinal organs following treatment. After the seventh day of administration of either Untagged Control (UC), Tagged Control (TC), Tagged Polyphenols (TP), or Untagged Polyphenols (UP), the GI tract was imaged using the iBright 1500 Imaging System under the FITC filter (495nm/520nm) and, using ImageJ, the CTCF was determined for the duodenum (navy), jejunum (orange), ileum (green), caecum (turquoise), colon (purple), and liver (red). Between treatment groups, there was no significant difference in CTCF in any organs (RFU = relative fluorescence units, each group n = 4, error bars = \pm SEM).

3.4.2.4. Polyphenol detection using HPLC

In an attempt to conclusively determine whether SLN-tagged and untagged polyphenols could be absorbed in the GI tract, HPLC was performed on the small intestine, and colon. Furthermore, to determine whether polyphenols became systemic following administration, liver samples also underwent HPLC. Only initial data is available and compares the liver of mice from the UC and TP groups (Figure 3.15.). There were no additional peaks in the TP chromatogram, suggesting no polyphenols are present in the liver and were not systemic. Therefore, polyphenols may not have been absorbed in the GI tract, but with only an n of 1 and without HPLC analysis on the small intestine and the colon, this cannot be confirmed. From this initial, limited data, it is unclear whether SLN-tagged polyphenol absorption occurred or whether SLN tagging has improved bioavailability.

Liver- Untagged Control:

(NPE) uppdosqy -100 -1

Liver- Tagged Polyphenol:

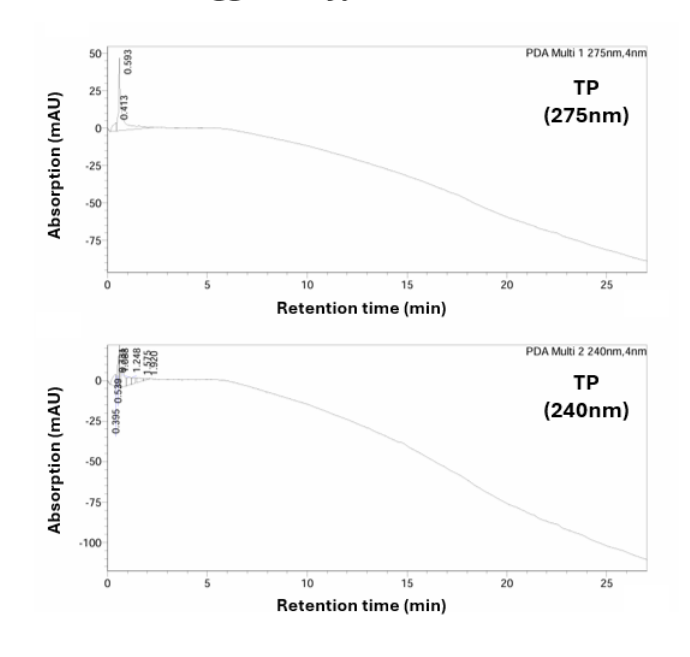


Figure 3.15. Chromatograms from HPLC analysis of liver tissue between Untagged Control and Tagged Control treatments. Following seven days of administration of either Untagged Control (UC), Tagged Control (TC), Tagged Polyphenols (TP), or Untagged Polyphenols (UP), HPLC was performed on harvested liver tissue. Preliminary data (n = 1 for each treatment) did not indicate the presence of polyphenols in the liver.

4. Discussion

4.1. Immunological state of the defunctioned ileum prior to reanastomosis

Due to ostensible compromised intestinal barrier function and increased potential for bacterial translocation, immune cell populations in the defunctioned ileum of stoma patients were hypothesised to be elevated. However, the results in 3.2. show no significant difference in total DC, CD103* DC, or T cell populations between the functional and defunctioned ileum. The immunological impacts of stoma formation on the defunctioned ileum have scarcely been investigated and findings vary amongst such studies. Previous research has focused on adaptive immunity, particularly T cells (Watanabe et al., 2022; Li et al., 2022; Turki et al., 2019), so DC populations in the defunctioned ileum have not been investigated in stoma patients. Although not identical to the environment in the defunctioned ileum, rats administered TPN experienced an increase in intestinal DC populations, suggesting nutrient deprivation may increase innate immune cell populations (Hagiwara et al., 2011). However, DC populations were measured after just seven days of nutrient deprivation, so results are not directly comparable as the environment in the defunctioned ileum was examined over a year since the defunctioning loop ileostomy was inserted.

Adaptive immune cells have been previously studied and a decrease in CD3⁺ T cells in the defunctioned ileum was reported (Watanabe et al., 2022; Li et al., 2022). However, another study found no change in T cell numbers (Turki et al., 2019) and there is further disagreement between studies when examining specific subsets; for example, Watanabe et al., 2022 found no change in IFN-γ⁺ T cells whereas a separate study found a decrease (Schmit et al., 2000). A notable explanation for the difference in results could be the profile of participants for each study. Immune cell populations were studied in IBD patients (Watanabe et al., 2022; Schmit et al., 2000), colorectal cancer patients (Li et al., 2022), and graft-versus-host disease (GVHD) patients (Turki et al., 2019) and the wide variety of pathologies had a range of associated treatments such as chemotherapies and immunosuppressants. Changes in immune cell populations may differ between patients with different pathologies and are likely influenced by

treatments the patients are undergoing. For example, chemotherapy has been shown to reduce T cell populations (McCoy et al., 2012) so possible immunological changes may be caused by patient-specific determinants rather than solely due to nutrient deprivation in the defunctioned ileum. As well as variations in treatments, patients with certain pathologies will already have disrupted immune cell populations prior to loop ileostomy surgery. For example, Crohn's disease is characterised by ileal inflammation (ileitis) resulting in elevated Th1 and Th17 cell numbers (Brand, 2009). For these patients, stoma formation may cause a decrease in pro-inflammatory T cells, although, this decrease would likely be to return T cells to homeostatic levels, rather than a physiological decrease below normal levels. Therefore, direct comparison cannot be made between the results in this study and previous studies that employed IBD and GVHD patients due to pre-existing dysregulated T cell populations. Notably, this pilot study excluded participants with IBD and a study that employed participants with both IBD and non-IBD showed non-IBD patients experienced a less extensive reduction in IFN- γ secreting T cells (Schmit et al., 2000). This indicates immunological changes observed in other studies may result from pre-existing T cell dysregulation. Therefore, contradicting the hypothesis that immune cells would be upregulated, there is limited evidence to suggest immune cell populations are affected by stoma formation. Additionally, the impact of ileostomy may be unique to each pathology and its associated treatment, making it difficult to draw conclusions at present.

The hypothesised increase in immune cell populations would likely correspond to chronic inflammation. Prior to reanastomosis, historic signs of inflammation have been reported in the defunctioned ileum, namely increased fibrosis and collagen type 1 expression (Beamish et al., 2017). However, inflammation scores immediately prior to reanastomosis did not differ between the functional and defunctioned ileum, indicating a lack of ongoing, chronic inflammation. This proposes a mechanism where, following stoma formation, there was an initial period of inflammation caused by an upregulation of immune cells but, with time, a possible 'dysbiotic equilibrium' was established where immune cell populations are not perturbed. Therefore, nutrient deprivation and subsequent reduction in bacterial load does not appear to have a long-term impact on immune cell populations and a new homeostasis is achieved, albeit at a potentially

compromised capacity. The consistency in CD103⁺ DC proportions between the functional and defunctioned ileum (3.2.) supports this theory, as elevated numbers of this subset would correlate to an increase in T cell activity and abundance. However, total T cell numbers were not changed, indicating immune cell responses are not dysregulated.

Despite these proposed mechanisms, the limited sample size must be considered, and a larger cohort may yield more accurate results. Additionally, investigation into specific T cell subsets would be more indicative to elucidate the immunological state of the defunctioned ileum. Only total CD3⁺ T cell populations were examined in this study, whereas specific quantification of pro- and anti-inflammatory T cell populations would confirm whether pro-inflammatory T cells are upregulated in the defunctioned ileum, confirming if there is ongoing inflammation. Performing flow cytometry to identify certain pro-inflammatory T cell subsets like Th1 and Th17 and ELISA (enzyme-linked immunosorbent assay) to measure levels of pro-inflammatory cytokines like IFN-γ, IL-2, and TNF-β would highlight any upregulated inflammatory responses occurring in the defunctioned ileum. Furthermore, only mucosal and LP immunity was assessed in this study, but the activity of these T cell subsets could be further elucidated by performing flow cytometry on small intestine-associated MLNs. This would provide a more accurate representation of CD103⁺ DC activity and T cell activation which occurs in the MLNs. For more accurate results, Cytometry by Time of Flight (CyTOF) could be implemented as multiple immune cells can be analysed and without the need for spectral compensation, reducing the risk of spectral overlap which can impact the accuracy of flow cytometry.

4.2. Physiological state of the defunctioned ileum prior to reanastomosis

Although well reported in previous studies, the physiological impacts of nutrient deprivation in the defunctioned ileum were still assessed. Work by Beamish et al., 2017 and numerous other studies had already reported a decrease in villus height in the defunctioned ileum (Williams et al., 2007; Li et al., 2022; Oh et al., 2005; Wieck et al.,

2017; Watanabe et al., 2022). As hypothesised, results in 3.2.2. confirmed that nutrient deprivation and lack of luminal stimulation in the defunctioned ileum caused villus atrophy. Crypt physiology was also assessed in a handful of these papers (Williams et al., 2007; Li et al., 2022; Watanabe et al., 2022) but no changes in crypt depth was observed in the defunctioned ileum, agreeing with the results in 3.3.3. However, other human studies (Wieck et al., 2017; Oh et al., 2005) and several rodent stoma models (Fowler et al., 2017; Józsa et al., 2009) reported a reduction in crypt depth and width following stoma formation.

Variation in results may depend on the duration with stoma and the type of participant included in each study. Stoma duration is an important consideration as the physiological environment in the defunctioned ileum changes over time. In the short term (two months with ileostomy), the functional ileum experienced post-surgical inflammation, causing hypertrophy characterised by an increase in villus height and mucosal thickness (Oh et al., 2005) as well as increased enterocyte proliferation (Józsa et al., 2009). In contrast, observations after nine months with ileostomy showed hypertrophy in the functional ileum was ameliorated, indicating prolonged duration with a stoma eventually leads to restoration of homeostasis and a reduction of inflammation in the functional ileum. Rodent stoma studies that reported a reduction in crypt depth in the defunctioned ileum took measurements less than a week following stoma formation. Therefore, differences between functional and defunctioned ileal crypt depth may not be a result of a decrease in the defunctioned ileum but more so hypertrophy in the functional ileum.

In the human studies that reported a reduction in crypt depth, one study examined physiological changes in neonates (Wieck et al., 2017). Similarly to the rodent studies, patients did not have a stoma for a prolonged period and newborns are known to have different intestinal environments than adults such as reduced gut microbial diversity (Hu et al., 2013). Crypt depth reduction observed in the second human stoma study (Oh et al., 2005) did not disclose the cohort demographic, so it is unknown whether age, pathologies, or associated treatments influenced these results.

Therefore, cohort age and stoma duration in these studies means they cannot be directly comparable to the findings of this study. Oppositely, all other studies which did

not report changes in crypt depth, employed adult patients who lived with the stoma for a prolonged period. These studies and our findings support a mechanism where there is an initial immunological response leading to physiological changes in both the functional and defunctioned ileum but, with time, immune responses cease, and homeostasis is achieved, restoring normal crypt depth.

4.3. Physiological impacts of DLS in the defunctioned ileum prior to reanastomosis

DLS in the defunctioned ileum was hypothesised to boost the diminished bacterial load and improve mucosal physiology, particularly by reversing villus atrophy. Nutrient deprivation models have previously demonstrated the effectiveness of DLS to improve the intestinal environment. For example, after just three days of refeeding, villus and crypt atrophy and reduced enterocyte thickness was reversed in starved rats (Dunel-Erb et al., 2001). Furthermore, return to enteral feeding increased villus height and gut weight in a TPN rat model (Mukau et al., 1994), proving intestinal atrophy can be reversed with luminal stimulation. However, despite all nutrient deprivation models sharing similarities in intestinal environments, the defunctioned ileum is unique and may respond differently to DLS.

Prebiotic DLS has previously demonstrated its success at reducing post-reanastomosis complications (Abrisqueta et al., 2014; Garfinkle et al., 2023) so a prebiotic approach was selected for this study. Despite the hypothesis that restoration of eubiosis in the defunctioned ileum would reverse mucosal atrophy, villus height in the defunctioned ileum was not increased. Despite no change to villus height, a significant increase in crypt depth was observed, potentially demonstrating the replenishment of proliferative activity in the crypt base. Although increased crypt depth can be associated with intestinal damage or inflammation (Bereswill et al., 2010), this is unlikely to be the case, as macroscopically, tissue samples appeared healthier and less shrunken following DLS.

Although not employing a prebiotic approach, one comparable study showed PCNA expression was increased following succus entericus (digestive enzyme mixture) reinfusion (Zhu et al., 2011). Cells in the crypt base are known to secrete PCNA (Yamada et al., 1992) and these cells are reported to be decreased in the defunctioned ileum (Beamish et al., 2017). Therefore, an increase in PCNA-positive cells following DLS suggests crypt base-located PCNA-positive cells are replenished, possibly indicating the upregulation of proliferative activity in the defunctioned ileum. Another form of DLS, faecal recycling, was also shown to boost proliferative activity, causing an increase in Ki67-positive cell numbers in the defunctioned ileum (Uga et al., 2021). Therefore, the observed increase in crypt depth following DLS may be attributed to a potential increase in proliferating cells, making the crypts appear deeper. Intestinal crypts are the initial responders to changes in intestinal environment and an increase in crypt depth may be the first sign of the restoration of intestinal homeostasis.

Cells local to the crypt base like Paneth cells are also reduced by stoma formation (Wieck et al., 2017) and an increase in crypt depth may correspond to an increase in Paneth cell numbers or activity. Paneth cells are responsible for maintaining the stem cell niche, so their replenishment would likely increase proliferative activity, such as an increase in PCNA-positive and Ki-67 positive cells in the crypt base. Restoration of the stem cell niche would correspond to increased ISC numbers and activity, allowing mucosal atrophy to be reversed. Using immunohistochemistry and fluorescence microscopy would confirm the replenishment of Paneth cells and to investigate whether their activity is increased and the stem cell niche is replenished, Wnt, EGF, and Notch signal levels before and after DLS could be compared using qPCR. Additionally, ISCs and goblet cells are reduced in the defunctioned ileum so determining if DLS increased numbers of these cells would give additional insight into intestinal barrier integrity and function. Another approach to elucidate changes to the intestinal environment could be to investigate changes in gut hormone levels associated with intestinal growth and repair such as gastrin, cholecystokinin, or glucagon-like peptide-2 (GLP-2).

However, despite the proposal of a mechanism where the stem cell niche and ISC activity is restored, villus height did not increase following DLS. The persistence of

villus atrophy may be attributed to the variation in feeding regime between patients, from three weeks to just three days prior to reanastomosis. The short period of time, accompanied by the small cohort, may limit the observable changes caused by DLS and with a prolonged, uniform feeding regime, villus height may increase, as seen following faecal recycling in mice (Uga et al., 2021). An n of 3 limits the confidence in these results as smaller cohorts reduce the study's statistical power and anomalous results contribute to poor representation of findings.

Although this study focused on prebiotic DLS, any potential changes to microbial composition are still unknown. The hypothesised mechanism, and rationale for this pilot study, was prebiotic DLS would increase the bacterial load, restore the normal intestinal environment, and reverse mucosal atrophy. Although further investigation is required, the findings in this study support this mechanism as initial signs of increased intestinal activity were observed, possibly attributed to an improvement in microbial composition. Functional and defunctioned ileal tissues have been prepared for 16S rDNA sequencing which will elucidate any changes to bacterial load and composition following DLS. Unfortunately, these data are not currently available, so it is unknown whether the prebiotic suspension used in this experiment successfully altered the gut microbiome. As well as 16S rDNA sequencing, other indicators of intestinal eubiosis, such as increased levels of SCFAs could also be investigated as this would indicate an increase in beneficial bacteria and improvement to the intestinal environment. Goblet cells are regulated by the gut microbiome (Engevick et al., 2019) so assessing goblet cell abundance and activity would not only be indicative of the condition of the intestinal environment but would also indirectly give insight into the state of the microbiome.

Although these findings are limited, they indicate early signs of intestinal replenishment following DLS, despite a very small sample size. This indicates that the DLS-induced reduction of post-operative complications following reanastomosis may be caused by the restoration of intestinal homeostasis and normal mucosal physiology. These initial data support the inclusion of DLS prior to reanastomosis, not only to reduce post-operative morbidity but also to improve the intestinal environment.

4.4. Investigating polyphenol bioavailability

4.4.1. Polyphenol translocation through an intestinal epithelial monolayer

Polyphenol bioavailability is not completely elucidated, but previous studies report high variability in metabolism and absorption. HPLC was used to investigate ferulic acid and apigenin translocation through a Caco-2 epithelial monolayer. As expected, both ferulic acid and apigenin were detected in the basolateral chamber, suggesting polyphenols were transported through the apical epithelial membrane and released through the basolateral membrane. However, polyphenols were detected at extremely low concentrations and, for ferulic acid, were only detected under the optimal wavelength (240nm). Additionally, without the inclusion of a calibration curve with known polyphenol concentrations, the exact amount of ferulic acid and apigenin present in the basolateral chamber cannot be calculated. Although both ferulic acid and apigenin were previously shown to pass through an epithelial monolayer (Sánchez-Marzo et al., 2019; Konishi and Shimizu, 2003), this gives limited insight into their metabolism and absorption in situ. Polyphenol metabolism is reliant on enteric bacteria-produced digestive enzymes (Zhu et al., 2018; Gaur et al., 2020; Szwajgier and Jakubczyk, 2010) but in vitro experiments are performed under a sterile environment, without a microbiome. Therefore, these experiments do not reflect the absorption of polyphenols in the GI tract and cannot give complete insight. Additionally, it is not confirmed that the added polyphenols are passing through the apical and basolateral membranes of the cells to reach the basolateral chamber and may be translocating the monolayer via adherens junctions or tight junctions. Future work could visualise polyphenol translocation through the monolayer by fluorescently tagging the polyphenols and using confocal microscopy to determine whether polyphenols pass through or in between cells. For further confirmation, membrane transport blockers such as phloretin and benzoic acid could be introduced into the apical chamber and assess whether this hinders polyphenol translocation, indicating polyphenols are reliant on transport through the apical membrane.

Low detection on the basolateral side of the monolayer may not result from low translocation but could be due to too small a concentration of polyphenols used in the experiment. Other studies, for example, added ferulic acid at 5mM (Konishi and Shimizu, 2003) and apigenin at 1.4µg/ml (Sato et al., 2024) whereas 10µmol/l was used in this study. Therefore, increasing the concentration added to the apical side of the monolayer will make detection in the basolateral chamber easier and will be helpful when detecting polyphenol translocation.

4.4.2. Attempts to improve polyphenol bioavailability

4.4.2.1. Impact of SLNs and EVOO extracts on colonic physiology

Colonic crypt depth was compared between treatment groups to identify if polyphenol or SLN administration altered mucosal physiology. The colon was selected as it has the greatest microbial density (Rastall, 2004) and is the location for the majority of polyphenol absorption (Clifford, 2004). As expected, crypt depth did not vary between treatments, indicating there was no detrimental impacts on physiology. Because the mice involved in the study were healthy, wildtype mice with normal mucosal physiology, potentially beneficial physiological effects may not be observed. Comparatively, previous studies have used disease models to highlight EVOO's ability to improve intestinal barrier function and reverse intestinal atrophy. EVOO was able to ameliorate mucosal crypt loss following DSS-induced colitis and demonstrated crypt regeneration (Sánchez-Fidalgo et al., 2011) as well as reduce the number of dystrophic goblet cells and crypt abscesses (Cariello et al., 2020). Using an ileitis model to assess the effects of EVOO administration on mucosal atrophy would demonstrate possible benefits conveyed to ileal physiology.

4.4.2.2. Impact of SLNs on polyphenol bioavailability

Following imaging of the liver and lower GI tract, fluorescence was hypothesised to be greatest in SLN-tagged treatments. However, organs showed no difference in fluorescence between treatment groups, confirmed by calculating CTCF, which did not

differ significantly between mice. This suggests no fluorescently tagged SLNs were present in the tissue, indicating SLNs were not absorbed or transported to the liver. However, there was no confirmation that the BODIPY fluorophore could be detected by the iBright 1500 so SLNs may be present in tissues but just cannot be visualised. In future experiments, treatments should be pipetted out and imaged to confirm that the fluorophore can be imaged and, if not, a different fluorophore should be employed such as fluorescein. Nevertheless, initial results from HPLC analysis did not detect SLN-tagged polyphenols in the liver, suggesting polyphenols were not systemic. However, with just an n of 1, no conclusions can be made regarding polyphenol absorption in this experiment. It is therefore unknown whether SLN-tagged EVOO extracts are absorbed and, if so, at a greater rate than untagged extracts. Previous administration of polyphenols only resulted in less than 1% of the original dose detected in the liver, (Soleas et al., 2001); therefore, the sensitivity of HPLC may limit polyphenol detection in these tissues.

Previous studies have not analysed liver tissue to identify the presence of polyphenols, but plasma concentrations of resveratrol (Zhang et al., 2019; Pandita et al., 2017) and curcumin (Baek and Cho, 2017; Ban et al., 2020) were increased by SLN-tagging.

Therefore, with further analysis, SLN-tagged EVOO extracts may be detected in the liver and at a greater concentration than untagged extracts. Due to the lack of data available and lack of repeats, no conclusions can be made regarding the effectiveness of SLNs in increasing polyphenol bioavailability. Based off previous studies, SLNs appear to increase polyphenol absorption and have been suggested to enhance uptake in the small intestine, making them a promising inclusion for DLS. Upcoming data will aim to reveal whether SLNs increase polyphenol bioavailability and whether SLN-tagged polyphenols are absorbed in the small intestine. Furthermore, to improve accuracy of future results and eliminate potential sex-specific biological responses, groups of both male and female mice should be employed for each treatment.

4.4.2.3. Suitability for SLN-tagged EVOO extracts in DLS

For EVOO and its polyphenolic extracts to be a useful inclusion in DLS, they must improve iteal dysbiosis and reverse mucosal atrophy. EVOO has previously successfully reversed atrophy, but this has only been demonstrated in the colon. Improvements to iteal atrophy (essential for DLS) have not been reported in EVOO extracts but resveratrol and grape seed extract (GSE) have reduced the extent of intestinal shortening and crypt deepening in mouse iteitis models (Bereswill et al., 2010; Yang et al., 2014). Although these studies are promising, this study has hypothesised that atrophy in the defunctioned iteum results from nutrient deprivation and a reduced bacterial load, rather than long term inflammation (Beamish et al., 2017). Therefore, for EVOO to be beneficial to DLS, it must reverse dysbiosis and stimulate intestinal cell activity. EVOO has previously been shown to increase the abundance of beneficial bacteria in disease models (Vezza et al., 2019; Martín-Peláez et al., 2017) but this has not been demonstrated in nutrient deprivation models. Additionally, microbial analysis is traditionally performed on faecal samples, so it is unclear whether the iteal microbiome is improved by polyphenol intake.

Low bioavailability in the small intestine also discourages the inclusion of EVOO in DLS; previous studies have demonstrated SLNs allow for nutraceuticals to be absorbed in the small intestine (Oehlke et al., 2014), but polyphenols are distinct in that they are proposed to transit the small intestine without being absorbed (Clifford, 2004). Additionally, SLN tagging may impair the prebiotic abilities of polyphenols by blocking their metabolism from enteric bacteria, further limiting their capabilities.

Future HPLC analysis will determine if SLNs can improve polyphenol bioavailability in the small intestine and using 16S rRNA or rDNA sequencing to compare microbial composition will determine whether ileal microbial composition is improved and whether SLN tagging effects this. If absorption in the small intestine is still limited and the ileal microbial composition is not influenced, polyphenols may not be appropriate for DLS.

4.5. Conclusion

Unexpectedly, comparison of DC and T cell populations found no difference between the functional and defunctioned ileum, suggesting no inflammatory or anti-pathogenic responses were upregulated at the time of reanastomosis. Therefore, villus atrophy, reported in this study, and other signs of atrophy in the defunctioned ileum such as a reduction in Paneth and goblet cells, were not attributed to dysregulation of immune responses. The preliminary findings of this pilot study are the first to investigate the impact of prebiotic DLS on intestinal physiology in the defunctioned ileum. Although the primary indicator of atrophy, villus height reduction, was not improved by DLS, crypt depth was increased. This could be an initial indication of restored proliferative activity in the crypt base and this study is the first to report this. This could indicate the start of restoration of the normal intestinal environment, supporting the use of DLS prior to reanastomosis to improve intestinal physiology. This may also improve bacterial dysbiosis and contribute to the reduction in post-operative complications reported in other studies. These findings demonstrate the pilot study's feasibility and, therefore, can be expanded to more participants and include a more in-depth investigation. For example, the effectiveness of DLS can be confirmed by analysis of activity of cells located in the crypt base such as Paneth cells and ISCs to determine whether proliferative activity is boosted in the crypts. Also, with a longer, uniform feeding regime other physiological changes caused by DLS may be observed. The study is also limited by the lack of optimisation of DLS suspension. The chemical composition of the nutrient stream that reaches the distal ileum via oral feeding likely differs from the nutritional composition of the DLS suspension used in this study. Therefore, further development of the suspension is required to best replicate the normal nutrient stream that passes through the distal ileum.

Alongside this pilot study, the murine study attempting to improve polyphenol bioavailability using SLNs was unable to yield sufficient evidence to conclude if SLNs increase polyphenol uptake. Despite their proposed prebiotic benefits, the inclusion of polyphenols in DLS is currently still unfeasible due to their low bioavailability in the small intestine. Hopefully upcoming data will determine whether SLN-tagged

polyphenols are absorbed in the small intestine at a greater rate than untagged polyphenols, increasing their usefulness in DLS.

5. Appendix

5.1. APES-coated microscope slides

In the fume hood, microscope slides placed in a slide rack were immersed in 1% acid alcohol (1% (v/v) concentrated HCl, 70% ethanol, 29% H_2O) for thirty minutes to clean the slides. Slides were then rinsed under running water, immersed in distilled water, then removed and allowed to dry. Once dry, slides were immersed in acetone [Sigma-Aldrich®] for ten minutes followed by immersion in 2% (v/v) APES (aminopropyltriethoxysilane [Sigma® A3648]) for a further five minutes. Slides were then briefly immersed in two sequential rinses of distilled water and left to dry overnight. Once dry, APES-coated slides were transferred to a dust-free container and stored for up to several months.

5.2. Flow cytometry

5.2.1. Cell surface antibodies

Table 5.1. Cell surface antibody panels used in flow cytometry acquisition.

Human T cell panel	Human DC/macrophage panel
CD45 (PE/Cy7)	CD45 (BV750)
CD3 (PerCP)	CD3, CD19, CD20, CD56 (FITC- 'dump' channel
CD4 (Spark violet 500)	HLA-DR (PE/Cy7)
CD25 (BV650)	CD11c (PERCP)
CD127 (PE)	CD68 (APC)
CD8 (PE/Dazzle 594)	CD163 (BV605)
	CD86 (PE)
	CD103 (BV421)

5.2.2. Patient filter panels

Table 5.2. Flow cytometry filter panel for Patient BCRG003.

BCRG003		FL-1	FL-2	FL-3	FL-4	FL-5
Functional	Defunctioned	FITC	PE	APC	PE-Cy7	APC-Cy7
1	8	TLR5	CD103	Cocktail	HLA-DR	Dye
2	9	TLR5	CD11c	Cocktail	HLA-DR	Dye
3	10	TLR5	CD163	Cocktail	HLA-DR	Dye
4	11	IgG2a	CD103	Cocktail	HLA-DR	Dye
5	12	IgG2a	CD11c	Cocktail	HLA-DR	Dye
6	13	IgG2a	CD163	Cocktail	HLA-DR	Dye
7	14	TLR5	lgG1	Cocktail	HLA-DR	Dye
	Comp. ctrl					
	15	lgG2a				
	16		IgG1			
	17			CD3		
	18				IgG2a	

Table 5.3. Flow cytometry filter panel for Patient BCRG004.

BCRG004		FL-1	FL-2	FL-3	FL-4	FL-5
Functional	Defunctioned	FITC	PE	APC	PE-Cy7	APC-Cy7
1	6	TLR5	CD103	Cocktail	HLA-DR	Dye
2	7	TLR5	CD11c	Cocktail	HLA-DR	Dye
3	8	lgG2a	CD103	Cocktail	HLA-DR	Dye
4	9	lgG2a	CD11c	Cocktail	HLA-DR	Dye
5	10	TLR5	lgG1	Cocktail	HLA-DR	Dye
	Comp. ctrl					
	11	lgG2a				
	12		lgG1			
	13			CD3		
	14				IgG2a	

Table 5.4. Flow cytometry filter panel for Patient BCRG006.

BCRG006		FL-1	FL-2	FL-3	FL-4	FL-5
Functional	Defunctioned	FITC	PE	APC	PE-Cy7	APC-Cy7
1	9	TLR5	CD163	CD14	HLA-DR	Dye
2	10	IgG2a	CD163	CD14	HLA-DR	Dye
3	11	TLR5	CD163	lgG1	HLA-DR	Dye
4	12	TLR5	CD103	Cocktail	HLA-DR	Dye
5	13	TLR5	CD11c	Cocktail	HLA-DR	Dye
6	14	IgG2a	CD103	Cocktail	HLA-DR	Dye
7	15	IgG2a	CD11c	Cocktail	HLA-DR	Dye
8	16	TLR5	lgG1	Cocktail	HLA-DR	Dye
	Comp. ctrl					
	17	lgG2a				
	18		lgG1			
	19			CD3		
	20				IgG2a	

Table 5.5. Flow cytometry filter panel for Patient BCRG007.

BCRG007		FL-1	FL-2	FL-3	FL-4	FL-5
Functional	Defunctioned	FITC	PE	APC	PE-Cy7	APC-Cy7
1	9	TLR5	CD163	CD14	HLA-DR	Dye
2	10	lgG2a	CD163	CD14	HLA-DR	Dye
3	11	TLR5	CD163	lgG1	HLA-DR	Dye
4	12	TLR5	CD103	Cocktail	HLA-DR	Dye
5	13	TLR5	CD11c	Cocktail	HLA-DR	Dye
6	14	IgG2a	CD103	Cocktail	HLA-DR	Dye
7	15	IgG2a	CD11c	Cocktail	HLA-DR	Dye
8	16	TLR5	lgG1	Cocktail	HLA-DR	Dye
	Comp. ctrl					
	17	lgG2a				
	18		lgG1			
	19			CD3		
	20				IgG2a	

Table 5.6. Flow cytometry filter panel for Patient BCRG018.

BCRG018		FL-1	FL-2	FL-3	FL-4	FL-5
Functional	Defunctioned	FITC	PE	APC	PE-Cy7	APC-Cy7
1	8	TLR5	-	CD3	CD14	Dye
2	9	TLR5	CD64	Cocktail	HLA-DR	Dye
3	10	IgG2a	-	CD3	CD14	Dye
4	11	IgG2a	CD64	Cocktail	HLA-DR	Dye
5	12	-	lgG1	Cocktail	HLA-DR	Dye
6	13	-	-	CD14	IgG2a	Dye
7	14	-	-	lgG1	CD14	Dye
	Comp. ctrl					
	15	IgG2a				
	16		lgG1			
	17			lgG1		
	18				IgG2a	
	19					Dye

Table 5.7. Flow cytometry filter panel for Patient BCRG020.

BCRG020		FL-1	FL-2	FL-3	FL-4	FL-5
Functional	Defunctioned	FITC	PE	APC	PE-Cy7	APC-Cy7
1	8	-	-	CD3	CD14	_/+
2	9	-	CD163	Cocktail	HLA-DR	_/+
3	10	-	-	CD3	CD14	_/+
4	11	-	CD161	Cocktail	HLA-DR	_/+
5	12	-	lgG1	Cocktail	HLA-DR	_/+
6	13	-	-	lgG1	CD14	_/_
7	14	-	-	CD3	IgG2a	_/_
	Comp. ctrl					
	15	lgG2a				
	16		lgG1			
	17			lgG1		
	18				IgG2a	
	19					Dye

Table 5.8. Flow cytometry filter panel for Patient BCRG021.

BCRG021		FL-1	FL-2	FL-3	FL-4	FL-5
Functional	Defunctioned	FITC	PE	APC	PE-Cy7	APC-Cy7
1	7	-	CD11c	Cocktail	HLA-DR	Dye
2	8	-	lgG1	Cocktail	HLA-DR	Dye
3	9	-	CD11c	CD3	CD14	Dye
4	10	-	lgG1	CD3	CD14	Dye
5	11	-	CD163	CD3	CD14	Dye
6	12	-	lgG1	lgG1	IgG2a	Dye
	Comp. ctrl					
	13	IgG2a				
	14		lgG1			
	15			CD3		
	16				IgG2a	
	17					Dye

Table 5.9. Flow cytometry filter panel for Patient BCRG022.

BCRG022		FL-1	FL-2	FL-3	FL-4	FL-5
Functional	Defunctioned	FITC	PE	APC	PE-Cy7	APC-Cy7
1	9	CD25	CD4	CD19	CD14	Dye
2	10	lgG1	CD4	CD19	CD14	Dye
3	11	lgG1	lgG1	lgG1	IgG2a	Dye
4	12	-	CD33	CD14	HLA-DR	Dye
5	13	-	lgG1	CD14	HLA-DR	Dye
6	14	-	CD33	lgG1	HLA-DR	Dye
7	15	-	CD11c	Cocktail	HLA-DR	Dye
8	16	-	lgG1	Cocktail	HLA-DR	Dye
	Comp. ctrl					
	17	lgG2a				
	18		lgG1			
	19			CD3		
	20				lgG2a	
	21					Dye

Table 5.10. Flow cytometry filter panel for Patient BCRG023.

BCRG023		FL-1	FL-2	FL-3	FL-4	FL-5
Functional	Defunctioned	FITC	PE	APC	PE-Cy7	APC-Cy7
1	9	CD25	CD4	CD19	CD14	Dye
2	10	lgG1	CD4	CD19	CD14	Dye
3	11	lgG1	lgG1	lgG1	IgG2a	Dye
4	12	-	CD33	CD14	HLA-DR	Dye
5	13	-	lgG1	CD14	HLA-DR	Dye
6	14	-	CD33	lgG1	HLA-DR	Dye
7	15	-	CD11c	Cocktail	HLA-DR	Dye
8	16	-	lgG1	Cocktail	HLA-DR	Dye
	17	CD25	CD4	CD19	CD14	-
	18	CD25	CD4	CD19	CD14	Dye
	Comp. ctrl					
	19	lgG1				
	20		lgG1			
	21			CD3		
	22				IgG2a	
	23					Dye

6. References

Aboui Mehrizi, M., Eidi, A., & Mortazavi, P. (2016). Study of effect of olive oil on reepithelialization of epithelial tissue in excision wound healing model in rats. *Journal Of Comparative Pathobiology Iran, 13 (2 (53)),* 1875-1883.

Abrisqueta, J., Abellan, I., Luján, J., Hernández, Q., & Parrilla, P. (2014). Stimulation of the efferent limb before ileostomy closure: a randomized clinical trial. *Diseases of the colon and rectum*, *57*(12), 1391–1396.

Ahuja A (2008). Immune system and immunodeficiency. *Encyclopedia of Infant and Early Childhood Development*, 137-146.

Alaziqi, B., Beckitt, L., Townsend, D. J., Morgan, J., Price, R., Maerivoet, A., Madine, J., Rochester, D., Akien, G., & Middleton, D. A. (2024). Characterization of Olive Oil Phenolic Extracts and Their Effects on the Aggregation of the Alzheimer's Amyloid-β Peptide and Tau. *ACS omega*, 9(30), 32557–32578.

Albenberg, L., Esipova, T. V., Judge, C. P., Bittinger, K., Chen, J., Laughlin, A., Grunberg, S., Baldassano, R. N., Lewis, J. D., Li, H., Thom, S. R., Bushman, F. D., Vinogradov, S. A., & Wu, G. D. (2014). Correlation between intraluminal oxygen gradient and radial partitioning of intestinal microbiota. *Gastroenterology*, *147*(5), 1055–63.e8.

Alberts B, Johnson A, Lewis J, Raff M, Roberts K, and Walter P (2002). The Adaptive Immune System. Helper T Cells and Lymphocyte Activation. *Molecular Biology of the Cell.* 4th Edition.

Ali, A., Tan, H., & Kaiko, G. E. (2020). Role of the Intestinal Epithelium and Its Interaction With the Microbiota in Food Allergy. *Frontiers in immunology*, *11*, 604054.

Alverdy, J. C., & Burke, D. (1992). Total parenteral nutrition: iatrogenic immunosuppression. *Nutrition (Burbank, Los Angeles County, Calif.)*, 8(5), 359–365.

Alverdy, J. C., Aoys, E., & Moss, G. S. (1988). Total parenteral nutrition promotes bacterial translocation from the gut. *Surgery*, *104*(2), 185–190.

Alverdy, J. C., Chi, H. S., Selivanov, V., Morris, J., & Sheldon, G. F. (1985). The effect of route of nutrient administration on the secretory immune system. *Current surgery*, *42*(1), 10–13.

Andrusaite, A., Lewis, J., Frede, A., Farthing, A., Kästele, V., Montgomery, J., Mowat, A., Mann, E., & Milling, S. (2024). Microbiota-derived butyrate inhibits cDC development via HDAC inhibition, diminishing their ability to prime T cells. *Mucosal immunology*, *17*(6), 1199–1211.

Annes, J. P., Munger, J. S., & Rifkin, D. B. (2003). Making sense of latent TGFbeta activation. *Journal of cell science*, *116*(Pt 2), 217–224.

Arredondo, F., Echeverry, C., Abin-Carriquiry, J. A., Blasina, F., Antúnez, K., Jones, D. P., Go, Y. M., Liang, Y. L., & Dajas, F. (2010). After cellular internalization, quercetin causes Nrf2 nuclear translocation, increases glutathione levels, and prevents neuronal death against an oxidative insult. *Free radical biology & medicine*, *49*(5), 738–747.

Baek, J. S., & Cho, C. W. (2017). Surface modification of solid lipid nanoparticles for oral delivery of curcumin: Improvement of bioavailability through enhanced cellular uptake, and lymphatic uptake. *European journal of pharmaceutics and biopharmaceutics*: official journal of Arbeitsgemeinschaft fur Pharmazeutische Verfahrenstechnik e.V, 117, 132–140.

Bai, X., Ihara, E., Tanaka, Y., Minoda, Y., Wada, M., Hata, Y., Esaki, M., Ogino, H., Chinen, T., & Ogawa, Y. (2025). From bench to bedside: the role of gastrointestinal stem cells in health and disease. *Inflammation and regeneration*, *45*(1), 15.

Bain, C. C., Montgomery, J., Scott, C. L., Kel, J. M., Girard-Madoux, M. J. H., Martens, L., Zangerle-Murray, T. F. P., Ober-Blöbaum, J., Lindenbergh-Kortleve, D., Samsom, J. N., Henri, S., Lawrence, T., Saeys, Y., Malissen, B., Dalod, M., Clausen, B. E., & Mowat, A. M. (2017). TGFβR signalling controls CD103⁺CD11b⁺ dendritic cell development in the intestine. *Nature communications*, 8(1), 620.

Ban, C., Jo, M., Park, Y. H., Kim, J. H., Han, J. Y., Lee, K. W., Kweon, D. H., & Choi, Y. J. (2020). Enhancing the oral bioavailability of curcumin using solid lipid nanoparticles. *Food chemistry*, *302*, 125328.

Ban, C., Park, S. J., Lim, S., Choi, S. J., & Choi, Y. J. (2015). Improving Flavonoid Bioaccessibility using an Edible Oil-Based Lipid Nanoparticle for Oral Delivery. *Journal of agricultural and food chemistry*, 63(21), 5266–5272.

Banaszkiewicz, Z., Woda, Ł. P., Zwoliński, T., Tojek, K., Jarmocik, P., & Jawień, A. (2015). Intestinal stoma in patients with colorectal cancer from the perspective of 20-year period of clinical observation. *Przeglad gastroenterologiczny*, *10*(1), 23–27.

Bang, S. H., Hyun, Y. J., Shim, J., Hong, S. W., & Kim, D. H. (2015). Metabolism of rutin and poncirin by human intestinal microbiota and cloning of their metabolizing α-L-rhamnosidase from Bifidobacterium dentium. *Journal of microbiology and biotechnology*, 25(1), 18–25.

Baxter, N. T., Schmidt, A. W., Venkataraman, A., Kim, K. S., Waldron, C., & Schmidt, T. M. (2019). Dynamics of Human Gut Microbiota and Short-Chain Fatty Acids in Response to Dietary Interventions with Three Fermentable Fibers. *mBio*, *10*(1), e02566-18.

Beamish, E. L., Johnson, J., Shaw, E. J., Scott, N. A., Bhowmick, A., & Rigby, R. J. (2017). Loop ileostomy-mediated fecal stream diversion is associated with microbial dysbiosis. *Gut microbes*, *8*(5), 467–478.

Beamish, E. L., Johnson, J., Shih, B., Killick, R., Dondelinger, F., McGoran, C., Brewster-Craig, C., Davies, A., Bhowmick, A., & Rigby, R. J. (2023). Delay in loop ileostomy reversal surgery does not impact upon post-operative clinical outcomes.

Complications are associated with an increased loss of microflora in the defunctioned intestine. *Gut microbes*, *15*(1), 2199659.

Bereswill, S., Fischer, A., Plickert, R., Haag, L. M., Otto, B., Kühl, A. A., Dasti, J. I., Zautner, A. E., Muñoz, M., Loddenkemper, C., Gross, U., Göbel, U. B., & Heimesaat, M. M. (2011). Novel murine infection models provide deep insights into the "ménage à trois" of Campylobacter jejuni, microbiota and host innate immunity. *PloS one*, *6*(6), e20953.

Bereswill, S., Muñoz, M., Fischer, A., Plickert, R., Haag, L. M., Otto, B., Kühl, A. A., Loddenkemper, C., Göbel, U. B., & Heimesaat, M. M. (2010). Anti-inflammatory effects

of resveratrol, curcumin and simvastatin in acute small intestinal inflammation. *PloS* one, 5(12), e15099.

Bindels, L. B., Delzenne, N. M., Cani, P. D., & Walter, J. (2015). Towards a more comprehensive concept for prebiotics. *Nature reviews. Gastroenterology & hepatology*, *12*(5), 303–310.

Blanco, N., Oliva, I., Tejedor, P., Pastor, E., Alvarellos, A., Pastor, C., Baixauli, J., & Arredondo, J. (2023). ILEOSTIM trial: a study protocol to evaluate the effectiveness of efferent loop stimulation before ileostomy reversal. *Techniques in coloproctology*, *27*(12), 1251–1256.

Bokkenheuser, V. D., Shackleton, C. H., & Winter, J. (1987). Hydrolysis of dietary flavonoid glycosides by strains of intestinal Bacteroides from humans. *The Biochemical journal*, *248*(3), 953–956.

Boussenna, A., Cholet, J., Goncalves-Mendes, N., Joubert-Zakeyh, J., Fraisse, D., Vasson, M.-P., Texier, O. and Felgines, C. (2016), Polyphenol-rich grape pomace extracts protect against dextran sulfate sodium-induced colitis in rats. J. Sci. Food Agric., 96: 1260-1268.

Boussenna, A., Joubert-Zakeyh, J., Fraisse, D., Pereira, B., Vasson, M. P., Texier, O., & Felgines, C. (2016). Dietary Supplementation with a Low Dose of Polyphenol-Rich Grape Pomace Extract Prevents Dextran Sulfate Sodium-Induced Colitis in Rats. *Journal of medicinal food*, *19*(8), 755–758.

Brand S. (2009). Crohn's disease: Th1, Th17 or both? The change of a paradigm: new immunological and genetic insights implicate Th17 cells in the pathogenesis of Crohn's disease. *Gut*, 58(8), 1152–1167.

Buey, B., Forcén, A., Grasa, L., Layunta, E., Mesonero, J. E., & Latorre, E. (2023). Gut Microbiota-Derived Short-Chain Fatty Acids: Novel Regulators of Intestinal Serotonin Transporter. *Life (Basel, Switzerland)*, *13*(5), 1085.

Burghgraef, T. A., Amelung, F. J., Verheijen, P. M., Broeders, I. A. M. J., & Consten, E. C. J. (2020). Intestinal motility distal of a deviating ileostomy after rectal resection with the

construction of a primary anastomosis: results of the prospective COLO-MOVE study. *International journal of colorectal disease*, *35*(10), 1959–1962.

Calame, W., Weseler, A. R., Viebke, C., Flynn, C., & Siemensma, A. D. (2008). Gum arabic establishes prebiotic functionality in healthy human volunteers in a dosedependent manner. *The British journal of nutrition*, *100*(6), 1269–1275.

Cao, Z., Sugimura, N., Burgermeister, E., Ebert, M. P., Zuo, T., & Lan, P. (2022). The gut virome: A new microbiome component in health and disease. *EBioMedicine*, *81*, 104113.

Carabotti, M., Scirocco, A., Maselli, M. A., & Severi, C. (2015). The gut-brain axis: interactions between enteric microbiota, central and enteric nervous systems. *Annals of gastroenterology*, *28*(2), 203–209.

Cariello, M., Contursi, A., Gadaleta, R. M., Piccinin, E., De Santis, S., Piglionica, M., Spaziante, A. F., Sabbà, C., Villani, G., & Moschetta, A. (2020). Extra-Virgin Olive Oil from Apulian Cultivars and Intestinal Inflammation. *Nutrients*, *12*(4), 1084.

Chance, W. T., Zhang, X., Zuo, L., Balasubramaniam, A. (1998). Reduction of gut hypoplasia and cachexia in tumour-bearing rats maintained on total parenteral nutrition and treated with peptide YY and clenbuterol. *Nutrition*, *14*(6), 502-507.

Chen, W., Jin, W., Hardegen, N., Lei, K. J., Li, L., Marinos, N., McGrady, G., & Wahl, S. M. (2003). Conversion of peripheral CD4+CD25- naive T cells to CD4+CD25+ regulatory T cells by TGF-beta induction of transcription factor Foxp3. *The Journal of experimental medicine*, 198(12), 1875–1886.

Cheng, H. Y., Ning, M. X., Chen, D. K., & Ma, W. T. (2019). Interactions Between the Gut Microbiota and the Host Innate Immune Response Against Pathogens. *Frontiers in immunology*, *10*, 607.

Cheng, L. K., O'Grady, G., Du, P., Egbuji, J. U., Windsor, J. A., & Pullan, A. J. (2010). Gastrointestinal system. *Wiley interdisciplinary reviews*. *Systems biology and medicine*, *2*(1), 65–79.

Christensen, K. Y., Naidu, A., Parent, M. É., Pintos, J., Abrahamowicz, M., Siemiatycki, J., & Koushik, A. (2012). The risk of lung cancer related to dietary intake of flavonoids. *Nutrition and cancer*, *64*(7), 964–974.

Clifford M. N. (2004). Diet-derived phenols in plasma and tissues and their implications for health. *Planta medica*, 70(12), 1103–1114.

Collado, M. C., Meriluoto, J., & Salminen, S. (2007). Role of commercial probiotic strains against human pathogen adhesion to intestinal mucus. *Letters in applied microbiology*, *45*(4), 454–460.

Collins, J., Borojevic, R., Verdu, E. F., Huizinga, J. D., & Ratcliffe, E. M. (2014). Intestinal microbiota influence the early postnatal development of the enteric nervous system. *Neurogastroenterology and motility*, *26*(1), 98–107.

Coombes, J. L., Siddiqui, K. R., Arancibia-Cárcamo, C. V., Hall, J., Sun, C. M., Belkaid, Y., & Powrie, F. (2007). A functionally specialized population of mucosal CD103+ DCs induces Foxp3+ regulatory T cells via a TGF-beta and retinoic acid-dependent mechanism. *The Journal of experimental medicine*, *204*(8), 1757–1764.

Cummings, J. H., Pomare, E. W., Branch, W. J., Naylor, C. P., & Macfarlane, G. T. (1987). Short chain fatty acids in human large intestine, portal, hepatic and venous blood. *Gut*, *28*(10), 1221–1227.

Demehri, F. R., Barrett, M., Ralls, M. W., Miyasaka, E. A., Feng, Y., & Teitelbaum, D. H. (2013). Intestinal epithelial cell apoptosis and loss of barrier function in the setting of altered microbiota with enteral nutrient deprivation. *Frontiers in cellular and infection microbiology*, *3*, 105.

Derrien, M., Vaughan, E. E., Plugge, C. M., & de Vos, W. M. (2004). Akkermansia muciniphila gen. nov., sp. nov., a human intestinal mucin-degrading bacterium. *International journal of systematic and evolutionary microbiology*, *54*(Pt 5), 1469–1476.

Dilke, S. M., Gould, L., Yao, M., Souvatzi, M., Stearns, A., Ignjatovic-Wilson, A., Tozer, P., & Vaizey, C. J. (2020). Distal feeding-bowel stimulation to treat short-term or long-term pathology: a systematic review. *Frontline gastroenterology*, *12*(7), 677–682.

Ding, X., Hu, X., Xie, J., Ying, M., Wang, Y., Yu, Q. (2021). Differentiated Caco-2 cell models in food-intestine interaction study: Current applications and future trends. Trends in Food Science and Technology, 107, 455-465.

Donovan, J. L., Crespy, V., Manach, C., Morand, C., Besson, C., Scalbert, A., & Rémésy, C. (2001). Catechin is metabolized by both the small intestine and liver of rats. *The Journal of nutrition*, *131*(6), 1753–1757.

Duan, L., An, X., Zhang, Y., Jin, D., Zhao, S., Zhou, R., Duan, Y., Zhang, Y., Liu, X., & Lian, F. (2021). Gut microbiota as the critical correlation of polycystic ovary syndrome and type 2 diabetes mellitus. *Biomedicine & pharmacotherapy = Biomedecine & pharmacotherapie*, *142*, 112094.

Ducatelle, R., Goossens, E., De Meyer, F., Eeckhaut, V., Antonissen, G., Haesebrouck, F., Van Immerseel, F. (2018). Biomarkers for monitoring intestinal health in poultry: present status and future perspectives. *Vet Res* 49, 43.

Duncan, S. H., Louis, P., & Flint, H. J. (2004). Lactate-utilizing bacteria, isolated from human feces, that produce butyrate as a major fermentation product. *Applied and environmental microbiology*, 70(10), 5810–5817.

Dunel-Erb, S., Chevalier, C., Laurent, P., Bach, A., Decrock, F., & Le Maho, Y. (2001). Restoration of the jejunal mucosa in rats refed after prolonged fasting. *Comparative biochemistry and physiology*. *Part A, Molecular & integrative physiology*, *129*(4), 933–947.

Eckburg, P. B., Bik, E. M., Bernstein, C. N., Purdom, E., Dethlefsen, L., Sargent, M., Gill, S. R., Nelson, K. E., & Relman, D. A. (2005). Diversity of the human intestinal microbial flora. *Science (New York, N.Y.)*, 308(5728), 1635–1638.

El-Hussuna, A., Lauritsen, M., & Bülow, S. (2012). Relatively high incidence of complications after loop ileostomy reversal. *Danish medical journal*, 59(10), A4517

Engevik, M. A., Luk, B., Chang-Graham, A. L., Hall, A., Herrmann, B., Ruan, W., Endres, B. T., Shi, Z., Garey, K. W., Hyser, J. M., & Versalovic, J. (2019). Bifidobacterium dentium Fortifies the Intestinal Mucus Layer via Autophagy and Calcium Signaling Pathways. *mBio*, *10*(3), e01087-19.

Estrada, D. M. L., Benghi, L. M., & Kotze, P. G. (2021). Practical insights into stomas in inflammatory bowel disease: what every healthcare provider needs to know. *Current opinion in gastroenterology*, *37*(4), 320–327.

Everts, B., Tussiwand, R., Dreesen, L., Fairfax, K. C., Huang, S. C., Smith, A. M., O'Neill, C. M., Lam, W. Y., Edelson, B. T., Urban, J. F., Jr, Murphy, K. M., & Pearce, E. J. (2016). Migratory CD103+ dendritic cells suppress helminth-driven type 2 immunity through constitutive expression of IL-12. *The Journal of experimental medicine*, *213*(1), 35–51.

Feliciano, R. P., Mills, C. E., Istas, G., Heiss, C., & Rodriguez-Mateos, A. (2017).

Absorption, Metabolism and Excretion of Cranberry (Poly)phenols in Humans: A Dose Response Study and Assessment of Inter-Individual Variability. *Nutrients*, 9(3), 268.

Feng, Y., Sun, X., Yang, H., & Teitelbaum, D. H. (2009). Dissociation of E-cadherin and beta-catenin in a mouse model of total parenteral nutrition: a mechanism for the loss of epithelial cell proliferation and villus atrophy. *The Journal of physiology*, 587(3), 641–654.

Fernández López, F., González López, J., Paz Novo, M., Ladra González, M. J., & Paredes Cotoré, J. (2019). Stimulation the efferent limb before loop ileostomy closure with short chain fatty acids. Estimulación preoperatoria del asa eferente de la ileostomía con ácidos grasos de cadena corta. *Cirugia espanola*, 97(1), 59–61.

Fiorentino, D. F., Zlotnik, A., Vieira, P., Mosmann, T. R., Howard, M., Moore, K. W., & O'Garra, A. (1991). IL-10 acts on the antigen-presenting cell to inhibit cytokine production by Th1 cells. *Journal of immunology (Baltimore, Md. : 1950), 146*(10), 3444–3451.

Fowler, K. L., Wieck, M. M., Hilton, A. E., Hou, X., Schlieve, C. R., & Grikscheit, T. C. (2017). Marked stem/progenitor cell expansion occurs early after murine ileostomy: a new model. *The Journal of surgical research*, *220*, 182–196.

Freeland, K. R., & Wolever, T. M. (2010). Acute effects of intravenous and rectal acetate on glucagon-like peptide-1, peptide YY, ghrelin, adiponectin and tumour necrosis factor-alpha. *The British journal of nutrition*, 103(3), 460–466.

Fucikova, J., Palova-Jelinkova, L., Bartunkova, J., and Spisek, R. (2019). Induction of Tolerance and Immunity by Dendritic Cells: Mechanisms and Clinical Applications. *Frontiers in immunology*, *10*, 2393.

Fukuda, S., Toh, H., Taylor, T. D., Ohno, H., & Hattori, M. (2012). Acetate-producing bifidobacteria protect the host from enteropathogenic infection via carbohydrate transporters. *Gut microbes*, *3*(5), 449–454.

Garfinkle, R., Demian, M., Sabboobeh, S., Moon, J., Hulme-Moir, M., Liberman, A. S., Feinberg, S., Hayden, D. M., Chadi, S. A., Demyttenaere, S., Samuel, L., Hotakorzian, N., Quintin, L., Morin, N., Faria, J., Ghitulescu, G., Vasilevsky, C. A., Boutros, M., & Bowel Stimulation Research Collaborative (2023). Bowel stimulation before loop ileostomy closure to reduce postoperative ileus: a multicenter, single-blinded, randomized controlled trial. *Surgical endoscopy*, *37*(5), 3934–3943.

Garg, A., Bhalala, K., Tomar, D. S., & Wahajuddin (2017). In-situ single pass intestinal permeability and pharmacokinetic study of developed Lumefantrine loaded solid lipid nanoparticles. *International journal of pharmaceutics*, *516*(1-2), 120–130.

Gaur, G., Oh, J. H., Filannino, P., Gobbetti, M., van Pijkeren, J. P., & Gänzle, M. G. (2020). Genetic Determinants of Hydroxycinnamic Acid Metabolism in Heterofermentative Lactobacilli. *Applied and environmental microbiology*, 86(5), e02461-19.

Gavin, M. A., Rasmussen, J. P., Fontenot, J. D., Vasta, V., Manganiello, V. C., Beavo, J. A., & Rudensky, A. Y. (2007). Foxp3-dependent programme of regulatory T-cell differentiation. *Nature*, *445*(7129), 771–775.

Gilbert, J. A., Blaser, M. J., Caporaso, J. G., Jansson, J. K., Lynch, S. V., & Knight, R. (2018). Current understanding of the human microbiome. *Nature medicine*, *24*(4), 392–400.

Guo, P., Zhang, K., Ma, X. He, P. (2020). Clostridium species as probiotics: potentials and challenges. *Journal of Animal Science and Biotechnology* 11(24).

Gurka, S., Hartung, E., Becker, M., & Kroczek, R. A. (2015). Mouse Conventional Dendritic Cells Can be Universally Classified Based on the Mutually Exclusive Expression of XCR1 and SIRPa. *Frontiers in immunology*, 6, 35.

Hagiwara, S., Iwasaka, H., Kusaka, J., Asai, N., Uchida, T., & Noguchi, T. (2011). Total parenteral-nutrition-mediated dendritic-cell activation and infiltration into the small intestine in a rat model. *Journal of anesthesia*, 25(1), 57–64.

Hartman, A. L., Lough, D. M., Barupal, D. K., Fiehn, O., Fishbein, T., Zasloff, M., & Eisen, J. A. (2009). Human gut microbiome adopts an alternative state following small bowel transplantation. *Proceedings of the National Academy of Sciences of the United States of America*, 106(40), 17187–17192.

Hassan, M., Juanola, O., Huber, S., Kellmann, P., Zimmermann, J., Lazzarini, E., Ganal-Vonarburg, S. C., Gomez de Agüero, M., & Moghadamrad, S. (2023). Absence of gut microbiota impairs depletion of Paneth cells but not goblet cells in germfree *Atoh1*^{lox/lox} VilCreER^{T2} mice. *American journal of physiology. Gastrointestinal and liver physiology*, 324(6), G426–G437.

Hayashi, H., Takahashi, R., Nishi, T., Sakamoto, M., & Benno, Y. (2005). Molecular analysis of jejunal, ileal, caecal and recto-sigmoidal human colonic microbiota using 16S rRNA gene libraries and terminal restriction fragment length polymorphism. *Journal of medical microbiology*, *54*(Pt 11), 1093–1101.

Hemarajata, P., & Versalovic, J. (2013). Effects of probiotics on gut microbiota: mechanisms of intestinal immunomodulation and neuromodulation. *Therapeutic advances in gastroenterology*, 6(1), 39–51.

Heneghan, A. F., Pierre, J. F., Gosain, A., & Kudsk, K. A. (2014). IL-25 improves luminal innate immunity and barrier function during parenteral nutrition. *Annals of surgery*, 259(2), 394–400.

Heneghan, A. F., Pierre, J. F., Tandee, K., Shanmuganayagam, D., Wang, X., Reed, J. D., Steele, J. L., & Kudsk, K. A. (2014). Parenteral nutrition decreases paneth cell function and intestinal bactericidal activity while increasing susceptibility to bacterial enteroinvasion. *JPEN. Journal of parenteral and enteral nutrition*, 38(7), 817–824.

Hernández-Chirlaque, C., Aranda, C. J., Ocón, B., Capitán-Cañadas, F., Ortega-González, M., Carrero, J. J., Suárez, M. D., Zarzuelo, A., Sánchez de Medina, F., & Martínez-Augustin, O. (2016). Germ-free and Antibiotic-treated Mice are Highly

Susceptible to Epithelial Injury in DSS Colitis. *Journal of Crohn's & colitis*, 10(11), 1324–1335.

Hill, C., Guarner, F., Reid, G., Gibson, G. R., Merenstein, D. J., Pot, B., Morelli, L., Canani, R. B., Flint, H. J., Salminen, S., Calder, P. C., Sanders, M. E. (2014). The international scientific association of probiotics and prebiotics consensus statement on the scope and appropriate use of the term probiotic. *Nature Reviews:*Gastroenterology and Hepatology, 11, 506-514

Hoensch, H., Groh, B., Edler, L., & Kirch, W. (2008). Prospective cohort comparison of flavonoid treatment in patients with resected colorectal cancer to prevent recurrence. *World journal of gastroenterology*, *14*(14), 2187–2193.

Holderman, L. V. and Moore W. E. C. (1974). New genus, *Coprococcus*, twelve new species, and emended descriptions of for previously described species of bacteria from human feces. *International Journal of Systematic and Evolutionary Microbiology*, 24(2).

Hollman, PCH., van Trijp, JMP., Buysman, MNCP., Gaag, MS., Mengelers, MJB., de Vries, JHM., Katan MB. (1997). Relative Bioavailability of the Antioxidant Flavonoid Quercetin from Various Foods in Man. Federation of European Biochemical Societies (FEBS) Letters, 418(1-2), 152-156.

Hong, D. K., Yoo, M. S., Heo, K., Shim, J. J., & Lee, J. L. (2021). Effects of *L. plantarum* HY7715 on the Gut Microbial Community and Riboflavin Production in a Three-Stage Semi-Continuous Simulated Gut System. *Microorganisms*, 9(12), 2478.

Hong, D. K., Yoo, M. S., Heo, K., Shim, J. J., & Lee, J. L. (2021). Effects of *L. plantarum* HY7715 on the Gut Microbial Community and Riboflavin Production in a Three-Stage Semi-Continuous Simulated Gut System. *Microorganisms*, 9(12), 2478.

Hooper, L. V., Wong, M. H., Thelin, A., Hansson, L., Falk, P. G., & Gordon, J. I. (2001). Molecular analysis of commensal host-microbial relationships in the intestine. *Science* (New York, N.Y.), 291(5505), 881–884.

Horvath, T. D., Ihekweazu, F. D., Haidacher, S. J., Ruan, W., Engevik, K. A., Fultz, R., Hoch, K. M., Luna, R. A., Oezguen, N., Spinler, J. K., Haag, A. M., Versalovic, J., &

Engevik, M. A. (2022). *Bacteroides ovatus* colonization influences the abundance of intestinal short chain fatty acids and neurotransmitters. *iScience*, *25*(5), 104158.

Hosmer, J., McEwan, A. G., & Kappler, U. (2024). Bacterial acetate metabolism and its influence on human epithelia. *Emerging topics in life sciences*, 8(1), 1–13.

Houston, S. A., Cerovic, V., Thomson, C., Brewer, J., Mowat, A. M., & Milling, S. (2016). The lymph nodes draining the small intestine and colon are anatomically separate and immunologically distinct. *Mucosal immunology*, 9(2), 468–478.

Hu, J., Nomura, Y., Bashir, A., Fernandez-Hernandez, H., Itzkowitz, S., Pei, Z., Stone, J., Loudon, H., & Peter, I. (2013). Diversified microbiota of meconium is affected by maternal diabetes status. *PloS one*, *8*(11), e78257.

Huang, S., Theophilus, M., Cui, J., Bell, S. W., Wale, R., Chin, M., Farmer, C., & Warrier, S. K. (2017). Colonic transit: what is the impact of a diverting loop ileostomy?. *ANZ journal of surgery*, 87(10), 795–799.

Hui, C., Qi, X., Qianyong, Z., Xiaoli, P., Jundong, Z., & Mantian, M. (2013). Flavonoids, flavonoid subclasses and breast cancer risk: a meta-analysis of epidemiologic studies. *PloS one*, 8(1), e54318.

Hurtado-Romero A, Del Toro-Barbosa M, Garcia-Amezquita LE, Garcia-Cayuela (2020)-Innovative technologies for the production of food ingredients with prebiotic potential: Modifications, applications, and validation methods. Trends in Food Science & Technology. 104. 117-131.

Ikawa, Y., Moriyama, S., Furuta, H. (2008). Facile syntheses of BODIPY derivatives for fluorescent labelling of the 3' and 5' ends of RNAs. Analytical Biochemistry, 378(2), 166-170.

Inaba, K., Inaba, M., Romani, N., Aya, H., Deguchi, M., Ikehara, S., Muramatsu, S., & Steinman, R. M. (1992). Generation of large numbers of dendritic cells from mouse bone marrow cultures supplemented with granulocyte/macrophage colony-stimulating factor. *The Journal of experimental medicine*, *17*6(6), 1693–1702.

Janu, P., Li, J., Renegar, K. B., & Kudsk, K. A. (1997). Recovery of gut-associated lymphoid tissue and upper respiratory tract immunity after parenteral nutrition. *Annals of surgery*, 225(6), 707–717.

Ji, H., Tang, J., Li, M., Ren, J., Zheng, N., & Wu, L. (2016). Curcumin-loaded solid lipid nanoparticles with Brij78 and TPGS improved in vivo oral bioavailability and in situ intestinal absorption of curcumin. *Drug delivery*, *23*(2), 459–470.

Johansson-Lindbom, B., Svensson, M., Pabst, O., Palmqvist, C., Marquez, G., Förster, R., & Agace, W. W. (2005). Functional specialization of gut CD103+ dendritic cells in the regulation of tissue-selective T cell homing. *The Journal of experimental medicine*, 202(8), 1063–1073.

Józsa, T., Magyar, A., Cserni, T., Szentmiklósi, A. J., Erdélyi, K., Kincses, Z., Rákóczy, G., Balla, G., & Roszer, T. (2009). Short-term adaptation of rat intestine to ileostomy: implication for pediatric practice. *Journal of investigative surgery: the official journal of the Academy of Surgical Research*, 22(4), 292–300.

Jurgoński, A., Juśkiewicz, J., Zduńczyk, Z., Matusevicius, P., & Kołodziejczyk, K. (2014). Polyphenol-rich extract from blackcurrant pomace attenuates the intestinal tract and serum lipid changes induced by a high-fat diet in rabbits. *European journal of nutrition*, 53(8), 1603–1613.

Kansagra, K., Stoll, B., Rognerud, C., Niinikoski, H., Ou, C. N., Harvey, R., & Burrin, D. (2003). Total parenteral nutrition adversely affects gut barrier function in neonatal piglets. *American journal of physiology. Gastrointestinal and liver physiology*, 285(6), G1162–G1170.

Karlsson, F. H., Fåk, F., Nookaew, I., Tremaroli, V., Fagerberg, B., Petranovic, D., Bäckhed, F., & Nielsen, J. (2012). Symptomatic atherosclerosis is associated with an altered gut metagenome. *Nature communications*, 3, 1245.

Kastl, A. J., Jr, Terry, N. A., Wu, G. D., & Albenberg, L. G. (2020). The Structure and Function of the Human Small Intestinal Microbiota: Current Understanding and Future Directions. *Cellular and molecular gastroenterology and hepatology*, 9(1), 33–45.

Kelly, C. J., Zheng, L., Campbell, E. L., Saeedi, B., Scholz, C. C., Bayless, A. J., Wilson, K. E., Glover, L. E., Kominsky, D. J., Magnuson, A., Weir, T. L., Ehrentraut, S. F., Pickel, C., Kuhn, K. A., Lanis, J. M., Nguyen, V., Taylor, C. T., & Colgan, S. P. (2015). Crosstalk between Microbiota-Derived Short-Chain Fatty Acids and Intestinal Epithelial HIF Augments Tissue Barrier Function. *Cell host & microbe*, *17*(5), 662–671.

Kelsall, B. L., & Strober, W. (1996). Distinct populations of dendritic cells are present in the subepithelial dome and T cell regions of the murine Peyer's patch. *The Journal of experimental medicine*, 183(1), 237–247.

Kiela, P. R., & Ghishan, F. K. (2016). Physiology of Intestinal Absorption and Secretion. *Best practice & research*. *Clinical gastroenterology*, *30*(2), 145–159.

King, B. K., Li, J., & Kudsk, K. A. (1997). A temporal study of TPN-induced changes in gut-associated lymphoid tissue and mucosal immunity. *Archives of surgery (Chicago, Ill.:* 1960), 132(12), 1303–1309.

Knekt, P., Jarvinen, R., Reunanen, A., & Maatela, J. (1996). Flavonoid intake and coronary mortality in Finland: a cohort study. *BMJ (Clinical research ed.)*, *312*(7029), 478–481.

Konishi, Y., & Shimizu, M. (2003). Transepithelial transport of ferulic acid by monocarboxylic acid transporter in Caco-2 cell monolayers. *Bioscience*, *biotechnology*, *and biochemistry*, 67(4), 856–862.

Langford, D. J., Bailey, A. L., Chanda, M. L., Clarke, S. E., Drummond, T. E., Echols, S., Glick, S., Ingrao, J., Klassen-Ross, T., Lacroix-Fralish, M. L., Matsumiya, L., Sorge, R. E., Sotocinal, S. G., Tabaka, J. M., Wong, D., van den Maagdenberg, A. M., Ferrari, M. D., Craig, K. D., & Mogil, J. S. (2010). Coding of facial expressions of pain in the laboratory mouse. *Nature methods*, *7*(6), 447–449.

Lapidot, T., Harel, S., Granit, R., Kanner, J. (1998). Bioavailability of Red Wine Anthocyanins as Detected in Human Urine. Journal of Agricultural and Food Chemistry, 46(10), 4297-4302.

Lapthorne, S., Pereira-Fantini, P. M., Fouhy, F., Wilson, G., Thomas, S. L., Dellios, N. L., Scurr, M., O'Sullivan, O., Ross, R. P., Stanton, C., Fitzgerald, G. F., Cotter, P. D., &

Bines, J. E. (2013). Gut microbial diversity is reduced and is associated with colonic inflammation in a piglet model of short bowel syndrome. *Gut microbes*, *4*(3), 212–221.

Larsen, N., Vogensen, F. K., Gøbel, R., Michaelsen, K. F., Abu Al-Soud, W., Sørensen, S. J., Hansen, L. H., & Jakobsen, M. (2011). Predominant genera of fecal microbiota in children with atopic dermatitis are not altered by intake of probiotic bacteria Lactobacillus acidophilus NCFM and Bifidobacterium animalis subsp. lactis Bi-07. *FEMS microbiology ecology*, 75(3), 482–496.

Lau, E. C., Fung, A. C., Wong, K. K., & Tam, P. K. (2016). Beneficial effects of mucous fistula refeeding in necrotizing enterocolitis neonates with enterostomies. *Journal of pediatric surgery*, *51*(12), 1914–1916.

Laursen, M. F., Laursen, R. P., Larnkjær, A., Michaelsen, K. F., Bahl, M. I., & Licht, T. R. (2017). Administration of two probiotic strains during early childhood does not affect the endogenous gut microbiota composition despite probiotic proliferation. *BMC microbiology*, *17*(1), 175.

Lee, S. Y., Park, H. M., Kim, C. H., & Kim, H. R. (2023). Dysbiosis of gut microbiota during faecal stream diversion in patients with colorectal cancer. *Gut pathogens*, *15*(1), 40.

Lefranc-Millot, C., Guérin-Deremaux, L., Wils, D., Neut, C., Miller, L. E., & Saniez-Degrave, M. H. (2012). Impact of a resistant dextrin on intestinal ecology: how altering the digestive ecosystem with NUTRIOSE®, a soluble fibre with prebiotic properties, may be beneficial for health. *The Journal of international medical research*, 40(1), 211–224.

Lesniak, W. G., Jyoti, A., Mishra, M. K., Louissaint, N., Romero, R., Chugani, D. C., Kannan, S., & Kannan, R. M. (2013). Concurrent quantification of tryptophan and its major metabolites. *Analytical biochemistry*, *443*(2), 222–231.

Li, J., Chen, C., Yang, H., & Yang, X. (2021). Tea polyphenols regulate gut microbiota dysbiosis induced by antibiotic in mice. *Food research international (Ottawa, Ont.)*, *141*, 110153.

Li, X., Ma, H., Sun, Y., Li, T., Wang, C., Zheng, H., Chen, G., Du, G., Ji, G., Yang, H., Xiao, W., & Qiu, Y. (2022). Effects of fecal stream deprivation on human intestinal barrier after loop ileostomy. *Journal of gastroenterology and hepatology*, *37*(6), 1119–1130.

Liang, J., Huang, H. I., Benzatti, F. P., Karlsson, A. B., Zhang, J. J., Youssef, N., Ma, A., Hale, L. P., & Hammer, G. E. (2016). Inflammatory Th1 and Th17 in the Intestine Are Each Driven by Functionally Specialized Dendritic Cells with Distinct Requirements for MyD88. *Cell reports*, *17*(5), 1330–1343.

Libertucci, J., Young, V.B. The role of the microbiota in infectious diseases. *Nat Microbiol* **4**, 35–45 (2019).

Liu, Z., Fang, L., Lv, L., Niu, Z., Hou, L., Chen, D., Zhou, Y., & Guo, D. (2021). Self-administered succus entericus reinfusion before ileostomy closure improves short-term outcomes. *BMC surgery*, *21*(1), 440.

Liu, Z., Lin, X., Huang, G., Zhang, W., Rao, P., & Ni, L. (2014). Prebiotic effects of almonds and almond skins on intestinal microbiota in healthy adult humans. *Anaerobe*, *26*, 1–6.

Liu, Z., Qin, H., Yang, Z., Xia, Y., Liu, W., Yang, J., Jiang, Y., Zhang, H., Yang, Z., Wang, Y., & Zheng, Q. (2011). Randomised clinical trial: the effects of perioperative probiotic treatment on barrier function and post-operative infectious complications in colorectal cancer surgery - a double-blind study. *Alimentary pharmacology & therapeutics*, 33(1), 50–63.

Luda, K. M., Joeris, T., Persson, E. K., Rivollier, A., Demiri, M., Sitnik, K. M., Pool, L., Holm, J. B., Melo-Gonzalez, F., Richter, L., Lambrecht, B. N., Kristiansen, K., Travis, M. A., Svensson-Frej, M., Kotarsky, K., & Agace, W. W. (2016). IRF8 Transcription-Factor-Dependent Classical Dendritic Cells Are Essential for Intestinal T Cell Homeostasis. *Immunity*, *44*(4), 860–874.

Mabbott, N. A., Donaldson, D. S., Ohno, H., Williams, I. R., & Mahajan, A. (2013). Microfold (M) cells: important immunosurveillance posts in the intestinal epithelium. *Mucosal immunology*, 6(4), 666–677.

Madison, A., & Kiecolt-Glaser, J. K. (2019). Stress, depression, diet, and the gut microbiota: human-bacteria interactions at the core of psychoneuroimmunology and nutrition. *Current opinion in behavioral sciences*, *28*, 105–110.

Manrique, P., Bolduc, B., Walk, S. T., van der Oost, J., de Vos, W. M., & Young, M. J. (2016). Healthy human gut phageome. *Proceedings of the National Academy of Sciences of the United States of America*, *113*(37), 10400–10405.

Marín, L., Miguélez, E. M., Villar, C. J., & Lombó, F. (2015). Bioavailability of dietary polyphenols and gut microbiota metabolism: antimicrobial properties. *BioMed research international*, 2015, 905215.

Markey, L., Shaban, L., Green, E. R., Lemon, K. P., Mecsas, J., & Kumamoto, C. A. (2018). Pre-colonization with the commensal fungus Candida albicans reduces murine susceptibility to Clostridium difficile infection. *Gut microbes*, 9(6), 497–509.

Márquez-Flores, Y. K., Villegas, I., Cárdeno, A., Rosillo, M. Á., & Alarcón-de-la-Lastra, C. (2016). Apigenin supplementation protects the development of dextran sulfate sodium-induced murine experimental colitis by inhibiting canonical and non-canonical inflammasome signaling pathways. *The Journal of nutritional biochemistry*, 30, 143–152.

Martin-Gallausiaux, C., Marinelli, L., Blottière, H. M., Larraufie, P., & Lapaque, N. (2021). SCFA: mechanisms and functional importance in the gut. *The Proceedings of the Nutrition Society*, 80(1), 37–49.

Martín-Peláez, S., Mosele, J. I., Pizarro, N., Farràs, M., de la Torre, R., Subirana, I., Pérez-Cano, F. J., Castañer, O., Solà, R., Fernandez-Castillejo, S., Heredia, S., Farré, M., Motilva, M. J., & Fitó, M. (2017). Effect of virgin olive oil and thyme phenolic compounds on blood lipid profile: implications of human gut microbiota. *European journal of nutrition*, 56(1), 119–131.

Martins, Y. C., Ribeiro-Gomes, F. L., and Daniel-Ribeiro, C. T. (2023). A short history of innate immunity. *Memorias do Instituto Oswaldo Cruz*, *118*, e230023.

Mayer, J. U., Demiri, M., Agace, W. W., MacDonald, A. S., Svensson-Frej, M., & Milling, S. W. (2017). Different populations of CD11b⁺ dendritic cells drive Th2 responses in the small intestine and colon. *Nature communications*, 8, 15820.

Mayrhofer, G., Pugh, C. W., & Barclay, A. N. (1983). The distribution, ontogeny and origin in the rat of Ia-positive cells with dendritic morphology and of Ia antigen in epithelia,

with special reference to the intestine. *European journal of immunology*, *13*(2), 112–122.

McCallum, G., & Tropini, C. (2024). The gut microbiota and its biogeography. *Nature reviews*. *Microbiology*, *22*(2), 105–118.

McCoy, M. J., Lake, R. A., van der Most, R. G., Dick, I. M., & Nowak, A. K. (2012). Post-chemotherapy T-cell recovery is a marker of improved survival in patients with advanced thoracic malignancies. *British journal of cancer*, *107*(7), 1107–1115.

Merad, M., Sathe, P., Helft, J., Miller, J., & Mortha, A. (2013). The dendritic cell lineage: ontogeny and function of dendritic cells and their subsets in the steady state and the inflamed setting. *Annual review of immunology*, *31*, 563–604.

Millman, J., Okamoto, S., Kimura, A., Uema, T., Higa, M., Yonamine, M., Namba, T., Ogata, E., Yamazaki, S., Shimabukuro, M., Tsutsui, M., Matsushita, M., Ikematsu, S., & Masuzaki, H. (2020). Metabolically and immunologically beneficial impact of extra virgin olive and flaxseed oils on composition of gut microbiota in mice. *European journal of nutrition*, 59(6), 2411–2425.

Mims, T. S., Abdallah, Q. A., Stewart, J. D., Watts, S. P., White, C. T., Rousselle, T. V., Gosain, A., Bajwa, A., Han, J. C., Willis, K. A., & Pierre, J. F. (2021). The gut mycobiome of healthy mice is shaped by the environment and correlates with metabolic outcomes in response to diet. *Communications biology*, *4*(1), 281.

Minot, S., Bryson, A., Chehoud, C., Wu, G. D., Lewis, J. D., & Bushman, F. D. (2013). Rapid evolution of the human gut virome. *Proceedings of the National Academy of Sciences of the United States of America*, *110*(30), 12450–12455.

Molan, A. L., Liu, Z., & Plimmer, G. (2014). Evaluation of the effect of blackcurrant products on gut microbiota and on markers of risk for colon cancer in humans. *Phytotherapy research: PTR*, 28(3), 416–422.

Molina, M. F., Sanchez-Reus, I., Iglesias, I., & Benedi, J. (2003). Quercetin, a flavonoid antioxidant, prevents and protects against ethanol-induced oxidative stress in mouse liver. *Biological & pharmaceutical bulletin*, 26(10), 1398–1402.

Monagas, M., Urpi-Sarda, M., Sánchez-Patán, F., Llorach, R., Garrido, I., Gómez-Cordovés, C., Andres-Lacueva, C., & Bartolomé, B. (2010). Insights into the metabolism and microbial biotransformation of dietary flavan-3-ols and the bioactivity of their metabolites. *Food & function*, *1*(3), 233–253.

Moreno-Indias, I., Sánchez-Alcoholado, L., Pérez-Martínez, P., Andrés-Lacueva, C., Cardona, F., Tinahones, F., & Queipo-Ortuño, M. I. (2016). Red wine polyphenols modulate fecal microbiota and reduce markers of the metabolic syndrome in obese patients. *Food & function*, *7*(4), 1775–1787.

Mukau, L., Talamini, M. A., & Sitzmann, J. V. (1994). Elemental diets may accelerate recovery from total parenteral nutrition-induced gut atrophy. *JPEN. Journal of parenteral and enteral nutrition*, 18(1), 75–78.

Mukhopadhya, I., Hansen, R., El-Omar, E. M., & Hold, G. L. (2012). IBD-what role do Proteobacteria play?. *Nature reviews. Gastroenterology & hepatology*, 9(4), 219–230.

Murota, K., Shimizu, S., Miyamoto, S., Izumi, T., Obata, A., Kikuchi, M., & Terao, J. (2002). Unique uptake and transport of isoflavone aglycones by human intestinal caco-2 cells: comparison of isoflavonoids and flavonoids. *The Journal of nutrition*, *132*(7), 1956–1961.

Nakasaki, H., Tajima, T., Mitomi, T., Fujii, K., Kamijoh, A. (1996). Countermeasures for hypofunction of gut associated lymphoid tissue during TPN in rats. Journal of the Japanese Society of Calligraphy, 93 (11), 806-812.

Naseribafrouei, A., Hestad, K., Avershina, E., Sekelja, M., Linløkken, A., Wilson, R., & Rudi, K. (2014). Correlation between the human fecal microbiota and depression. *Neurogastroenterology and motility*, *26*(8), 1155–1162.

Nash, A. K., Auchtung, T. A., Wong, M. C., Smith, D. P., Gesell, J. R., Ross, M. C., Stewart, C. J., Metcalf, G. A., Muzny, D. M., Gibbs, R. A., Ajami, N. J., & Petrosino, J. F. (2017). The gut mycobiome of the Human Microbiome Project healthy cohort. *Microbiome*, *5*(1), 153.

Neves, A. R., Lúcio, M., Martins, S., Lima, J. L., & Reis, S. (2013). Novel resveratrol nanodelivery systems based on lipid nanoparticles to enhance its oral bioavailability. *International journal of nanomedicine*, 8, 177–187.

Ng S. K. C., Hamilton I.R. (1971) Lactate Metabolism by *Veillonella parvula*. Journal of Bacteriology 105(3), 999–1005.

Nguyen, H. N., Tanaka, M., Li, B., Ueno, T., Matsuda, H., & Matsui, T. (2019). Novel in situ visualisation of rat intestinal absorption of polyphenols via matrix-assisted laser desorption/ionisation mass spectrometry imaging. *Scientific reports*, 9(1), 3166.

Niedzielin, K., Kordecki, H., & Birkenfeld, B. (2001). A controlled, double-blind, randomized study on the efficacy of Lactobacillus plantarum 299V in patients with irritable bowel syndrome. *European journal of gastroenterology & hepatology*, *13*(10), 1143–1147.

Nielsen, S. E., Breinholt, V., Justesen, U., Cornett, C., & Dragsted, L. O. (1998). In vitro biotransformation of flavonoids by rat liver microsomes. *Xenobiotica*; the fate of foreign compounds in biological systems, 28(4), 389–401.

Ocaña, J., García-Pérez, J. C., Labalde-Martínez, M., Rodríguez-Velasco, G., Moreno, I., Vivas, A., Clemente-Esteban, I., Ballestero, A., Abadía, P., Ferrero, E., Fernández-Cebrián, J. M., & Die, J. (2022). Can physiological stimulation prior to ileostomy closure reduce postoperative ileus? A prospective multicenter pilot study. *Techniques in coloproctology*, 26(8), 645–653.

Oehlke, K., Adamiuk, M., Behsnilian, D., Gräf, V., Mayer-Miebach, E., Walz, E., & Greiner, R. (2014). Potential bioavailability enhancement of bioactive compounds using food-grade engineered nanomaterials: a review of the existing evidence. *Food & function*, 5(7), 1341–1359.

Oh, N. G., Son, G. M., Sin, J. Y., Ding, X. Z., & Adrian, T. E. (2005). Time-course of morphologic changes and peptide YY adaptation in ileal mucosa after loop ileostomy in humans. *Diseases of the colon and rectum*, *48*(6), 1287–1294.

Olalla, J., García de Lomas, J. M., Chueca, N., Pérez-Stachowski, X., De Salazar, A., Del Arco, A., Plaza-Díaz, J., De la Torre, J., Prada, J. L., García-Alegría, J., Fernández-

Sánchez, F., & García, F. (2019). Effect of daily consumption of extra virgin olive oil on the lipid profile and microbiota of HIV-infected patients over 50 years of age. *Medicine*, 98(42), e17528.

O'Shea, E. F., Cotter, P. D., Stanton, C., Ross, R. P., & Hill, C. (2012). Production of bioactive substances by intestinal bacteria as a basis for explaining probiotic mechanisms: bacteriocins and conjugated linoleic acid. *International journal of food microbiology*, *152*(3), 189–205.

Palade, C. M., Vulpoi, G. A., Vulpoi, R. A., Drug, V. L., Barboi, O. B., & Ciocoiu, M. (2022). The Biotics Family: Current Knowledge and Future Perspectives in Metabolic Diseases. *Life (Basel, Switzerland)*, *12*(8), 1263.

Palleja, A., Mikkelsen, K. H., Forslund, S. K., Kashani, A., Allin, K. H., Nielsen, T., Hansen, T. H., Liang, S., Feng, Q., Zhang, C., Pyl, P. T., Coelho, L. P., Yang, H., Wang, J., Typas, A., Nielsen, M. F., Nielsen, H. B., Bork, P., Wang, J., Vilsbøll, T., ... Pedersen, O. (2018). Recovery of gut microbiota of healthy adults following antibiotic exposure. *Nature microbiology*, *3*(11), 1255–1265.

Pandita, D., Kumar, S., Poonia, N., Lather, V. (2014). Solid lipid nanoparticles enhance oral bioavailability of resveratrol, a natural polyphenol. Food Research International, 62, 1165-1174.

Pareek, S., Kurakawa, T., Das, B., Motooka, D., Nakaya, S., Rongsen-Chandola, T., Goyal, N., Kayama, H., Dodd, D., Okumura, R., Maeda, Y., Fujimoto, K., Nii, T., Ogawa, T., Iida, T., Bhandari, N., Kida, T., Nakamura, S., Nair, G. B., & Takeda, K. (2019). Comparison of Japanese and Indian intestinal microbiota shows diet-dependent interaction between bacteria and fungi. *NPJ biofilms and microbiomes*, *5*(1), 37.

Park, J., Kim, M., Kang, S. G., Jannasch, A. H., Cooper, B., Patterson, J., & Kim, C. H. (2015). Short-chain fatty acids induce both effector and regulatory T cells by suppression of histone deacetylases and regulation of the mTOR-S6K pathway. *Mucosal immunology*, 8(1), 80–93.

Pasinetti, G. M., Singh, R., Westfall, S., Herman, F., Faith, J., & Ho, L. (2018). The Role of the Gut Microbiota in the Metabolism of Polyphenols as Characterized by Gnotobiotic Mice. *Journal of Alzheimer's disease*: *JAD*, 63(2), 409–421.

Patel, A., & Jialal, I. (2023). Biochemistry, Immunoglobulin A. StatPearls [Internet]. Treasure Island, StatPearls Publishing.

Peng, L., Li, Z. R., Green, R. S., Holzman, I. R., & Lin, J. (2009). Butyrate enhances the intestinal barrier by facilitating tight junction assembly via activation of AMP-activated protein kinase in Caco-2 cell monolayers. *The Journal of nutrition*, *139*(9), 1619–1625.

Persson, E. K., Uronen-Hansson, H., Semmrich, M., Rivollier, A., Hägerbrand, K., Marsal, J., Gudjonsson, S., Håkansson, U., Reizis, B., Kotarsky, K., & Agace, W. W. (2013). IRF4 transcription-factor-dependent CD103(+)CD11b(+) dendritic cells drive mucosal T helper 17 cell differentiation. *Immunity*, *38*(5), 958–969.

Petrick, J. L., Steck, S. E., Bradshaw, P. T., Trivers, K. F., Abrahamson, P. E., Engel, L. S., He, K., Chow, W. H., Mayne, S. T., Risch, H. A., Vaughan, T. L., & Gammon, M. D. (2015). Dietary intake of flavonoids and oesophageal and gastric cancer: incidence and survival in the United States of America (USA). *British journal of cancer*, *112*(7), 1291–1300.

Plamada, D., & Vodnar, D. C. (2021). Polyphenols-Gut Microbiota Interrelationship: A Transition to a New Generation of Prebiotics. *Nutrients*, *14*(1), 137.

Popescu, M., Van Belleghem, J. D., Khosravi, A., & Bollyky, P. L. (2021). Bacteriophages and the Immune System. *Annual review of virology*, 8(1), 415–435.

Porter, E., Bevins, C., Ghosh, D., Tanz, T. (2002). The multifaceted Paneth Cell. CMLS, Cell. Mol. Life Sci. 59, 156-170.

Pouille, C. L., Ouaza, S., Roels, E., Behra, J., Tourret, M., Molinié, R., Fontaine, J. X., Mathiron, D., Gagneul, D., Taminiau, B., Daube, G., Ravallec, R., Rambaud, C., Hilbert, J. L., Cudennec, B., & Lucau-Danila, A. (2022). Chicory: Understanding the Effects and Effectors of This Functional Food. *Nutrients*, *14*(5), 957.

Powell, D. N., Swimm, A., Sonowal, R., Bretin, A., Gewirtz, A. T., Jones, R. M., & Kalman, D. (2020). Indoles from the commensal microbiota act via the AHR and IL-10 to tune the

cellular composition of the colonic epithelium during aging. *Proceedings of the National Academy of Sciences of the United States of America*, *117*(35), 21519–21526.

Pull, S. L., Doherty, J. M., Mills, J. C., Gordon, J. I., & Stappenbeck, T. S. (2005). Activated macrophages are an adaptive element of the colonic epithelial progenitor niche necessary for regenerative responses to injury. *Proceedings of the National Academy of Sciences of the United States of America*, 102(1), 99–104.

Putsep, K., Axelsson, L. G., Boman, A., Midtvedt, T., Normark, S., Boman, H. G., & Andersson, M. (2000). Germ-free and colonized mice generate the same products from enteric prodefensins. *The Journal of biological chemistry*, *275*(51), 40478–40482.

Qin, J., Li, R., Raes, J., Arumugam, M., Burgdorf, K. S., Manichanh, C., Nielsen, T., Pons, N., Levenez, F., Yamada, T., Mende, D. R., Li, J., Xu, J., Li, S., Li, D., Cao, J., Wang, B., Liang, H., Zheng, H., Xie, Y., ... Wang, J. (2010). A human gut microbial gene catalogue established by metagenomic sequencing. *Nature*, *464*(7285), 59–65.

Rakoff-Nahoum, S., Paglino, J., Eslami-Varzaneh, F., Edberg, S., & Medzhitov, R. (2004). Recognition of commensal microflora by toll-like receptors is required for intestinal homeostasis. *Cell*, *118*(2), 229–241.

Ramnani, P., Gaudier, E., Bingham, M., van Bruggen, P., Tuohy, K. M., & Gibson, G. R. (2010). Prebiotic effect of fruit and vegetable shots containing Jerusalem artichoke inulin: a human intervention study. *The British journal of nutrition*, *104*(2), 233–240.

Rastall R. A. (2004). Bacteria in the gut: friends and foes and how to alter the balance. *The Journal of nutrition*, 134(8 Suppl), 2022S–2026S.

Redpath, S. A., Heieis, G. A., Reynolds, L. A., Fonseca, N. M., Kim, S. S., & Perona-Wright, G. (2018). Functional specialization of intestinal dendritic cell subsets during Th2 helminth infection in mice. *European journal of immunology*, 48(1), 87–98.

Reichardt, N., Duncan, S. H., Young, P., Belenguer, A., McWilliam Leitch, C., Scott, K. P., Flint, H. J., & Louis, P. (2014). Phylogenetic distribution of three pathways for propionate production within the human gut microbiota. *The ISME journal*, 8(6), 1323–1335.

Ren, J., Yue, B., Wang, H., Zhang, B., Luo, X., Yu, Z., Zhang, J., Ren, Y., Mani, S., Wang, Z., & Dou, W. (2021). Acacetin Ameliorates Experimental Colitis in Mice via Inhibiting Macrophage Inflammatory Response and Regulating the Composition of Gut Microbiota. *Frontiers in physiology*, *11*, 577237.

Rivière, A., Selak, M., Lantin, D., Leroy, F., & De Vuyst, L. (2016). Bifidobacteria and Butyrate-Producing Colon Bacteria: Importance and Strategies for Their Stimulation in the Human Gut. *Frontiers in microbiology*, *7*, 979.

Rodríguez-Padilla, Á., Morales-Martín, G., Pérez-Quintero, R., Gómez-Salgado, J., Balongo-García, R., & Ruiz-Frutos, C. (2021). Postoperative Ileus after Stimulation with Probiotics before Ileostomy Closure. *Nutrients*, *13*(2), 626.

Romero, R., Zarzycka, A., Preussner, M., Fischer, F., Hain, T., Herrmann, J. P., Roth, K., Keber, C. U., Suryamohan, K., Raifer, H., Luu, M., Leister, H., Bertrams, W., Klein, M., Shams-Eldin, H., Jacob, R., Mollenkopf, H. J., Rajalingam, K., Visekruna, A., & Steinhoff, U. (2022). Selected commensals educate the intestinal vascular and immune system for immunocompetence. *Microbiome*, *10*(1), 158.

Sakaguchi, S., Sakaguchi, N., Shimizu, J., Yamazaki, S., Sakihama, T., Itoh, M., Kuniyasu, Y., Nomura, T., Toda, M., & Takahashi, T. (2001). Immunologic tolerance maintained by CD25+ CD4+ regulatory T cells: their common role in controlling autoimmunity, tumor immunity, and transplantation tolerance. *Immunological reviews*, *182*, 18–32.

Sakai, S. A., Aoshima, M., Sawada, K., Horasawa, S., Yoshikawa, A., Fujisawa, T., Kadowaki, S., Denda, T., Matsuhashi, N., Yasui, H., Goto, M., Yamazaki, K., Komatsu, Y., Nakanishi, R., Nakamura, Y., Bando, H., Hamaya, Y., Kageyama, S. I., Yoshino, T., Tsuchihara, K., ... Yamashita, R. (2022). Fecal microbiota in patients with a stoma decreases anaerobic bacteria and alters taxonomic and functional diversities. *Frontiers in cellular and infection microbiology*, *12*, 925444.

Sallusto, F., Lenig, D., Förster, R., Lipp, M., & Lanzavecchia, A. (1999). Two subsets of memory T lymphocytes with distinct homing potentials and effector functions. *Nature*, *401*(6754), 708–712.

Sánchez-Fidalgo, S., Sánchez de Ibargüen, L., Cárdeno, A., & Alarcón de la Lastra, C. (2012). Influence of extra virgin olive oil diet enriched with hydroxytyrosol in a chronic DSS colitis model. *European journal of nutrition*, *51*(4), 497–506.

Sánchez-Marzo, N., Pérez-Sánchez, A., Ruiz-Torres, V., Martínez-Tébar, A., Castillo, J., Herranz-López, M., & Barrajón-Catalán, E. (2019). Antioxidant and Photoprotective Activity of Apigenin and its Potassium Salt Derivative in Human Keratinocytes and Absorption in Caco-2 Cell Monolayers. *International journal of molecular sciences*, 20(9), 2148.

Sasaki, M., Schwab, C., Ramirez Garcia, A., Li, Q., Ferstl, R., Bersuch, E., Akdis, C. A., Lauener, R., CK-CARE study group, Frei, R., & Roduit, C. (2022). The abundance of Ruminococcus bromii is associated with faecal butyrate levels and atopic dermatitis in infancy. *Allergy*, 77(12), 3629–3640. Advance online publication.

Satchithanandam, S., Vargofcak-Apker, M., Calvert, R. J., Leeds, A. R., & Cassidy, M. M. (1990). Alteration of gastrointestinal mucin by fiber feeding in rats. *The Journal of nutrition*, *120*(10), 1179–1184.

Sato, V. H., Sato, H., Sangfuang, M., Nontakham, J., Junyaprasert, V. B., Teeranachaideekul, V., & Morakul, B. (2024). Enhancement of in vitro transcellular absorption and in vivo oral bioavailability of apigenin by self-nanoemulsifying drug delivery systems. *Scientific reports*, *14*(1), 32148.

Savage D. C. (1986). Gastrointestinal microflora in mammalian nutrition. *Annual review of nutrition*, 6, 155–178.

Scalbert, A., & Williamson, G. (2000). Dietary intake and bioavailability of polyphenols. *The Journal of nutrition*, *130*(8S Suppl), 2073S–85S.

Schmit, A., Van Gossum, A., Carol, M., Houben, J. J., & Mascart, F. (2000). Diversion of intestinal flow decreases the numbers of interleukin 4 secreting and interferon gamma secreting T lymphocytes in small bowel mucosa. *Gut*, *46*(1), 40–45.

Schoenborn, A. A., von Furstenberg, R. J., Valsaraj, S., Hussain, F. S., Stein, M., Shanahan, M. T., Henning, S. J., & Gulati, A. S. (2019). The enteric microbiota regulates

jejunal Paneth cell number and function without impacting intestinal stem cells. *Gut microbes*, *10*(1), 45–58.

Shimizu, M., Fukutomi, Y., Ninomiya, M., Nagura, K., Kato, T., Araki, H., Suganuma, M., Fujiki, H., & Moriwaki, H. (2008). Green tea extracts for the prevention of metachronous colorectal adenomas: a pilot study. *Cancer epidemiology, biomarkers & prevention: a publication of the American Association for Cancer Research, cosponsored by the American Society of Preventive Oncology, 17*(11), 3020–3025.

Shiokawa, A., Kotaki, R., Takano, T., Nakajima-Adachi, H., & Hachimura, S. (2017). Mesenteric lymph node CD11b⁻ CD103⁺ PD-L1^{High} dendritic cells highly induce regulatory T cells. *Immunology*, *152*(1), 52–64.

Shkoporov, A. N., & Hill, C. (2019). Bacteriophages of the Human Gut: The "Known Unknown" of the Microbiome. *Cell host & microbe*, *25*(2), 195–209.

SickKids Staff (2013). GI (Gastrointestinal) tract. Sick Kids, About Kids Health. https://www.aboutkidshealth.ca/gi-gastrointestinal-tract [last accessed 17/07/2025].

Siddiqui, K. R., & Powrie, F. (2008). CD103+ GALT DCs promote Foxp3+ regulatory T cells. *Mucosal immunology*, *1 Suppl 1*, S34–S38.

Silk, D. B., Davis, A., Vulevic, J., Tzortzis, G., & Gibson, G. R. (2009). Clinical trial: the effects of a trans-galactooligosaccharide prebiotic on faecal microbiota and symptoms in irritable bowel syndrome. *Alimentary pharmacology & therapeutics*, *29*(5), 508–518.

Soderholm, A. T., and Pedicord, V. A. (2019). Intestinal epithelial cells: at the interface of the microbiota and mucosal immunity. *Immunology*, *158*(4), 267–280.

Soleas, G. J., Angelini, M., Grass, L., Diamandis, E. P., & Goldberg, D. M. (2001). Absorption of trans-resveratrol in rats. *Methods in enzymology*, 335, 145–154.

Spinler, J. K., Taweechotipatr, M., Rognerud, C. L., Ou, C. N., Tumwasorn, S., & Versalovic, J. (2008). Human-derived probiotic Lactobacillus reuteri demonstrate antimicrobial activities targeting diverse enteric bacterial pathogens. *Anaerobe*, *14*(3), 166–171.

Stappenbeck, T. S., Hooper, L. V., & Gordon, J. I. (2002). Developmental regulation of intestinal angiogenesis by indigenous microbes via Paneth cells. *Proceedings of the National Academy of Sciences of the United States of America*, 99(24), 15451–15455. Stoeva, M. K., Garcia-So, J., Justice, N., Myers, J., Tyagi, S., Nemchek, M., McMurdie, P. J., Kolterman, O., & Eid, J. (2021). Butyrate-producing human gut symbiont, *Clostridium butyricum*, and its role in health and disease. *Gut microbes*, *13*(1), 1–28.

Sun, J., Fang, D., Wang, Z., & Liu, Y. (2023). Sleep Deprivation and Gut Microbiota Dysbiosis: Current Understandings and Implications. *International journal of molecular sciences*, *24*(11), 9603.

Szwajgier D & Jakubczyk A (2010)- Biotransformation of ferulic acid by *Lactobacillus acidophilus* K1 and selected *Bifidobacterium* strains. Acta Sci. Pol., Technol. Aliment. 9(1). 45-59.

Tagaino, R., Washio, J., Abiko, Y., Tanda, N., Sasaki, K., & Takahashi, N. (2019). Metabolic property of acetaldehyde production from ethanol and glucose by oral Streptococcus and Neisseria. *Scientific reports*, 9(1), 10446.

Takashima, T., Sakata, Y., Iwakiri, R., Shiraishi, R., Oda, Y., Inoue, N., Nakayama, A., Toda, S., & Fujimoto, K. (2014). Feeding with olive oil attenuates inflammation in dextran sulfate sodium-induced colitis in rat. *The Journal of nutritional biochemistry*, 25(2), 186–192.

Tamboli, C. P., Neut, C., Desreumaux, P., & Colombel, J. F. (2004). Dysbiosis in inflammatory bowel disease. *Gut*, *53*(1), 1–4.

Tandon, D., Haque, M. M., Gote, M., Jain, M., Bhaduri, A., Dubey, A. K., & Mande, S. S. (2019). A prospective randomized, double-blind, placebo-controlled, dose-response relationship study to investigate efficacy of fructo-oligosaccharides (FOS) on human gut microflora. *Scientific reports*, 9(1), 5473.

Teng, Z., Yuan, C., Zhang, F., Huan, M., Cao, W., Li, K., Yang, J., Cao, D., Zhou, S., & Mei, Q. (2012). Intestinal absorption and first-pass metabolism of polyphenol compounds in rat and their transport dynamics in Caco-2 cells. *PloS one*, *7*(1), e29647.

Topping, D. L., & Clifton, P. M. (2001). Short-chain fatty acids and human colonic function: roles of resistant starch and nonstarch polysaccharides. *Physiological reviews*, *81*(3), 1031–1064.

Turki, A. T., Bayraktar, E., Basu, O., Benkö, T., Yi, J. H., Kehrmann, J., Tzalavras, A., Liebregts, T., Beelen, D. W., & Steckel, N. K. (2019). Ileostomy for steroid-resistant acute graft-versus-host disease of the gastrointestinal tract. *Annals of hematology*, 98(10), 2407–2419.

Turnbaugh, P. J., Ley, R. E., Hamady, M., Fraser-Liggett, C. M., Knight, R., & Gordon, J. I. (2007). The human microbiome project. *Nature*, *44*9(7164), 804–810.

Uga, N., Nakatani, M., Yoshimura, A., Kumamoto, K., Tsuchida, K., Nagao, S., Tsuchiya, T., Kondo, Y., Naoe, A., Watanabe, S., Yasui, T., Hara, F., & Suzuki, T. (2021). A new murine ileostomy model: recycling stool prevents intestinal atrophy in the distal side of ileostomy. *Fujita medical journal*, *7*(2), 41–49.

Vaishnava, S., Yamamoto, M., Severson, K. M., Ruhn, K. A., Yu, X., Koren, O., Ley, R., Wakeland, E. K., & Hooper, L. V. (2011). The antibacterial lectin RegIllgamma promotes the spatial segregation of microbiota and host in the intestine. *Science (New York, N.Y.)*, 334(6053), 255–258.

Velasquez M. T. (2018). Altered Gut Microbiota: A Link Between Diet and the Metabolic Syndrome. *Metabolic syndrome and related disorders*, *16*(7), 321–328.

Vezza, T., Rodríguez-Nogales, A., Algieri, F., Garrido-Mesa, J., Romero, M., Sánchez, M., Toral, M., Martín-García, B., Gómez-Caravaca, A. M., Arráez-Román, D., Segura-Carretero, A., Micol, V., García, F., Utrilla, M. P., Duarte, J., Rodríguez-Cabezas, M. E., & Gálvez, J. (2019). The metabolic and vascular protective effects of olive (Olea europaea L.) leaf extract in diet-induced obesity in mice are related to the amelioration of gut microbiota dysbiosis and to its immunomodulatory properties. *Pharmacological research*, *150*, 104487.

Vighi, G., Marcucci, F., Sensi, L., Di Cara, G., & Frati, F. (2008). Allergy and the gastrointestinal system. *Clinical and experimental immunology*, *153 Suppl 1*(Suppl 1), 3–6.

Villa-Rodriguez, J. A., Ifie, I., Gonzalez-Aguilar, G. A., & Roopchand, D. E. (2019). The Gastrointestinal Tract as Prime Site for Cardiometabolic Protection by Dietary Polyphenols. *Advances in nutrition (Bethesda, Md.)*, *10*(6), 999–1011.

Villmones HC, Haug ES, Ulvestad E, Grude N, Stenstad T, Halland A, & Kommedal <u>Ø</u> (2018)- Species level description of the human ileal bacterial microbiota. Nature, Scientific Reports. 8. 4736.

Vinolo, M. A., Rodrigues, H. G., Nachbar, R. T., & Curi, R. (2011). Regulation of inflammation by short chain fatty acids. *Nutrients*, *3*(10), 858–876.

Vlasova, A. N., Kandasamy, S., Chattha, K. S., Rajashekara, G., & Saif, L. J. (2016). Comparison of probiotic lactobacilli and bifidobacteria effects, immune responses and rotavirus vaccines and infection in different host species. *Veterinary immunology and immunopathology*, *172*, 72–84.

Walker, A. W., Duncan, S. H., McWilliam Leitch, E. C., Child, M. W., & Flint, H. J. (2005). pH and peptide supply can radically alter bacterial populations and short-chain fatty acid ratios within microbial communities from the human colon. *Applied and environmental microbiology*, 71(7), 3692–3700.

Wan, Y. Y., & Flavell, R. A. (2007). Regulatory T-cell functions are subverted and converted owing to attenuated Foxp3 expression. *Nature*, *445*(7129), 766–770.

Wang, K., Guo, J., Chang, X., & Gui, S. (2022). Painong-San extract alleviates dextran sulfate sodium-induced colitis in mice by modulating gut microbiota, restoring intestinal barrier function and attenuating TLR4/NF-κB signaling cascades. *Journal of pharmaceutical and biomedical analysis*, 209, 114529.

Wang, P., Li, D., Ke, W., Liang, D., Hu, X., & Chen, F. (2020). Resveratrol-induced gut microbiota reduces obesity in high-fat diet-fed mice. *International journal of obesity* (2005), 44(1), 213–225.

Wang, T., Leibrock, N., Plugge, C. M., Smidt, H., & Zoetendal, E. G. (2023). *In vitro* interactions between *Blautia hydrogenotrophica*, *Desulfovibrio piger* and *Methanobrevibacter smithii* under hydrogenotrophic conditions. *Gut microbes*, 15(2), 2261784.

Wang, X., Qi, Y., & Zheng, H. (2022). Dietary Polyphenol, Gut Microbiota, and Health Benefits. *Antioxidants (Basel, Switzerland)*, *11*(6), 1212.

Watanabe, Y., Mizushima, T., Okumura, R., Fujino, S., Ogino, T., Miyoshi, N., Takahashi, H., Uemura, M., Matsuda, C., Yamamoto, H., Takeda, K., Doki, Y., & Eguchi, H. (2022). Fecal Stream Diversion Changes Intestinal Environment, Modulates Mucosal Barrier, and Attenuates Inflammatory Cells in Crohn's Disease. *Digestive diseases and sciences*, 67(6), 2143–2157.

Weigmann, B., Tubbe, I., Seidel, D., Nicolaev, A., Becker, C., & Neurath, M. F. (2007). Isolation and subsequent analysis of murine lamina propria mononuclear cells from colonic tissue. *Nature protocols*, *2*(10), 2307–2311.

Weiss, J., Decker, E.A., McClements, D.J., Kristbergsson, K., Helgason, T., Awad, T. (2008). Solid lipid nanoparticles as delivery systems for bioactive food components. Food Biophysics, (3), 146-154.

Welty, N. E., Staley, C., Ghilardi, N., Sadowsky, M. J., Igyártó, B. Z., & Kaplan, D. H. (2013). Intestinal lamina propria dendritic cells maintain T cell homeostasis but do not affect commensalism. *The Journal of experimental medicine*, *210*(10), 2011–2024.

Wen, L., & Duffy, A. (2017). Factors Influencing the Gut Microbiota, Inflammation, and Type 2 Diabetes. *The Journal of nutrition*, *147*(7), 1468S–1475S.

Wieck, M. M., Schlieve, C. R., Thornton, M. E., Fowler, K. L., Isani, M., Grant, C. N., Hilton, A. E., Hou, X., Grubbs, B. H., Frey, M. R., & Grikscheit, T. C. (2017). Prolonged Absence of Mechanoluminal Stimulation in Human Intestine Alters the Transcriptome and Intestinal Stem Cell Niche. *Cellular and molecular gastroenterology and hepatology*, 3(3), 367–388.e1.

Wildhaber, B. E., Lynn, K. N., Yang, H., & Teitelbaum, D. H. (2002). Total parenteral nutrition-induced apoptosis in mouse intestinal epithelium: regulation by the Bcl-2 protein family. *Pediatric surgery international*, *18*(7), 570–575.

Williams, L., Armstrong, M. J., Finan, P., Sagar, P., & Burke, D. (2007). The effect of faecal diversion on human ileum. *Gut*, *56*(6), 796–801.

Wolin M. J. (1969). Volatile fatty acids and the inhibition of Escherichia coli growth by rumen fluid. *Applied microbiology*, *17*(1), 83–87.

Wong, K. K., Lan, L. C., Lin, S. C., Chan, A. W., & Tam, P. K. (2004). Mucous fistula refeeding in premature neonates with enterostomies. *Journal of pediatric gastroenterology and nutrition*, 39(1), 43–45.

Woo, H. D., Lee, J., Choi, I. J., Kim, C. G., Lee, J. Y., Kwon, O., & Kim, J. (2014). Dietary flavonoids and gastric cancer risk in a Korean population. *Nutrients*, 6(11), 4961–4973.

Worthington, J. J., Czajkowska, B. I., Melton, A. C., & Travis, M. A. (2011). Intestinal dendritic cells specialize to activate transforming growth factor-β and induce Foxp3+ regulatory T cells via integrin ανβ8. *Gastroenterology*, *141*(5), 1802–1812.

Wrzosek, L., Miquel, S., Noordine, M. L., Bouet, S., Joncquel Chevalier-Curt, M., Robert, V., Philippe, C., Bridonneau, C., Cherbuy, C., Robbe-Masselot, C., Langella, P., & Thomas, M. (2013). Bacteroides thetaiotaomicron and Faecalibacterium prausnitzii influence the production of mucus glycans and the development of goblet cells in the colonic epithelium of a gnotobiotic model rodent. *BMC biology*, *11*, 61.

Wurster, A. L., Rodgers, V. L., Satoskar, A. R., Whitters, M. J., Young, D. A., Collins, M., & Grusby, M. J. (2002). Interleukin 21 is a Thelper (Th) cell 2 cytokine that specifically inhibits the differentiation of naive Th cells into interferon gamma-producing Th1 cells. *The Journal of experimental medicine*, 196(7), 969–977.

Xu, S., Wang, Y., Wang, J., & Geng, W. (2022). Kombucha Reduces Hyperglycemia in Type 2 Diabetes of Mice by Regulating Gut Microbiota and Its Metabolites. *Foods* (Basel, Switzerland), 11(5), 754.

Xu, X., Wang, H-J., Murphy, PA., Cook, L., Hendrich, S. (1994). Daidzein is a More Bioavailable Soymilk Isoflavone than is Genistein in Adult Women. The Journal of Nutrition, 124(6), 825-832.

Yamada, K., Yoshitake, K., Sato, M., & Ahnen, D. J. (1992). Proliferating cell nuclear antigen expression in normal, preneoplastic, and neoplastic colonic epithelium of the rat. *Gastroenterology*, *103*(1), 160–167.

Yang, G., Wang, H., Kang, Y., & Zhu, M. J. (2014). Grape seed extract improves epithelial structure and suppresses inflammation in ileum of IL-10-deficient mice. *Food & function*, *5*(10), 2558–2563.

Yang, H., Fan, Y., & Teitelbaum, D. H. (2003). Intraepithelial lymphocyte-derived interferon-gamma evokes enterocyte apoptosis with parenteral nutrition in mice. *American journal of physiology. Gastrointestinal and liver physiology*, 284(4), G629–G637.

Yang, H., Gumucio, D. L., & Teitelbaum, D. H. (2008). Intestinal specific overexpression of interleukin-7 attenuates the alternation of intestinal intraepithelial lymphocytes after total parenteral nutrition administration. *Annals of surgery*, *248*(5), 849–856.

Yousefi, Y., Haider, Z., Grondin, J. A., Wang, H., Haq, S., Banskota, S., Seto, T., Surette, M., & Khan, W. I. (2025). Gut microbiota regulates intestinal goblet cell response and mucin production by influencing the TLR2-SPDEF axis in an enteric parasitic infection. *Mucosal immunology*, S1933-0219(25)00033-9.

Zhan, Y., Chen, P. J., Sadler, W. D., Wang, F., Poe, S., Núñez, G., Eaton, K. A., & Chen, G. Y. (2013). Gut microbiota protects against gastrointestinal tumorigenesis caused by epithelial injury. *Cancer research*, 73(24), 7199–7210.

Zhang, L., Zhu, K., Zeng, H., Zhang, J., Pu, Y., Wang, Z., Zhang, T., & Wang, B. (2019). Resveratrol solid lipid nanoparticles to trigger credible inhibition of doxorubicin cardiotoxicity. *International journal of nanomedicine*, *14*, 6061–6071.

Zhang, X., Zhang, D., Jia, H., Feng, Q., Wang, D., Liang, D., Wu, X., Li, J., Tang, L., Li, Y., Lan, Z., Chen, B., Li, Y., Zhong, H., Xie, H., Jie, Z., Chen, W., Tang, S., Xu, X., Wang, X., ... Wang, J. (2015). The oral and gut microbiomes are perturbed in rheumatoid arthritis and partly normalized after treatment. *Nature medicine*, *21*(8), 895–905.

Zhao, Z., Shi, A., Wang, Q., & Zhou, J. (2019). High Oleic Acid Peanut Oil and Extra Virgin Olive Oil Supplementation Attenuate Metabolic Syndrome in Rats by Modulating the Gut Microbiota. *Nutrients*, *11*(12), 3005.

Zhou, L., Zhang, M., Wang, Y., Dorfman, R. G., Liu, H., Yu, T., Chen, X., Tang, D., Xu, L., Yin, Y., Pan, Y., Zhou, Q., Zhou, Y., & Yu, C. (2018). Faecalibacterium prausnitzii

Produces Butyrate to Maintain Th17/Treg Balance and to Ameliorate Colorectal Colitis by Inhibiting Histone Deacetylase 1. *Inflammatory bowel diseases*, *24*(9), 1926–1940.

Zhu, J.-G & Yu, R. & Ge, H.-F & Jiang, B.-F & Tao, G.-Q. (2011). Effects of succus entericus reinfusion with continuous enteral nutrition on the barrier function of intestinal mucosa in patients with stomal type fistulas. Chinese Journal of Clinical Nutrition. 19. 239-241.

Zhu, Y., Sun, H., He, S., Lou, Q., Yu, M., Tang, M., & Tu, L. (2018). Metabolism and prebiotics activity of anthocyanins from black rice (Oryza sativa L.) in vitro. *PloS one*, *13*(4), e0195754.

Zong, X., Fu, J., Xu, B., Wang, Y., & Jin, M. (2020). Interplay between gut microbiota and antimicrobial peptides. *Animal nutrition (Zhongguo xu mu shou yi xue hui)*, 6(4), 389–396.